MOL.19960924.0193

CRWMS/M&O

Design Analysis Cover Sheet

Complete only applicable items.

①

QA: L

Page: 1 Of: 64

2. DESIGN ANALYSIS TITLE (SCPB: N/A)
Second Waste Package Probabilistic Criticality Analysis: Generation and Evaluation of Internal Criticality Configurations

3. DOCUMENT IDENTIFIER (Including Rev. No.)
BBA000000-01717-2200-00005 REV00

4. TOTAL PAGES
64

5. TOTAL ATTACHMENTS
9

6. ATTACHMENT NUMBERS - NO. OF PAGES IN EACH
I-7, II-5, III-3, IV-7, V-3, VI-7, VII-13, VIII-7, IX- 5 (see Sect.9 for Att. list)

	Printed Name	Signature	Date
7. Originator	P. Gottlieb J.R. Massari J.K. McCoy	P. Gottlieb John Massari J K McCoy	3/27/96
8. Checker	J.K. McCoy D. Stahl	J K McCoy David Stahl	3/27/96
9. Lead Design Engineer	P. Gottlieb	P. Gottlieb	3/27/96
10.QA Manager	Hyde Griffith	Hyde Griffith	3/27/96
11. Department Manager	Hugh A. Benton	Hugh A. Benton	3/27/96

12. REMARKS

Initial Issue

PCG compliance review of checked doucment completed by Wayne E. Wallin WEW 3/27/96

Summary of originator and checker responsibilities:

Section(s)	Responsible Individual(s)	Checked By
1.0, 3.0, 4.0	**P. Gottlieb**	**J.K. McCoy**
2.0, 5.0, 6.0	**J.R. Massari**	**J.K. McCoy**
7.1	**P. Gottlieb**	**J.K. McCoy**
7.2	**P. Gottlieb**	**J.K. McCoy**
7.3	**P. Gottlieb**	**J.K. McCoy**
7.4	**P. Gottlieb**	**J.K. McCoy**
7.5	**J.R. Massari**	**J.K. McCoy**
8.0	**P. Gottlieb**	**J.K. McCoy**
9.0	**J.R. Massari**	**J.K. McCoy**
Att. I	**P. Gottlieb**	**J.K. McCoy**
Att. II	**P. Gottlieb**	**J.K. McCoy**
Att. III	**J. R. Massari**	**J.K. McCoy**
Att. IV	**J.K. McCoy (author of included white paper)**	**D. Stahl**
Att. V	**P. Gottlieb**	**J.K. McCoy**
Att. VI	**J.R. Massari**	**J.K. McCoy**
Att. VII	**J.R. Massari**	**J.K. McCoy**
Att. VIII	**J.R. Massari**	**J.K. McCoy**
Att. IX	**J.R. Massari**	**J.K. McCoy**

CRWMS/M&O

Design Analysis Revision Record

Complete only applicable items.

①

2. DESIGN ANALYSIS TITLE Second Waste Package Probabilistic Criticality Analysis: Generation and Evaluation of Internal Criticality Configurations	
3. DOCUMENT IDENTIFIER (Including Rev. No.) BBA000000-01717-2200-00005 REV00	

4. Revision No.	5. Description of Revision
00	Initial Issue - Issued Approved

1. Purpose -

This analysis is prepared by the Mined Geologic Disposal System (MGDS) Waste Package Development (WPD) department to provide an evaluation of the criticality potential within a waste package having some or all of its contents degraded by corrosion and removal of neutron absorbers. This analysis is also intended to provide an estimate of the consequences of any internal criticality, particularly in terms of any increase in radionuclide inventory. These consequence estimates will be used as part of the WPD input to the Total System Performance Assessment.

The ultimate objective of this analysis is to augment the information gained from the Initial Waste Package Probabilistic Criticality Analyses (Ref. 5.8 and 5.9, hereafter referred to as IPA) to a degree which will support preliminary waste package design recommendations intended to reduce the risk of waste package criticality and the risk to total repository system performance posed by the consequences of any criticality. The IPA evaluated the criticality potential under the assumption that the waste package basket retained its structural integrity, so that the assemblies retained their initial separation, even when the neutron absorbers had been leached from the basket. This analysis is based on the more realistic condition that removal of the neutron absorbers is a consequence of the corrosion of the steel in which they are contained, which has the additional consequence of reducing the structural support between assemblies. The result is a set of more reactive configurations having a smaller spacing between assemblies, or no inter-assembly spacing at all.

Another difference from the IPA is the minimal attention to probabilistic evaluation given in this study. Although the IPA covered a time horizon to 100,000 years, the lack of consideration of basket degradation modes made it primarily applicable to the first 10,000 years. In contrast, this study, by focusing on the degraded modes of the basket, is primarily applicable to the post 10,000 year time horizon.

The principal probability related objective of this analysis is to estimate the earliest time at which a criticality can possibly occur, as a function of several environmental and material performance parameters, the specific values of which are subject to great uncertainty. It should be noted that the longer the possibility of criticality is delayed, the less will be the probability of any criticality at all, because of the increased probability that the waste package bottom will be penetrated by corrosion so that the waste package can no longer hold enough water to provide the necessary moderation to support the criticality.

2. Quality Assurance -

The Quality Assurance (QA) program applies to this analysis. The work reported in this document is part of the probabilistic evaluation of the waste package (WP). This activity can affect the proper functioning of the Mined Geologic Disposal System (MGDS) waste package; the waste package has been identified as an MGDS Q-List item important to safety and waste isolation (pp.

5, 16, Ref. 5.1). The waste package is on the Q-List by direct inclusion by the Department of Energy (DOE); a QAP-2-3 evaluation has yet to be conducted. The work performed for this analysis is covered by a WPD QAP-2-0 work control Activity Evaluation entitled *Perform Probabilistic Waste Package Design Analyses* (Ref. 5.2). This QAP-2-0 evaluation determined that such activities are subject to *Quality Assurance Requirements and Description* (QARD) (Ref. 5.3) requirements. Applicable procedural controls are listed in the evaluation.

All design inputs which are identified in this document are for preliminary design and shall be treated as unqualified data; these design inputs will require subsequent qualification (or superseding inputs) as the waste package design proceeds. This document will not directly support any construction, fabrication or procurement activity and therefore is not required to be procedurally controlled as TBV (to be verified). In addition, the inputs associated with this analysis are not required to be procedurally controlled as TBV. However, use of any data from this analysis for input into documents supporting procurement, fabrication, or construction is required to be controlled as TBV in accordance with the appropriate procedures.

3. Method -

The following methods are used for this analysis:

- Calculation of amounts of neutron absorbers within the waste package as a function of time, using numerical integration of the set of linear, first order differential equations coupling the steel, oxide, and solution phases. The implementation of this numerical integration in a simple program is called the configuration generator.

- Calculation of k_{eff}, using the QA qualified code MCNP, for a set of partially degraded configurations which reflect the expected corrosion processes for the basket materials, carbon steel, and borated stainless steel.

- Parameterization of the dependence of k_{eff} on concentration of the principal neutron absorbers, iron and boron, by a linear regression developed from the k_{eff} data. This regression also incorporates the effects of basket collapse causing increased reactivity.

- Application of the k_{eff} regression to the calculation of the amounts of neutron absorbers remaining in the WP. This is used to estimate times to when sufficient neutron absorber has been depleted to permit criticality ($k_{eff}>0.91$ after considering the 5% margin of safety and the bias and uncertainty of MCNP in accordance with Ref. 5.12).

- Estimation of the consequences of a criticality of 1,000, 5,000 and 10,000 years duration. The increase in radionuclide inventory of the fuel assemblies involved is estimated using the code ORIGEN-S (which computes the radionuclide inventory for fuel assemblies irradiated in a reactor at a specified power for a specified time).

Further detail on the specific analytical methods employed for each step is available in Section 7 of this analysis.

4. Design Inputs -

All design inputs are for preliminary design; these design inputs will require subsequent qualification (or superseding inputs) as the waste package design proceeds to final design.

4.1 Design Parameters -

4.1.1 Material Property Parameters

The material property parameters (density, composition) used in this analysis are shown in Table 4.1-1 below. This information was obtained from Reference 5.5. See assumption 4.3.23.

Table 4.1-1. Material Property Parameters Used

Material Property	A516 Carbon Steel	Borated 316 Stainless Steel (316B6A)
Density (g/cm^3)	7.832	7.770
Weight % Fe	98.535%	60.445%
Weight % B	n/a	1.600%
Weight % Cr	n/a	19.00%
Weight % Ni	n/a	13.500%
Weight % Mn	0.900%	2.000%
Weight % N	n/a	0.100%
Weight % S	0.035%	0.030%
Weight % Si	0.275%	0.750%
Weight % C	0.220%	0.030%
Weight % P	0.035%	0.045%
Weight % Mo	n/a	2.500%

The density of iron oxide was taken to be that of Fe_2O_3, 5.24 g/cm^3 (Reference 5.17).

4.1.2 Intact Waste Package Geometry Parameters

The intact waste package geometry parameters used in this analysis are taken from conceptual figures of the design, Reference 5.6. See assumption 4.3.25. The dimensions are listed in Table 4.1-2 below. Figure 4.1-1 depicts the 21 Pressurized Water Reactor (PWR) Advanced Uncanistered Fuel (AUCF) WP, its internals, and the material specifications (Ref. 5.34).

Table 4.1-2. Intact WP Dimensions

Component:	Dimension: (cm)
Outer barrier length (skirt edge to skirt edge)	533.5
Outer barrier skirt length (both ends)	22.5
Outer barrier inner radii	73.1
Outer barrier outer radii	83.1
Inner barrier length (overall)	466.5
Inner barrier inner radii	71.095
Inner barrier outer radii	73.095
Fuel cell tube opening	22.9
Fuel cell tube thickness	0.5
Fuel cell tube height	457.5
Criticality control panel thickness	0.7
Criticality control panel width	113.4
Criticality control long panel (16 total) length	122.1
Criticality control short panel (16 total) length	73.0
Criticality control panel cutout length (4 per long panel/2 per short panel)	56.7
Criticality control panel cutout width	0.7

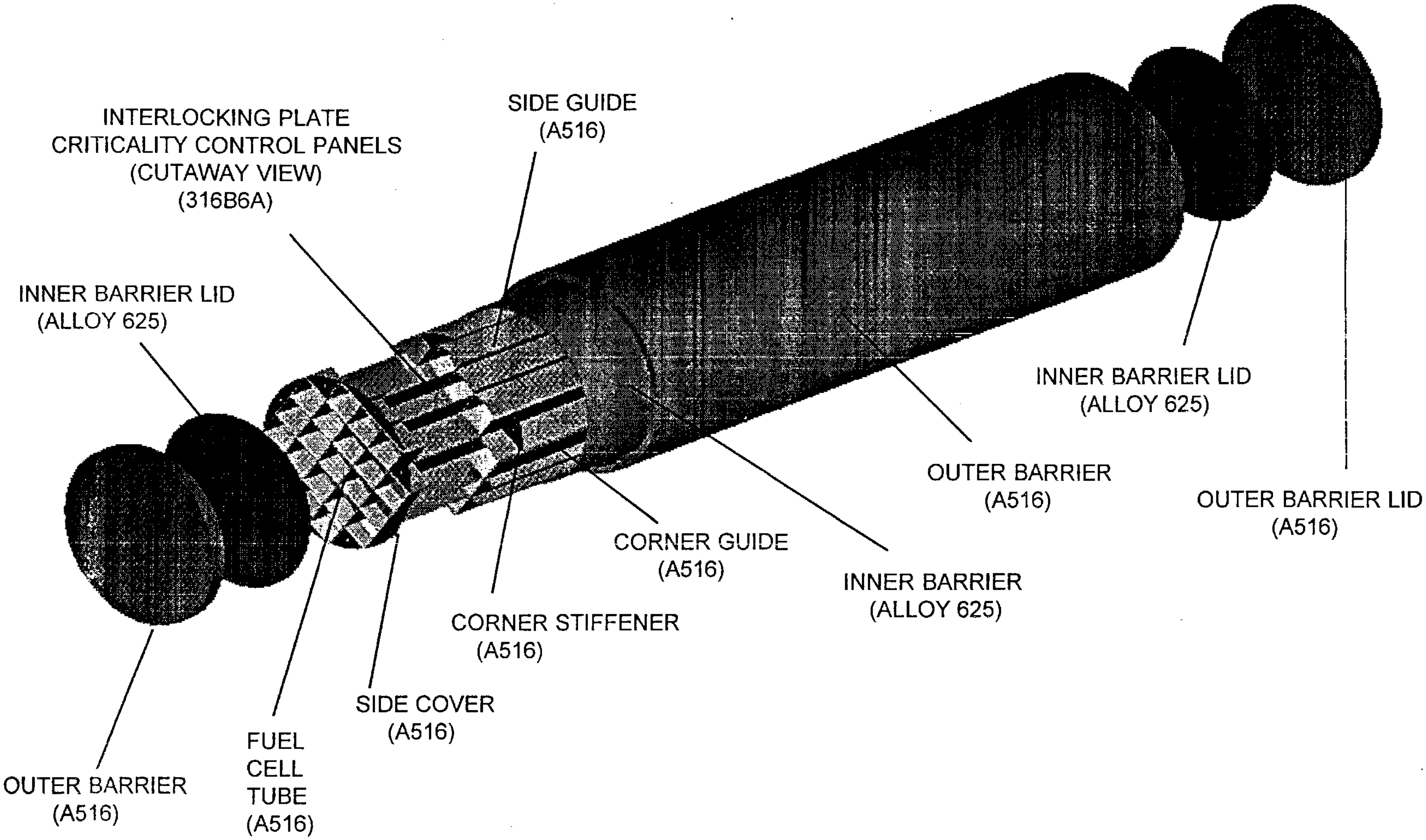

Figure 4.1-1. Advanced Uncanistered Fuel Waste Package with Internals Shown

4.1.3 Calculated WP k_{eff} For Various Intact and Degraded Geometries

4.1.3.1 Calculated k_{eff}

Tables 4.1-3 and 4.1-4 provide the results of k_{eff} calculations for various degraded geometries (without filler material) which were performed using the Monte Carlo neutronics code MCNP. Further detail on these calculations is contained in Reference 5.4.

Table 4.1-3. Progressive Degradation of Borated Stainless Steel Control Panels (Ref. 5.4)

% SS-B Plate Thickness Remaining	% of WP Void Space Filled With Fe_2O_3	k_{eff}
80	0	0.894
50	0	0.917
50	10	0.851
25	20	0.857
25	15	0.880
10	25	0.887
10	20	0.908
10	10	0.944

Table 4.1-4. Basket Structure Gone, Uniform Iron Oxide and Boron Concentration (Ref. 5.4)

% of WP Void Filled With Fe_2O_3	% of Original B-10 Remaining In WP	k_{eff}
0	0	1.093
30	0	0.928
30	2	0.913
30	5	0.890
20	0	0.979
20	5	0.941
20	10	0.902
20	15	0.872
20	25	0.812
20	100	0.572
10	10	0.947
10	15	0.909
10	20	0.879

4.1.3.2 Effects of Moderator Density Changes on k_{eff}

The effects of moderator density reductions on the k_{eff} of two Advanced Conceptual Design (ACD) Uncanistered Fuel (UCF) WP geometries were reported in Reference 5.16, and are summarized in Table 4.1-5 below.

Table 4.1-5. Effects of Moderator Density Changes on WP k_{eff}

% of Moderator Density at 300 K	Calculated k_{eff}	
	Intact Basket w/ No Boron	Collapsed Basket w/ No Boron
100%	1.0079	1.0180
98%	1.0044	1.0152
95%	0.9959	1.0085
90%	0.9870	not available
80%	0.9705	not available

4.1.4 PWR (Pressurized Water Reactor) Fuel Assembly Parameters

The PWR fuel assembly parameters used in this analysis are based on a B&W 15x15 fuel assembly. See assumption 4.3.24.

Active Length:	3.602 m	(Reference 5.7)
Assembly Width:	0.217 m	(Reference 5.7)
Mass of U per Assembly:	464 kg	(Reference 5.7)
Volume Displaced:	0.0807 m^3	(Reference 5.19, P.II 3.6-98)

The spent fuel thermal parameters used in this analysis are taken from Reference 5.30 and are given in Table 4.1-6 below. The criticality design basis PWR Spent Nuclear Fuel (SNF) of 3.00% U-235 initial enrichment and 20,000 MWd/MTU burnup (Ref. 5.10) was used. For comparison, PWR SNF assemblies discharged through 1990 had an average burnup of ≈29,800 MWd/MTU and an average initial enrichment of 2.98 % (Ref. 5.7). The total projected discharges of PWR SNF assemblies from existing reactors are expected to have an average burnup of ≈44,800 MWD/MTU and an average initial enrichment of 4.14% (Ref. 5.7).

Table 4.1-6. Thermal Output of Criticality Design Basis PWR SNF

Age (years)	Thermal Output (W/MTU)
5,000	13.26
10,000	9.95
20,000	6.22
50,000	2.38
100,000	0.831

4.1.5 WP Environmental Parameters

TSPA-95 Climate Model (Ref. 5.18 pp. 7-12, 7-20, 7-21)

Climate Cycle Period:	100,000 years
Cycle Peak Multiplier:	1 to 5 (uniform distrib.)
Low Infil. Scenario Min. Infiltration Rate:	0.01 to 0.05 mm/yr (uniform distrib.)
High Infil. Scenario Min. Infiltration Rate:	0.5 to 2.0 mm/yr (uniform distrib.)
Fracture Flow Concentration Factor:	4

The relationship between the rate of infiltration into Yucca Mountain and the rate of water dripping on a WP is given in Table 4.1-7 below, which was abstracted from TSPA-95 Figures 7.3-7 and 7.3-8 These values were used in conjunction with a linear interpolation function in the MathCad v5.0+ worksheet in Attachment VII.

Table 4.1-7. TSPA-95 Relationship Between Infiltration and Drip Rates

Infiltration Rate (q_{inf}) (mm/yr)	Drip Rate (q_{drip}) (mm/yr)
0.01	4.00e-04
0.02	1.40e-03
0.03	2.80e-03
0.04	4.60e-03
0.05	6.60e-03
0.5	0.22
1.0	0.53
1.5	0.90
2.0	1.27

TSPA-95 Temp. and RH at times > 15,000 years for 83 MTU/acre, no backfill (Ref. 5.18)

Drift Relative Humidity:	≈96%	
Drift Wall/WP Surface Temperature:	≈30°C	
Other Information		
Drift Diameter:	5 m	(Reference 5.32)

4.1.6 Properties of Liquid Water

4.1.6.1 Specific Volume and Saturation Pressure

Values for the saturation pressure and specific volume of liquid water as a function of temperature are listed in Table 4.1-8 for the temperature ranges of interest in this analysis. These values were obtained from Reference 5.15 and were used in conjunction with a cubic spline interpolation function in the MathCad v5.0+ worksheets in Attachments III, VII, VIII, and IX.

Table 4.1-8. Saturation Pressure and Specific Volume of Water

Temperature (°C)	Sat. Pressure (bars)	Specific Volume (cm^3/g)
26	0.03363	1.0032
28	0.03782	1.0037
30	0.04246	1.0043
32	0.04759	1.0050
34	0.05324	1.0056
36	0.05947	1.0063
38	0.06632	1.0071
40	0.07384	1.0078
45	0.09593	1.0099
50	0.1235	1.0121
55	0.1576	1.0146
60	0.1994	1.0172

4.1.6.2 Specific Heat and Viscosity

Values for the viscosity and specific heat of liquid water as a function of temperature are listed in Table 4.1-9 for the temperature ranges of interest in this analysis. These values were obtained from Reference 5.14 and were used in conjunction with a cubic spline interpolation function in the MathCad v5.0+ worksheets in Attachments IV, VI, VII, VIII, IX.

Table 4.1-9. Viscosity and Specific Heat of Water

Temperature (°C)	Viscosity (kg/m*s)	Specific Heat (kJ/kg*K)
26.67	8.60×10^{-4}	4.179
32.22	7.65×10^{-4}	4.174
37.78	6.82×10^{-4}	4.174
43.33	6.16×10^{-4}	4.174
48.89	5.62×10^{-4}	4.174
54.44	5.13×10^{-4}	4.179
60	4.71×10^{-4}	4.179

4.1.6.3 Other Properties of Water Used

Molecular Volume:	18.8 cm^3/mole	(Ref. 5.14)
Molecular Weight:	18.02 kg/kmol	(Ref. 5.17)
Coefficient of Thermal Expansion:	320.6×10^{-6} K^{-1} at 32°C	(Ref. 5.28)
Thermal Conductivity:	0.620 W/m*K	(Ref. 5.28)
Diffusion Coefficient at 8°C:	0.239 cm^2/s	(Ref. 5.17)
For Water Into Air at 25°C:	0.256 cm^2/s	(Ref. 5.14)

4.1.7 Constants and Other Miscellaneous Information Used

Universal Gas Constant:	8.315 kJ/kmol*K	(Ref. 5.14)
Stephan-Boltzman Constant:	5.669×10^{-8} W/m^2K^4	(Ref. 5.14)
Avogadro's Number	6.022×10^{23} atoms/mole	(Ref. 5.33)
Carbon Steel Emissivity:	0.80	(Ref. 5.31)
TSw2 Drift Wall Emissivity:	0.85	(Ref. 5.31)
Crushed Tuff Avg. Thermal Conductivity:	0.66 W/m*K	(Ref. 5.32)
Acceleration of Gravity:	9.807 m/s^2	(Ref. 5.15)
Atmospheric Pressure:	1.0132×10^5 Pa	(Ref. 5.15)
Molecular Volume of Air*:	29.9 cm^3/mole	(Ref. 5.14)
Molecular Weight of Air:	28.97 kg/kmol	(Ref. 5.15)
Molecular Volume of O_2*:	7.4 cm^3/mole	(Ref. 5.14)
Molecular Weight of O_2:	32 kg/kmol	(Ref. 5.14)
Diffusion Coefficient of O_2 in Water:	1.8×10^{-5} cm^2/s at 20°C	(Ref. 5.26)
Molecular Weight of N:	14 kg/kmol	(Ref. 5.33)
Volume % N in Air:	78.08%	(Ref. 5.17)
Abundance of ^{14}N:	99.63%	(Ref. 5.33)
^{14}N (n,p) Thermal Cross Section:	1.81 barns	(Ref. 5.33)
Abundance of ^{17}O:	0.04%	(Ref. 5.33)
^{17}O (n,α) Thermal Cross Section:	0.24 barns	(Ref. 5.33)
Molecular Weight of Cl:	35.453 kg/kmol	(Ref. 5.33)

Concentration of Cl^- in J-13 Well Water:	7.5 μg/mL	(Ref. 5.35)
after boiling for 1 yr:	161 μg/mL	(Ref. 5.35)
Abundance of ^{35}Cl:	75.77%	(Ref. 5.33)
^{35}Cl (n,γ) Thermal Cross Section:	43.6 barns	(Ref. 5.33)
^{36}Cl Half-Life	3.01×10^5 years	(Ref. 5.33)
^{14}C Half-Life	5730 years	(Ref. 5.33)

* for gas diffusivity calculations

4.1.8 WP Radionuclide Inventories

Radionuclide inventories for WPs containing the criticality design basis fuel (3.0% initial enrichment, 20,000 MWd/MTU) at various ages were obtained from ORIGEN-S runs detailed in Ref. 5.4. Reference 5.4 also indicated that the average neutron flux for a WP which is critical at 2.182 kW would be 2.9×10^8 neutrons/cm^{2}s and that 10.9% of the flux would be in the thermal part of the spectrum. See assumption 4.3.11.

4.2 Criteria -

The repository criticality control design criteria for waste packages are based upon criteria from requirements documents. The requirements from the higher level requirement documents, such as the Mined Geological Disposal System Requirements Document (Reference 5.11), are only listed if they are not explicitly echoed in the Engineered Barrier Design Requirements Document (EBDRD, Reference 5.12). The criteria cited in requirement documents that have bearing on this analysis include:

4.2.1 From the EBDRD (Reference 5.12);

"**3.2.2.6 CRITICALITY PROTECTION**

A. The Engineered Barrier Segment shall be designed to ensure that a nuclear criticality accident is not possible unless at least two unlikely, independent, and concurrent or sequential changes have occurred in the conditions essential to nuclear criticality safety. Each system shall be designed for criticality safety under normal and accident conditions. The calculated effective multiplication factor must be sufficiently below unity to show at least a five percent margin, after allowance for the bias in the method of calculation and the uncertainty in the experiments used to validate the methods of calculation. [MGDS-RD 3.2.2.6.A][10CFR60.131(b)(7)]"

4.2.2 From the EBDRD (Reference 5.12);

"**3.7.1.3 INTERNAL STRUCTURE REQUIREMENTS**

A. The internal structure shall provide separation of the waste forms such that nuclear criticality shall not be possible unless at least two unlikely, independent, and concurrent or sequential changes have occurred in the conditions essential to nuclear criticality safety. The calculated effective multiplication factor (k_{eff}) must be sufficiently below unity to show at least a five percent margin after allowance for the bias in the method of calculation and the uncertainty in the experiments used to validate the methods of calculation (TBD). [MGDS-RD 3.2.2.6.A] [10CFR60.131(b)(7)]"

4.2.3 The Waste Package Implementation Plan (WPIP) (Reference 5.13) briefly echoes the criteria from the EBDRD. One of the design goals stated in the WPIP is to "Ensure subcriticality" (Reference 5.13, Page 2-5, Table 2-1).

4.3 Assumptions -

4.3.1 It is assumed that the principal precondition for the occurrence of a waste package internal criticality, is the filling of the waste package with water to serve as moderator, and the waste package remaining filled long enough to remove corrosion products and sustain criticality. It is further assumed that this precondition does occur. The basis for the first assumption (the designation of the precondition) is the fact that calculations of k_{eff} for the design basis commercial SNF, show that criticality cannot be supported without a major portion of the waste package being filled with water to serve as moderator.

The basis for the second assumption (occurrence of the precondition) is that it is the most conservative configuration possible within the present uncertainty range of long term corrosion rates for waste package barrier materials. A scenario which could lead to this configuration is based on the assumption that there will be very little probability of penetration of the lower portion of the waste package barriers before penetration of the upper portion, because such an "outside-in" process would require pit growth to a depth of 12 centimeters against gravity. The scenario begins with penetration of the upper portion of the barrier in 3000 to 5000 years; during much of the time before 3000 years the barrier temperature is above 90°C, and the aqueous corrosion rate of corrosion resistant inner barrier is modeled as being relatively high (Ref. 5.18), which is the reason why the penetration time is so short. After penetration of the upper portion of the barrier, penetration of the lower portion can begin from the inside out. By this time, however, the temperature is likely to have dropped below 60°C, where the corrosion rate is small (Ref. 5.18). Because of the present uncertainty in the corrosion model, the probability for achieving a water-filled configuration as a result of this scenario has not yet been estimated. It is expected to be extremely small.

These assumptions are used in Sections 7.3.1 and 7.3.2.

4.3.2 It is assumed that for the purpose of worst case analysis it is reasonable to define low and high values for infiltration rates of 1 and 10 mm/yr, respectively, even though the estimates of present infiltration rate are less than, or equal to only .1 mm/yr. The basis for this assumption is that there is some significant probability that the infiltration rate will increase within the next 50,000 years, based on evidence that it has been higher in the past 50,000 years. Consistent with TSPA-95 (Ref. 5-18), these low and high infiltration rates can be mapped into drip rates of 0.53, and 7.19 mm/yr respectively. The high value is a linear extrapolation from Ref. 5.18, figure 7.3-8. The calculation of this extrapolation is given in Attachment VII, pg 8, with the result of 1.91×10^5 cm^3/yr impinging on the waste package, which is converted to mm/yr by dividing by the waste package internal area projected on a horizontal plane (6.63 m^2), dividing by the concentration factor (4), dividing by the number of square centimeters in a square meter, and multiplying by the number of millimeters in a centimeter. This assumption is used in Sections 7.3.3 and 7.5.1.

4.3.3 It is assumed that the filling rate for water entering the package can be approximated by neglecting evaporation and using the simple formula: id*il*eff*infl*cf/1000, where the parameters are defined in 7.3.3. The basis for this assumption is that is a simple physical model of an admittedly complex flow problem. The neglect of evaporation is a conservative approximation, which has the effect of lowering the estimate of filling rate, particularly for low infiltration rates. A more sophisticated model of the flow process is not warranted, since the condition of the substrate on which this flow takes place (upper surface of the waste package) cannot be accurately estimated at this time. This assumption is used in Section 7.3.2

4.3.4 It is assumed that the entry of water into the waste package from dripping on the waste package can be approximated by two factors: a filling efficiency and a transfer efficiency. The filling efficiency pertains to a waste package which is not already filled with water. The transfer efficiency pertains to a package which is filled with water and represents the process of exchanging inside water for outside water. It is assumed that the filling efficiency can range from a low value of 0.01 to a high value of 1.0. The values in the range of transfer efficiencies are assumed to be a factor of 10 smaller (0.001 to 0.1). It is also assumed that both the filling efficiency and the transfer efficiency will increase with time. The basis for these assumptions is that the amount of water getting into the waste package will increase with corrosion of the waste package upper surface, which will increase with time. The maximum value for filling efficiency can be no larger than 1.0. It will be smaller if only a small fraction of the surface is covered with holes. Transfer efficiency should be at least an order of magnitude smaller than filling efficiency because even in the most favorable hole geometry (water flowing in one hole and out another) there will be some faster path for the entering water to leave than for some general parcel of water already in the package to be exchanged. This assumption is used in Section 7.3.2.

4.3.5 It is assumed for the consequence analyses that the filling efficiency is 1.0. This assumption is based on the expectation that any prolonged dripping onto a waste package would eventually corrode/erode a sufficient size hole beneath the drip to allow entry of the entire flow. This assumption is consistent with the conservative high value for this parameter defined, and justified in Section 7.3.2, and in Assumption 4.3.4, above. This assumption is used in Section 7.5.

4.3.6 It is assumed for the consequence analyses that the negative reactivity insertion resulting from moderator density reductions during heating of the water in a critical waste package will be insufficient to cause the waste package to go subcritical. The basis for this assumption is that Reference 5.16 indicates that the first 5% reduction in moderator density produces approximately a 1% reduction in k_{eff}. The moderator density reductions resulting from the temperature increases discussed in Section 7.5 are only on the order of 1%. This assumption is used in section 7.5.1.

4.3.7 It is assumed for the consequence analyses that under the appropriate conditions the waste package will gradually approach a critical condition ($k_{eff} = 1.0$), and, once criticality is achieved, the reactor period will be so large that the waste package will take several days to reach the indicated peak power level. The basis for this is that the postulated criticality scenarios occur due to slow positive reactivity insertions which are a result of gradual losses of boron and iron from the waste package interior. This assumption is used in Section 7.5.

4.3.8 It is assumed that the waste package is in the center of the drift for heat transfer calculations. The basis for this assumption is that it is conservative for this analysis and the actual placement has yet to be determined. This assumption is used in Section 7.5.

4.3.9 It is assumed for the consequence analyses that the partial pressure of water in air is that given by the saturation pressure at the water surface of the flooded WP, and that given by the absolute humidity (relative humidity * sat. pressure) at the WP surface. The basis of this assumption is that it provides a conservative estimate of the power output of a criticality in a waste package. This assumption is used in Section 7.5.

4.3.10 It is assumed for the consequence analyses that the estimated concentrations of N and Cl in the WP remain constant. The basis of this assumption is that the consumption during a criticality is calculated to be small. This assumption is used in Section 7.5.

4.3.11 It is assumed that the total neutron flux used by ORIGEN-S is within an order of magnitude of the actual flux in a critical WP. The basis for this assumption is found in Ref. 5.4. This assumption in used in Sections 4.18, and 7.5.

4.3.12 It is assumed that the water containing dissolved Fe, B, and oxygen is circulated (by convective cooling of the heat generating assembly) so that it passes in the vicinity of waste package holes through which it can overflow or otherwise exchange with the water outside the waste package. The basis for this assumption is the calculation of circulation parameters in Attachment VI, demonstrating that the Rayleigh number is above the minimum for buoyant circulation. The assumption is used in Section 7.1.1.

4.3.13 It is assumed (approximated) that carbon steel consists of 100% Fe, although it actually contains only 99% iron. The basis for this assumption is that it is conservative given that most of the remaining 1% is manganese (A516, Ref. 5.5) which is a stronger absorber of the thermal neutrons. This assumption is used in Section 7.1.1.

4.3.14 It is assumed that borated stainless steel is all Fe and B, even though borated stainless steel normally contains only 60% Fe (316B6A, Ref. 5.5). The basis for this assumption is that it is conservative given that most of the remainder is chromium, nickel, or manganese, all of which have higher thermal neutron absorption cross Sections than iron (Ref. 5.20). This assumption is used in Section 7.1.1.

4.3.15 It is assumed that the amount of Fe in solution is approximated by the maximum permitted by the solubility limit. The basis for this assumption is that the iron oxide pool is still more than several thousand times the limit (equal to fe_sol) at the time when the boron reaches very small values and the package reaches the criticality threshold, so that the solution remains saturated with iron. This assumption is used in Section 7.1.1.

4.3.16 It is assumed that the numerical integration of the differential equations can be accurately accomplished with a time step of 10 years. The basis for this assumption is that 10 years is much smaller than the typical fill times, so changes during a 10 year time period will be sufficiently small to preserve the linearity of the discrete approximation to the differential equations of the model. This assumption is used in Section 7.1.1.

4.3.17 It is assumed that the set of representative configurations selected for MCNP evaluation is representative of possible waste package degradation scenarios which could lead to internal criticality. The basis for this assumption is that they cover the range of Fe and B concentrations generated by the corrosion-dissolution-removal numerically integrated model. This assumption is used in Section 7.2.

4.3.18 It is assumed that the criticality design basis fuel (20,000 MWD/MTU burnup and 3% initial enrichment) is less stressing (lower k_{eff}) than 98% of the commercial PWR fuel. The basis for this assumption is the design basis fuel document (Ref.5.10). This assumption is used in Section 7.2.1.

4.3.19 It is assumed that the linear regression of k_{eff} as a function of the amounts of boron and iron remaining will accurately reflect the actual dependence on these parameters over the range of values of interest. More specifically, it is assumed that the two data sets fitted (one for partly oxidized/degraded borated stainless steel and the other for fully oxidized/degraded basket) are accurately reflected by two separate regression lines. The basis for this assumption is that the two individual regression fits have values of the R^2 statistic in excess of 0.9 while the linear regression of the pooled sample has R^2 only 0.54. This assumption is used in Section 7.2.

4.3.20 It is assumed that corrosion of borated stainless steel will release boron congruently, but a fraction, f, of the boron released thereby will be trapped in the solid iron oxide as it is being formed. More specifically, it is assumed that the trapping process will accurately model a more fundamental underlying process in which the boron in stainless steel is actually in the form of a boride of iron (or boride of the other metal components of stainless steel); since such borides are generally found to be very stable (as described in Ref. 5.25), the borides can be assumed to oxidize much more slowly than the iron, and will be trapped in the solid iron oxide matrix. Finally, it is assumed that the time of final release of the boron can be approximately modeled by the time of dissolution of the trapping iron oxide. The basis for the final assumption is that it is conservative. In this model it is implicit that by the time when the iron oxide is released into solution, the boride will have oxidized and dissolve also, in which case it will be quickly flushed out of the package. The alternative is that the boron would still be solid boride, in which case it could remain in place (clinging to the remaining solid iron oxide, or fuel rods) or it could fall to the bottom of the package through holes in the severely degraded basket. If the former case is true, this analysis will underestimate the criticality controlling effect of this remaining boron. If the latter case is true the effect will be approximately the same as is modeled in this study. This assumption is used in Sections 7.1.1 and 7.3.4.

4.3.21 It is assumed that the set of MCNP calculations for the completely corroded configuration, which has the remaining boron uniformly distributed throughout the waste package void space, is also a reasonable model for the boron being trapped in the solid oxide and located at the plates (or their remains in solid oxide form). The basis of this assumption is that it represents a balancing of conservative and non-conservative approximations. The conservative approximation is that the completely corroded basket has the assemblies touching, whereas, they would likely have some k_{eff} reducing separation due to the remaining solid iron oxide. The non-conservative approximation is that the uniformly distributed boron is somewhat more effective in lowering k_{eff} than the boron located on plates. This assumption is used in Section 7.2.1.

4.3.22 It is assumed that there is focusing of flow by the near-drift fracture network so that a large area of the drift (possibly spanning several waste packages) is drained onto one spot on one package. It is further assumed that this effect can be represented by a concentration factor of 4. The possibility of flow focusing is well recognized, but the specific value of concentration factor is highly speculative until actual fracture mapping from the repository horizon becomes available. The basis for this value is that it is consistent with TSPA-95 (Ref. 5.18). This assumption is used in Sections 7.3.1, 7.3.2, 7.3.4 and Section 7.5.1.

4.3.23 It is assumed that the material information from Reference 5.5 is appropriate for this analysis. The basis for this assumption is that the Reference 5.5 design analysis has been developed and approved in accordance with the applicable M&O (Management and Operating Contractor) QA procedures. This assumption is used in Section 4.1.1.

4.3.24 It is assumed that the B&W 15×15 PWR fuel assembly is an appropriate reference PWR fuel assembly for conceptual UCF development. The basis for this assumption is that the B&W 15×15 PWR fuel assembly has been established as one of the more reactive PWR fuel designs under intact fuel assembly and basket geometry conditions (Ref. 5.7). This assumption is used in Section 4.1.4 and throughout Section 7 and the attachments.

4.3.25 It is assumed that the geometry parameters from Reference 5.6 are appropriate for this analysis. The basis for this assumption is that the Reference 5.6 represents the latest information available on the AUCF WP design at the time in which this analysis was conducted. This assumption is used in Section 4.1.2.

4.3.26 It is assumed that the friction factor =0.08 for a narrow hole or crack in the bottom of the waste package which may provide a leakage path for draining the package. The basis for this assumption is that, considering the high asperity (roughness) likely for such a corrosion generated hole, the highest possible value of friction factor should be used. Reference 5.21, p. 362 indicates that this is 0.08. This assumption is used in Section 7.3.2.

4.3.27 It is assumed that once there are holes in the bottom of the waste package, the holes will not become subsequently plugged with deposits from corrosion products or other debris. The basis for this assumption is the mechanical argument that particles small enough to enter the hole will flow through it, and particles too large to enter the hole might collect at the entry, but would be large enough to permit significant flow through the interstices of such a collection. This assumption is used in Section 7.3.2.

4.3.28 It is assumed that if most of the waste package is filled with water, and there is no leakage out the bottom of the package, corrosion of the interior can be maintained only if there is sufficient circulation within the waste package. The basis for this assumption is that initial corrosion will quickly exhaust the oxygen dissolved in the original water, so without circulation and exchange of water with the environment there will be no source of oxygen to continue that process. This assumption is used in Section 7.3.3.

4.3.29 It is assumed that the hole configuration most favorable to both these exchanges (corrosion product and oxygen) has at least one hole near the top of the package and at least one hole in the waste package at a vertical displacement down from the top of the inner package wall of approximately 4.12 cm (half the distance from the upper assembly row to the package inner wall). The basis of this assumption is that such a hole configuration provides an optimum between (1) the buoyant circulation which is strengthened by increasing distance between the upper limit of the fluid and the heat source (top of the uppermost assembly) and (2) oxygen exchange which is strengthened by increasing the area of the air-water interface. This assumption is used in Section 7.3.4.

4.3.30 It is assumed that a circulation following the contours of the basket will be just as effective as a circulation moving continuously throughout the waste package. The basis for this assumption is provided by the discussion in Section 7.3.3, which is supported by calculations in Attachment VI, and will not be repeated here. This assumption is used in Section 7.3.3.

4.3.31 It is assumed that the carbon steel aqueous general corrosion rate, should range from a high value of 50 microns/yr for medium oxygen water, to a low value of 5 microns per year for low oxygen. Both these rates assume a near neutral pH. The basis for the corrosion rate assumptions is the family of curves giving corrosion rate as a function of pH given in reference 5.22. The basis of the pH assumption is that natural groundwater is nearly always near neutral, except under very special circumstances, such as intense microbial activity. Such special conditions could take place only over a small area and for a relatively short period of time, not sufficient to enhance the corrosion of a major portion of the basket. The only process which could acidify the entire waste package is radiolysis of the air immediately above the water surface to produce nitric acid, but this is expected to be insignificant, even inside the waste package.

However, the value of the carbon steel aqueous general corrosion rate used in the calculations is reduced to 1.18 microns/yr. The basis of this assumption is the limitation of available oxygen when the waste package is filled with water, as is explained in Sections 7.3.4 and 7.3.5 (where the reduced value is expressed in kg/yr). In applying this lower corrosion rate assumption, it is further assumed that any humid air corrosion which occurs before the waste package is filled with water can be neglected. The basis for this assumption is fact that humid air general corrosion rates are so low that no direct measurements have been reported. This assumption is used in Section 7.3.4.

4.3.32 It is assumed that the stainless steel aqueous general corrosion rate should range from a high value of 0.3 microns/yr to a low value of 0.1 microns per year. The basis for the high value is experimental data reported reference 5.23, pg 24 in which the highest value for 316L is for 80°C and gives a value calculated as (0.011mil/yr)*(25microns/mil)=0.28 microns/yr. The basis for the low value is the data reported in reference 5.24, p. 24, which shows approximately 0.1 microns/yr as the median of 3 values for the corrosion of 316L. This assumption is used in Section 7.3.4.

4.3.33 It is assumed that the upper limit of iron ion concentration in any waste package water should range from a high value of 0.00505 mol/liter to a low value of $8.0\text{x}10^{-5}$. The basis for this assumption is the estimation of highest possible acid normality given in Attachment IV as 0.01 equivalents/liter, and the assumption that the lowest acidity would simply be neutral. Since the J-13 well water, believed to be most typical of the repository environment, is somewhat basic (which would lead to an even lower iron ion solubility), this assumption of near neutrality is conservative. This assumption is used in Section 7.3.4.

4.3.34 It is assumed that the buildup of neutron absorbers during the course of an internal criticality will not be sufficient to reduce the k_{eff} below the criticality threshold, and thereby shut down the criticality. The basis of this assumption is that it is conservative. The assumption is used in Section 7.5.1.

4.3.35 It is assumed that airflow is stagnant in a drift at the 15,000 year-plus time frame under consideration, and evaporation can be modeled as diffusion of water vapor into air. The basis for this assumption is that there are no conceivable repository environmental processes which could agitate the air or otherwise increase the evaporation over the standard diffusion process. This assumption is used in Section 7.5.1.

4.3.36 It is assumed that in the event of a sustained criticality within a waste package, water will enter the waste package at a temperature of 30°C and will be to heated by the criticality to a temperature of 57.4°C so that the criticality maintains a steady state by evaporating as much water as is infiltrating (dripping) into the waste package. The basis for this assumption is that it is the only way for the criticality to maintain a steady state. If the power output spurts so that more water is evaporated, the resulting net loss of water will shut down the criticality. Of course, the criticality could start up again after the reactor cooled sufficiently to accumulate enough new water. However, such a pulsed operation is known to produce less total energy (and therefore less radionuclide inventory) than a steady state operation. This assumption is used in Section 7.5.1.

4.3.37 It is assumed for the consequence analyses that the WP criticality occurs when the fuel has aged/decayed for 15,000 years and will have a maximum duration of 10,000 years. The basis for the first part of this assumption is that it is the approximate time of the highest postclosure criticality potential for the PWR criticality design basis SNF (as has been demonstrated by many time-dependent k_{eff} calculations) and it is one of the earliest potential criticalities discussed in Section 7.4. The basis for the second part of this assumption is that it is the expected upper bound for the conditions supporting criticality (high infiltration, integrity of the lower part of the barrier, sufficient fissile material remaining). This assumption is used in Section 7.5.

4.3.38 It is assumed that the most likely thermal configuration for the waste package at time of criticality will be covered half-way with rubble, so that approximately half the surface area transfers heat by conduction and half transfers heat by radiation. The basis for this assumption is that rockfalls occur in mines that are in operation today, so a significant amount of rockfall might be expected by 15,000 years. This assumption is used in Section 7.5.1.

4.3.39 It is assumed that the volume of the basket is 0.873 m^3. The basis for this assumption is a calculation of the software system Pro/ENGINEER, used to design the waste package. The assumption is used to determine the volume of water in a filled waste package, which is used in Sections 7.3.3, 7.3.4, and 7.5.1.

4.3.40 It is assumed, for purposes of estimating the waste package water circulation parameters, that all the heat is transferred from the fuel rods to the waste package barrier by conduction. The basis for this assumption is that it is conservative. In actuality, the calculated circulation would provide convective cooling which would serve to lower the temperature difference, and hence lower the circulation. This assumption is used in Section 7.3.3, and in Attachment VI.

4.3.41 It is assumed that the products of corrosion from the basket materials, both carbon steel and borated stainless steel, remain in place where they may very slowly dissolve. Since the solubility of iron in water is low, the most important consequence of this assumption is that for a long period of time there will be significant amounts of corrosion products which serve the following two criticality control functions: (1) the oxidized metals remain in positions in which they can be fully effective as neutron absorbers; (2) the products of corrosion provide a substrate for trapping borides that could otherwise settle to the bottom of the package. The trapping may occur in two ways: (1) boride particles may be embedded in the corrosion products of the stainless steel; particles may settle on other components, such as the waste form or the carbon steel tube corrosion products. The basis for this assumption is that most experimental data show that the corrosion products remain on the surface of the corroding metal, frequently in the form of a hard scale. It has been suggested that it is possible, when the steel is covered with oxygen rich water, for the iron to go into solution and subsequently precipitate on adjacent surfaces away from the iron substrate; this scenario would be most likely in an acidic environment. Such precipitation would not necessarily be effective in controlling criticality, and it might not be fast enough to trap any borides. To the extent that any criticality enhancing consequences could result, the possibility of such dissolution and precipitation scenarios would make the assumption of the oxidation in place pathway non-conservative, and could significantly lower many of the earliest times to criticality calculated in this study, particularly for the acidic case, with the larger iron solubility. It is expected that current metal corrosion testing activities will resolve this issue before 1998. This assumption is used explicitly in Section 7.3.4, and is a strong determining factor of the results in Section 7.4.

4.4 Codes and Standards -

Not applicable.

5. References -

5.1 *Q-List*, YMP/90-55Q, REV 3, Yucca Mountain Site Characterization Project

5.2 Activity Evaluation, *Perform Probabilistic Waste Package Design Analyses*, Document Identifier Number (DI#): BB0000000-01717-2200-00030 REV 02, CRWMS (Civilian Radioactive Waste Management System) M&O (Management and Operating Contractor)

5.3 *Quality Assurance Requirements and Description*, DOE/RW-0333P, REV 5, Department of Energy (DOE) Office of Civilian Radioactive Waste Management (OCRWM)

5.4 *AUCF Waste Package Criticality and SAS2H Evaluations*, Interoffice Correspondence LV.WP.DAT.03/96.070, Dan Thomas, March 26, 1996, CRWMS M&O

5.5 *Material Compositions and Number Densities for Neutronics Calculations*, DI#: BBA000000-01717-0200-00002 REV 00, CRWMS M&O

5.6 *AUCF Waste Package Design (21 PWR) Tube Design*, Engineering Sketches, DI#: BBAA00000-01717-2100-16000 thru 16022 REV 00A, March 1996, CRWMS M&O

5.7 *Characteristics of Potential Repository Wastes*, DOE/RW-0184-R1, Volume 1, p. 2A-8, July 1992, DOE OCRWM

5.8 *Initial Waste Package Probabilistic Criticality Analysis: Uncanistered Fuel*, DI#: B00000000-01717-2200-00079 REV 01, CRWMS M&O

5.9 *Initial Waste Package Probabilistic Criticality Analysis: Multi-Purpose Canister With Disposal Container*, DI#: B00000000-01717-2200-00080 REV 01, CRWMS M&O

5.10 *Waste Package Design Basis Fuel Analysis,* DI#: B00000000-01717-0200-000127 REV 00A, 1996, CRWMS M&O

5.11 *Mined Geologic Disposal System Requirements Document*, DOE/RW-0404P, DI#: B00000000-00811-1708-00002 REV 01, DCN 01, DOE OCRWM

5.12 *Engineered Barrier Design Requirements Document*, YMP/CM-0024, REV 0, ICN 1, Yucca Mountain Site Characterization Project

5.13 *Waste Package Implementation Plan*, YMP/92-11Q, REV 1, Yucca Mountain Site Characterization Project

5.14 Holman, J.P., *Heat Transfer*, 7th Edition, McGraw-Hill Publishing Company, 1990

5.15 Moran, M.J., Shapiro, H.N., *Fundamentals of Engineering Thermodynamics*, John Wiley & Sons, 1988

5.16 *UCF Waste Package Criticality Analysis*, DI#: BBAA00000-01717-0200-00005 REV 00B, 1996, CRWMS M&O

5.17 *CRC Handbook of Chemistry and Physics*, 66th Edition, CRC Press, 1985

5.18 *Total System Performance Assessment - 1995: An Evaluation of the Potential Yucca Mountain Repository*, DI#: B00000000-01717-2200-00136 REV 00, CRWMS M&O

5.19 *Final Design Package, Babcock & Wilcox, BR-100 Ton Rail/Barge Spent Fuel Shipping Cask*, B&W Fuel Company, 51-1203400-01, November 1991

5.20 Lamarsh, J.R., *Introduction to Nuclear Engineering*, 2nd Edition, Addison-Wesley Publishing Company, 1983

5.21 Fox, R.W., McDonald, A.T., *Introduction to Fluid Mechanics*, 3rd Edition, John Wiley & Sons, 1985

5.22 *Corrosion Rates for Carbon Steel*, Interoffice Correspondence LV.WP.JKM.03/96.060, J.K. McCoy, March 15, 1996, CRWMS M&O

5.23 *Electrochemical Determination of The Corrosion Behavior of Candidate Alloys Proposed for Containment Of High Level Nuclear Waste in Tuff*, Lawrence Livermore National Laboratory (LLNL), UCID-20174, Livermore, CA, June 1984

5.24 *Progress Report on the Results of Testing Advanced Conceptual Design Metal Barrier Materials Under Relevant Environmental Conditions For A Tuff Repository*, LLNL, UCID-21044, December 1987

5.25 *Performance Assessment of the Direct Disposal in Unsaturated Tuff of Spent Nuclear Fuel and High-Level Waste Owned by U.S. Department of Energy*, Sandia National Laboratory, SAND94-2563/2, March 1995

5.26 *Chemical Engineers Handbook,* Third Edition, McGraw-Hill Book Company, 1950

5.27 Darken, L.S., Gurry, R.W., *Physical chemistry of Metals*, McGraw-Hill Book Company, 1953

5.28 Incropera, K.P., DeWitt, D.P., *Introduction to Heat Transfer*, John Wiley & Sons, 1985

5.29 *Engineer-in-Training Reference Manual*, Eighth Edition, Professional Publications, Inc., 1992

5.30 *Characteristics Database LWR Radiological PC Database*, Version 1.1, CSCI A00000000-02268-1200-20002, CRWMS M&O

5.31 *Emplacement Scale Thermal Evaluations of Large and Small WP Designs*, DI#: BB0000000-01717-0200-00009 REV 00, CRWMS M&O

5.32 *Waste Package/Engineered Barrier Segment Conceptual Design Report*, DI#: BBA000000-01717-5705-00006 REV 00A, 1995, CRWMS M&O

5.33 *Nuclides and Isotopes*, Fourteenth Edition, General Electric Company, 1989

5.34 *Material of 21 PWR AUCF Waste Container*, Interoffice Correspondence LV.WP.HW.03/96.059, Helen Wang, March 13, 1996, CRWMS M&O

5.35 *Pitting, Galvanic, and Long-Term Corrosion Studies on Candidate Container Alloys for the Tuff Repository*, U.S. Nuclear Regulatory Commission, NUREG/CR-5709, January 1992

5.36 *User Manual for the CDB_R*, DI#: A00000000-01717-2002-20002 REV 01, CRWMS M&O

5.37 Flint, A.L., Flint, L.E., *Spatial Distribution of Potential Near Surface Moisture Flux at Yucca Mountain*, High Level Radioactive Waste Management: Proceedings of the Fifth Annual International Conference, ANS & ASCE, pp. 2352-2358, May 1994

5.38 Long, A., Childs, S.W., *Rainfall and Net Infiltration Probabilities for Future Climate Conditions at Yucca Mountain*, High Level Radioactive Waste Management: Proceedings of the Fourth Annual International Conference, ANS & ASCE, pp. 112-121, April 1993

6. Use of Computer Software -

A. Scientific and Engineering Software:

The Characteristics Database (CDB) LWR Radiological PC Database, CSCI: A00000000-02268-1200-20002, Ver. 1.1 was used to obtain the thermal characteristics of the criticality design basis SNF. The CDB has been qualified by the Office of Civilian Radioactive Waste Management for use in work subject to the requirements of the QARD (Ref. 5.3). The CDB was installed on an IBM-compatible PC in accordance with the User Manual for the CDB_R (p. 1, Ref. 5.36) and was obtained in accordance with the QAP-SI series procedures. Use of the SNF thermal characteristics from the CDB is appropriate for this design analysis and is within the range of validation performed for the CDB. The data extracted from the CDB are given in Table 4.1-6 and are used in Attachment VII.

B. Computational Support Software:

6.1 MathCad v5.0+, loaded on a 66MHz 486 PC.

6.2 Microsoft Excel v5.0, loaded on a 66MHz 486 PC.

6.3 Pro/ENGINEER Release 15.0, loaded on an HP 9000 /735, used for computer aided design of the waste package.

6.4 Microsoft Visual C++ compiler, version 1.0, loaded on a 66MHz 486 PC used as computational support software with Excel or MathCad checking to verify the algorithms used.

deltasd.c	Deterministic accounting of boron (steel and dissolved oxide) and iron (steel and solid oxide, with the dissolved oxide always equal to saturation which is much smaller than the other phases until the very end). The package is assumed to be filled with water and is cyclically flushed at periods which can range from 5 years to 5,000 years. The filling of the package can be delayed by a specified time, thereby permitting corrosion to proceed by humid air, but delaying removal of any absorbers released by the humid air corrosion process. This program is included as Attachment I, together with sample inputs and outputs.
leak.c	Deterministic calculation of the rate at which water can drain from typical holes in the bottom of the waste package. This program starts with the waste package containing water to some height and then proceeds to drain through holes in the bottom. At first the flow through the holes is turbulent because of the pressure from the

head, but after most of the package has drained, the flow becomes laminar. This program is included as Attachment V, together with sample input and output.

7. Design Analysis -

This design analysis is presented in five sections. Section 7.1 explains the methodology for generating parameters of degraded modes as a function of time and degradation process rates. Section 7.2 describes the methodology for mapping the principal degradation mode parameters, boron and iron concentrations, into values of k_{eff} for the waste package. Section 7.3 analyzes the preconditions necessary for criticality (in addition to the degradation mode parameters, boron and iron concentration considered in sections 7.1 and 7.2), and identifies the environmental parameters which determine degradation process rates, and which are used as inputs to the calculations. Section 7.4 presents the results of calculation of earliest times to criticality, using the degradation mode generating methodology and the range of inputs defined in the previous sections, and assuming the existence of all the necessary preconditions, particularly the unlikely condition of the waste package filling and remaining filled with water. Section 7.5 presents the consequences of a criticality, in terms of increased radionuclide inventory, assuming that a criticality does occur.

7.1 Determination of Degraded modes

The degradation of the waste package interior begins with corrosive attack from a humid and/or aqueous environment containing oxygen. Since the waste package is sealed with an inert interior atmosphere, the corrosion process cannot start until the waste package barriers have been breached. The time of breach depends on the rate of corrosion of the waste package barriers. This process has been modeled in other studies, with first penetration times ranging from 2000 years to 5000 years with very conservative models which have relatively rapid corrosion (Ref. 5.18). This study will not include the value of this time explicitly, because it turns out to be much less than the times required to remove neutron absorbers from the package in sufficient quantity to permit a criticality.

7.1.1 Model of degradation processes and the configuration generator

The waste package interior degradation model solves the coupled first order differential equations which connect the concentrations of iron and boron in the three phases: steel, oxide, and in solution. The model follows directly from the standard interpretation of chemical processes in terms of first order, time dependent linear differential equations. The assumptions concern the values of the coefficients of the model, and these assumptions are listed in Section 4.3 and discussed in the narrative of this study as appropriate.

Corrosion of borated stainless steel is assumed to release boron congruently, but a fraction, f, of the boron released thereby is assumed to be trapped in the solid iron oxide as it is being formed. This is a reasonable assumption since the boron in the stainless steel is in the form of a boride of iron, or other metal component of stainless steel, and such borides are generally found to be very stable. In this study a range of values will be used for f, all well under 0.1.

The model assumes that the water containing dissolved Fe, B, and oxygen is circulated (by convective cooling of the heat generating assembly) so that it passes in the vicinity of waste package holes through which it can overflow or otherwise exchange with the water outside the waste package. The result of this circulatory exchange is the removal of the neutron absorbing corrosion products and the replenishing of the oxygen supply to support further corrosion. The principal processes, and the differential equations describing their time dependence and coupling, are as follows:

Carbon steel change:

dm_{fec}/dt = - c_rate_cs; provided $m_{fec}>0$.

Stainless steel change:

dm_{fes}/dt = - c_rate_ss*(1-alph); provided $m_{fes}>0$.

Iron oxide change:

dm_{feo}/dt = c_rate_ss + c_rate_cs - ex_rate*fe_sol;

in which the first and second terms on the right side are included if the mass of stainless steel and the mass of carbon steel are greater than zero, respectively.

Boron in stainless steel change:

dm_{bs}/dt= -c_rate_ss*alph; provided $m_{bs}>0$.

Boron trapped in the solid iron oxide change:

dm_{bot}/dt= f*c_rate_ss*alph - ex_rate*fe_sol*m_{bot}/m_{feo} ;

in which the last term on the right side represents the trapped boron released to solution as the iron oxide is permitted to go into solution to replace the amount which was exchanged.

Boron in solution change:

dm_{bosol}/dt = (1-f)*c_rate_ss*alph + ex_rate*fe_sol*m_{bot}/m_{feo} - ex_rate*m_{bosol} ;

in which the first term on the right side is included only if the mass of stainless steel is greater than 0, and the second term is the same as the second term of the previous equation but with opposite sign.

The following symbols have been used:

m_{fec}	Mass of the remaining carbon steel (conservatively assumed to be 100% Fe, although actually only 99% iron, because most of the remainder is manganese which has a higher neutron absorption cross section than iron; the carbon content, from which the steel gets its name is only 0.2%, A516, Ref. 5.5).
m_{fes}	Mass of the metallic fraction of the remaining borated stainless steel (conservatively assumed to be all Fe, because most of the remainder is chromium, nickel, or manganese,

all of which have higher neutron absorption cross section than iron, 316B6A, Ref. 5.5).

m_{feo}	Mass of iron as iron oxide not in solution (corrosion product of both the carbon steel and the stainless steel).
m_{bs}	Mass of boron in the remaining stainless steel.
m_{bosol}	Mass of boron oxide in solution.
m_{boi}	Mass of boron trapped in the solid iron oxide.
c_rate_cs	Corrosion rate of carbon steel (kg/yr).
c_rate_ss	Corrosion rate of borated stainless steel (kg/yr).
ex_rate	Exchange rate between the water in the waste package and the water in the immediate environment (per/yr).
f	Fraction of the boron being trapped in the oxide of the stainless steel being oxidized.
alph	Fraction of boron in stainless steel (used to compute the amount of boron going into solution as the stainless steel is oxidized).
fe_sol	The amount of Fe ion in solution at any given time, approximated by a constant equal to the maximum permitted by the solubility limit (kg).

It will be noted that the five differential equations do not include specific accounting for the iron oxide in solution or the boron oxide not in solution. As indicated in the definition of fe_sol, above, the amount of Fe in solution is approximated by the maximum permitted by the solubility limit. This assumption (approximation) is justified by the fact that the iron oxide pool is still more than several thousand times the fe_sol at the time when the boron reaches very small values and the package reaches the criticality threshold, so that the solution remains saturated with iron, as will be shown in the discussion of calculation results, below.

The model is implemented by the simple program "deltasd.c", the annotated listing of which is given in Attachment I. This implementation uses numerical integration of the differential equations with a time step of 10 years, which is assumed to be much shorter than the reciprocal of the exchange rate, so that the concentrations of absorber change little during the time step. The proper implementation of the algorithms is checked by MathCad. The model is intended to serve as a generator of configurations which represent the criticality potential of all the possible internally degraded states of the waste package.

In the exercises with this model the initial basket steel masses are fixed at the current design values, and the corrosion and exchange rates are varied over the range of physically possible values.

7.2 Estimation of k_{eff}

The evaluation of the criticality of the various generated configurations is determined by their k_{eff}. Since a separate neutronics code calculation for each configuration would be impractical, a set of representative configurations was selected and evaluated with MCNP, assuming the waste package filled with the design basis fuel for criticality (initial enrichment 3% and burnup 20,000 MWd/MTU, Ref. 5.4 and 5.10).

The selected configurations are defined by discrete values of neutron absorber amounts remaining inside the waste package, and the amount of basket material which remains to provide a certain amount of k_{eff} reducing interassembly spacing. In order to evaluate the continuous range of these parameters presented by the results of the model runs, the discrete MCNP configurations were abstracted by a tri-variate regression, which was then used to identify the stage in the degradation when k_{eff} exceeds 0.91, or the earliest time at which the waste package can go critical. The use of a k_{eff} of 0.91 to define criticality, rather than 1.0, is conservative and is based on the 5% margin of safety and the expected bias and uncertainty of the MCNP calculations, as required by EBDRD, Ref. 5.12. It is assumed that the dependence will be linear over the range of parameters of interest. The individual MCNP results, and the regression developed from them, are described in the following Sections.

7.2.1 MCNP calculations of k_{eff}

Of the discrete degraded mode configurations, two sets were found to be most relevant to this study. The k_{eff} calculations are reproduced from reference 5.4 as the two tables in Section 4.1.3.1. These values of k_{eff} are given as a function of percentages which must be converted into mass of boron and iron to be useful in the present model. These conversions are given in Attachment VIII. The results are presented in the tables below. In addition, a few of the lines from the tables of 4.1.3.1 are not used in the regression in order to limit the range of the dependent variables, iron and boron mass, to those expected to be encountered in an actual waste package under conditions which can cause criticality. This limitation will assure an optimum linear regression by minimizing the effect of any nonlinear variations. The specific reasons for the eliminations are stated in connection with the tables individually, below.

(1) The borated stainless steel has partially corroded, releasing oxides, with most of the boron oxides dissolving almost immediately after creation because of their high solubility, so that the relevant parameters are the oxide concentration. Although MCNP calculations did not explicitly model the trapped boron fraction, f, it is assumed that the results will be relatively insensitive to whether this small amount of boron is at the position initially occupied by the borated stainless steel plates or uniformly distributed throughout the package void space, as is assumed in the MCNP calculations. Table 7.2-1 below is

derived from Table 4.1-3, where the first line of the original table has been omitted because the low solubility of iron prevents the removal of all the corrosion product of the carbon steel before most of the stainless steel has been corroded. In this table, the iron mass is the sum of the iron in the remaining uncorroded stainless steel plus the undissolved oxide, and the only boron is that remaining in the uncorroded stainless steel.

Table 7.2-1. Partial Basket Degradation

kg Fe	kg B	k_{eff}
929	15.24	0.917
2978	15.24	0.851
4608	7.618	0.857
3572	7.618	0.880
5399	3.05	0.887
4392	3.05	0.908
2271	3.05	0.944

(2) The borated stainless steel is fully corroded, with only small amounts of boron remaining but with larger amounts of iron oxide remaining. This models the very rapid removal of B compared with iron caused by its much larger solubility in water. The MCNP calculations of reference 5.4 modeled this configuration set with both the Fe and B uniformly distributed throughout the package void space. It is assumed that the k_{eff} calculated is a conservative approximation to the values which would be obtained by a more explicit model with some specific fraction of the Fe and B remaining in solid form at the initial location of the basket. Table 7.2-2 below is derived from Table 4.1-4, where the first line is eliminated because the zero concentration of both absorbers is far beyond the limit of a linear regression (as is the resulting large k_{eff}). The two lines with 20% Fe_2O_3 and the two values of B-10 25% and 100% are eliminated because the resulting values of k_{eff} are far below any possible range of linearity.

Table 7.2-2. Assemblies Touching

kg Fe	kg B	k_{eff}
6283	0.0	0.928
6283	0.6	0.913
6283	1.5	0.890
4188	0.0	0.979
4188	1.5	0.941
4188	3.05	0.902
4188	4.57	0.872
2094	3.05	0.947
2094	4.57	0.909
2094	6.1	0.879

Both these sets also assumed that the carbon steel had already corroded by the time of the stated stainless steel corrosion, with the corrosion products contributing to the reservoir of iron oxide which is uniformly distributed throughout the water in the waste package.

7.2.2 Regression analysis of the data

The regression lines for these data sets are given by the following equations (where Fe is in metric tons and B is in kilograms):

Partial basket (7 data points):

$k=1.026 - 0.0242*Fe - 0.00645*B, R^2=0.91$

Assemblies touching (10 data points):

$k=1.068 - 0.0221*Fe - 0.0236*B, R^2=0.99$

Pooled data sets (17 data points):

$k=0.989 - 0.0132*Fe - 0.00679*B, R^2=0.54.$

The calculations are described in Attachment III.

It should be noted that the partial basket regression implicitly incorporates the effect of decreasing basket thickness, which is generally proportional to the explicitly decreasing amounts of boron and iron.

The fact that the pooled data set has such a small R^2 indicates that the two sets represent somewhat different physical processes, which is consistent with the fact that the partial basket variation incorporates the effect of varying assembly spacing, while the assemblies touching case does not. This distinction will be reflected in the calculations of earliest time to criticality. In those calculations (presented in Section 7.4.1) the boron and iron concentrations are decreased at each time step to reflect the corrosion and removal process, and at each time step the k_{eff} is calculated as a function of the remaining boron and iron, using the partially degraded regression while the stainless steel is still intact and the assemblies touching regression after the stainless steel has all corroded.

7.3 Evaluation of preconditions and inputs

The criticality evaluations presented in this study begin with the assumed occurrence of certain necessary preconditions. These preconditions are summarized in Section 7.3.1, with their probability of occurrence simply restated from References 5.8 and 5.9. Principal among these preconditions are the filling of the waste package with water, and the waste package remaining filled. The possible mechanisms for this process are discussed in Section 7.3.2, without presenting any probabilities.

The principal conditions required to sustain the corrosion and removal of the neutron absorbers are assumed to be an adequate oxygen supply and sufficient exchange of water. The adequacy of these processes is discussed in Section 7.3.3.

Design inputs and assumptions, documented in Sections 4.1 and 4.3, respectively, are used to compute the specific design inputs, as described in Section 7.3.4

7.3.1 Preconditions for criticality

This section provides a discussion of the major precondition requirements for the occurrence of a criticality, and the probabilities of the occurrence of these preconditions. The actual calculation of the probability of occurrence of a criticality is beyond the scope of this analysis, because of the present uncertainty of some of the most important probabilities.

The following precondition requirements reduce the probability of a criticality in a manner which can be estimated since they are determined by conditions existing at time of emplacement:

- Focusing of the infiltration flow by a fracture network so that a large area above the drift (possibly spanning several waste packages) is drained onto one spot on one package, thereby accelerating corrosion in that spot and facilitating the filling of the waste package through the resulting penetration. The analysis of this process in the IPA lead to the estimation of the probability of such a fracture flow contacting a given waste package as 0.075. However, that analysis was based on fracture and flow data from a saturated site in totally different geology. It was expected that actual fracture data from the ESF would be available for this analysis. That data is expected to be released shortly, but not in time for this analysis.

- The criticality design basis fuel used for the k_{eff} analysis is assumed to be more stressing than 98% of the fuel (reference 5.10), so there is at most a 0.02 probability of a commercial waste package being able to go critical at the earliest times specified by this study. If the amounts of neutron absorber are reduced still further after this earliest time then more of the fuel is able to go critical at later times.

The following precondition is quite unlikely. Therefore, its requirement will greatly reduce the probability of a criticality.

- Waste package remains filled (absence of holes in the bottom of the package) for a sufficiently long time after penetration of the waste package barriers (assumed to be from the top) to remove corrosion products and sustain criticality.

The estimation of the probability of occurrence of this precondition may be unreliable because of the lack of precise information on corrosion mechanisms and rates for corrosion resistant metals, such as Alloy 625, which is presently designated as the material for the waste package inner barrier. Therefore, for this analysis, it will be assumed that a waste package configuration with penetrations in the upper half of the barrier, but no penetrations in the lower half of the barrier can occur. It is recognized that this is a very conservative assumption, and the basis for the assumption is given in Assumption 4.3.1. It is expected that ongoing corrosion testing programs will provide more precise information on corrosion resistant metals so that by 1997 it will be possible to make reliable probability estimates. At that time the probabilities of these three preconditions will provide the basis for a reliable estimate of the upper bound for the probability that any package will go critical.

7.3.2 Evaluation of Processes for Filling the WP with Water and Remaining Filled

The purpose of this section is to estimate the range of possible waste package filling and draining times, in order to understand whether there can be any dynamic balance between filling and draining which would support a waste package filled with water once the bottom has been penetrated to permit some draining. The conclusion, given at the end of this section is that there cannot.

Package filling

The range of filling rates is calculated according to the formula

Filling rate = id*il*eff*dripr*cf/1000,

where the following definitions apply,

id: Inside diameter of the waste package, in meters,
il: Inside length of the waste package, in meters,
eff: Filling efficiency, which is the fraction of the water impinging on the waste package which actually gets into the package,
dripr: Drip rate in mm/yr, related to the more commonly referred to infiltration rate according to a scheme presented in TSPA-95 with details of the application to this study in Attachment VII,
cf: Concentration factor, degree of focusing, from the drift ceiling to the package surface.

and where the factor of 1000 converts the input drip rate from millimeters to meters, so that the filling rate is in m^3/yr.

The filling time is given by the package interior void space volume divided by the filling rate. Potential losses due to evaporation are not considered. This is a conservative approximation, as explained in Assumption 4.3.3. This calculation is presented in Attachment VII.

For this analysis, the waste package design parameters id=1.42 m, il=4.67 m, void space volume=4.84 m^3 are used. A concentration factor of 4 is assumed, and a range of infiltration rates and filling efficiencies are used to determine the filling times. Since the present-day infiltration rates are believed to range from 0.02 mm/yr (vertical infiltration only) to 1 mm/yr (significant lateral flow from the north) (Ref. 5.37 and 5.18), the higher infiltration rates are unlikely in the near future, but their likelihood may increase with time as a consequence of climate change; hence, it will be assumed that increasing infiltration rates are associated with increasing time horizons. The transfer efficiency is a function of the amount of corrosion of the waste package, and is therefore also assumed to increase with time. Reasonable values for the time associations are given in the following table of filling times.

Table 7.3-1. Range of Possible Filling Times (years)

Flow Rate (Drip, Infil) in mm/yr	Filling efficiency		
	1.0 (>100,000 yrs)	0.1 (>50,000 yrs)	0.01 (>10,000 yrs)
0.0004, 0.01	$4.56x10^5$	$4.56x10^6$	$4.56x10^7$
0.03, 0.1	$6.02x10^3$	$6.02x10^4$	$6.02x10^5$
0.53, 1.0	$3.44x10^2$	$3.44x10^3$	$3.44x10^4$
7.19, 10	$2.54x10^1$	$2.54x10^2$	$2.54x10^3$

Package draining

The purpose of this part of the analysis is to estimate the range of times which would be required to drain the waste package once there had been some small penetration near the bottom of the package.

The method of analysis is to apply laminar and turbulent flow rate formulas to flow through narrow holes (or tubes) having a range of diameters and lengths (since we do not know the dimensions of the holes which will actually penetrate the waste package bottom). The time to empty is determined by numerically summing the increments of water level decrease multiplied by the water surface area (in the waste package) and divided by the calculated flow rate using the program "leak.c". The value of flow rate used to calculate each time increment is taken as the lower of the values calculated by the laminar and turbulent flow formulas. This is conservative, since it provides the longest estimate of drain time. The equations used are as follows:

Turbulent volumetric flow:
$qturb=2*\pi*r^2sqrt(g*h*r/f_r/l)$ (derived from Ref. 5.21 as described in Attachment V)

Laminar volumetric flow:
$qlam=\pi*r^4*\rho*((h/l)+1.0)/8/\mu;$

Incrementing time (time increment corresponding to the distance integration step, dh)
$\text{Time increment}=2*\alpha*il*sqrt(rp^2-(rp-h)^2)*dh/q;$

with the following parameter definitions:

l	Length of the narrow portion of the hole (which will generally be significantly less than the thickness of the package wall)
r	Radius of the narrow portion of the hole
rp	Inner radius of the package
g	Acceleration due to gravity
il	Inside length of the waste package
q	Lesser of qturb, qlam
f_r	Friction factor (conservatively assumed to be 0.08, Ref. 5.21, p. 362)
ρ	Density of water
μ	Viscosity of water
α	Fraction of the waste package interior which can be occupied by water (void space, 0.653)

and the time increments are summed from h=1.4 meters (slightly less than the largest water depth possible, 1.422 meters; see assumption 4.3.40) to h=0, the bottom of the package, decreasing h by dh at each step.

The high and low values are summarized in Table 7.3-2 below. Inputs and outputs are given in Attachment V.

Table 7.3-2. Waste Package Drainage Times

Parameter	High rate	Low rate
Hole diameter	0.4 mm	0.1 mm
Hole length	2 mm	1 mm
Drain time	1.02 yrs	133 yrs

If there many holes in the package bottom, the single hole leak rate would have to be multiplied accordingly.

It should be noted that the high aspect ratio hole is also the one most likely to plug, although we have no quantitative analysis of the process at this time.

Since the waste package drainage times are generally much shorter than the filling times, it will be assumed that the very unlikely plugging has not occurred so that the package cannot maintain a filled condition once the bottom has been penetrated to permit draining.

7.3.3 Estimate of the Adequacy of Processes Supporting Corrosion and Corrosion Product Removal

The results presented in this subsection are not used as direct inputs to the calculations of the earliest time to criticality. They are used only to demonstrate the adequacy of certain processes which support the corrosion process. For this reason the formulae, references, and calculation details are given in Attachment VI, and only the results are presented here. The basic technical assumption is that if the most of the waste package is filled with water, corrosion can be maintained only if there is sufficient circulation within the waste package to support exchange with the environment of:

- Corrosion products (which requires a liquid exchange interface)
- Oxygen (which requires an air interface)

It will be assumed that the hole configuration most favorable to both these exchanges has at least one hole near the top of the package and at least one hole in the waste package at a vertical displacement down from the top of the inner package wall of approximately 4.12 cm (half the distance from the upper assembly row to the package inner wall). This hole configuration provides an optimum between (1) the buoyant circulation which is strengthened by increasing distance between the upper limit of the fluid and the heat source (top of the uppermost assembly) and (2) oxygen exchange which is strengthened by increasing the area of the air-water interface. Such a hole configuration also permits the most efficient water exchange between a filled package and its environment: water flowing in the topmost hole, and flowing out at the upper surface of the water.

The above described fluid/fuel geometry is used as the basis for the calculation of: (1) temperature difference driving the circulation, (2) Rayleigh number characterizing the circulation, and (3) circulation time. The formulae and calculations are presented in Attachment VI. Since the driving temperature difference and the resulting circulation are strong functions of the heat generation by the SNF, and since that heat generation decreases with time, these parameters have been calculated for representative times as given in Table 7.3-3 below. The values of ΔT and, hence, Rayleigh number have been calculated under the assumption that all of the heat transfer is by conduction. This is conservative, as is explained in Assumption 4.3.40

Table 7.3-3. Results of WP Circulation and Oxygen Supply Calculations

Time (yrs)	ΔT (°C)	Rayleigh Num	Circ time (sec)	O_2 exchg (kg/yr)
5000	1.32×10^{-1}	2.55×10^{5}	2.73×10^{3}	0.709
10000	9.88×10^{-2}	1.91×10^{5}	2.93×10^{3}	0.684
20000	6.17×10^{-2}	1.20×10^{5}	3.30×10^{3}	0.645
50000	2.36×10^{-2}	4.58×10^{4}	4.20×10^{3}	0.572
100000	8.25×10^{-3}	1.60×10^{4}	5.46×10^{3}	0.501

As expected, the parameters of circulation get weaker with increasing time. However, even the weakest in the table (for 100,000 years) is more than adequate, with Rayleigh number well above the threshold of 1708 and circulation time less than one day.

If the highest value of oxygen exchange rate In Table 7.3-3 is converted to iron oxidation capability, at the stoichiometric ratio of (2*55.8/3/16), the result is sufficient to oxidize no more than 1.65 kg/yr of iron. This limit will be used in the adjustment of the carbon steel corrosion rate as described in Section 7.3.4 below.

Since the Rayleigh number is proportional to the fourth power of the scale length involved in the circulation process (as is shown by the formulas for Ra and ΔT in Attachment VI) , a circulation throughout the waste package (in contrast to the top 8 cm used in the above calculation) would be much stronger. However, the basket serves as a baffle inhibiting such a large scale circulation. It might even be suggested that this inhibiting effect is large enough to significantly reduce the amount of oxygen in the lower portions of the basket and thereby greatly inhibit corrosion; this could reduce the effective corrosion rate by a factor of 10 (a factor of 5 for the number of layers in the waste package and a factor of 2 because the corrosion would be only on one side at a time of a basket plate). However, the following heuristic argument casts doubt on such an extreme concept: (1) there will certainly be as much hole area corroded in the major basket plates as in the much thicker waste package upper barrier; (2) water will be flowing past such holes in adjacent layers and will have opportunity to exchange oxygen and corrosion products; (3) an estimate of the water circulation velocity driven only by the small driving ΔT present at the end of 100,000 years is more than 6 meters/day, as shown in Attachment VI, and is consistent with package transverse dimension and the circulation time in the above table). It is, therefore, assumed that a circulation following the contours of the basket will be just as effective as a circulation moving continuously throughout the waste package.

7.3.4 Input data

Carbon steel aqueous general corrosion rate: (Ref. 5.22)

- High value in medium oxygen water: 50 microns/yr
- Low value in low oxygen water: 5 microns/yr

To convert to kg/yr multiply by :

- 7830 density of carbon steel in kg/m^3
- 178 surface area of carbon steel tubes in m^2 (Attachment VIII)
- 10^{-6} meters/micron

This process gives a high value of 69.7 kg/yr and a low value of 6.97 kg/yr. Since it has been shown in the discussion following table 7.3-3 that the maximum oxygen exchange rate can oxidize no more than 1.65 kg of Fe per year, these estimates must be adjusted downward. As a conservative approximation, this study will use only the limiting value of 1.65 kg/yr.

Stainless steel aqueous general corrosion rate:

- High value measured near 100°C: 0.3 microns/yr (Ref. 5.23, pg 24)
- Low value measured near 28°C: 0.1 microns/yr (Ref. 5.24, pg 24)

To convert to kg/yr multiply by:

- 7770 density of stainless steel in kg/m^3
- 70 surface area of stainless steel plate in m^2 (Attachment VIII)
- 10^{-6} meters/micron

This process gives a high value of 0.163 kg/yr and a low value of 0.0544 kg/yr. Both are well below the 1.65 kg/yr upper limit supportable by the oxygen exchange rate, so they will be used for the calculations. This approximation is conservative, since the upper limit must be shared between the carbon steel and the stainless steel, so the actual rates should be lower.

Flush/exchange rate:

The water in the package will be flushed much faster if there are holes in the bottom. However, it is extremely unlikely that holes in the package bottom could be subsequently plugged to support filling the package with water, as is required for any criticality. Therefore, the flush rate is calculated under the assumption that the principal physical mechanism is exchange of water through holes near the top of the package. It is recognized that this is not conservative with respect to corrosion rates; however, with our present understanding of the effectiveness of hole plugging, it is the only mechanism for producing criticality.

Multiply the following:

- Drip rate (high 7.19 mm/yr, medium 0.53 mm/yr, low 0.03 mm/yr), derived in Attachment VII.
- Efficiency of exchange through holes in the top of the package (high 0.1, medium 0.01, low 0.001); note that the exchange efficiency values are an order of magnitude smaller than the filling efficiency discussed in Section 7.3.3; this distinction is justified in the discussion of assumption 4.3.4 given in Section 4.3
- Concentration factor (4)
- Waste package area projected on a horizontal plane (6.63 m^2) (Attachment VII)

Divide by:

- Waste package void volume (4.84 m^3) (Attachment VIII)

The 4 possible combinations of the high and medium values of drip rate and exchange efficiency give the 4 exchange rate values 0.00394, 0.000291, 0.000394, 0.0000291. These are all used in the calculations of Section 7.4.1, below, but they are tracked according to the individual drip rate and exchange efficiency values, so they will be presented that way in the input summary Table 7.3-4.

Upper limit of dissolved iron in the waste package filled with water:

- High value 0.00505 mole/liter, more acidic environment than is likely to be produced by radiolysis in the waste package,
- Low value 8.0×10^{-5} mole/liter, for neutral water

To convert to total kg in the waste package solution multiply by:

- 55.8 molecular weight of iron (gm/mole)
- 4.84 cubic meters of water in the waste package.

High result: 1.33 kg; Low result: 0.021 kg

Boron fraction trapped in solid iron oxide:

There has been virtually no quantitative investigation of this phenomenon, neither theoretical nor experimental. It is therefore appropriate to try a range of values to test the sensitivity to this parameter. It will be seen that the range 0.02 to 0.05 shows a large variation in the effect on earliest possible time of criticality, so these two values will represent the low and high values of the parameter f. Since f is the only parameter for which increasing values act to decrease k_{eff}, the value 0.02 will be referred to as the high value, and 0.05 will be considered the low value. Of course the actual values could turn out to be outside this rather narrow range after all.

These input parameters are summarized in Table 7.3-4 below.

Table 7.3-4. Summary of Input Parameters

Parameter	High	Low
Dissolved Fe upper limit (kg)	1.33	0.021
Stainless steel corrosion rate (kg/yr)	0.163	0.0544
Trapped B fraction, f	0.02.	0.05
Exchange efficiency	0.1	0.01*
Drip rate (mm/yr)	7.19	0.53*

* These values correspond to the medium values given in the analysis above; they are given here because they are the ones which will be used as the basis for the variations for the calculations of Section 7.4.1.

Although the temperature dependence of the above parameters could have been explicitly modeled, as was done to some degree in IPA, a constant temperature approximation has been used for this analysis. This is justified because the temperature change is small over the period of interest and the resulting parameter changes would be smaller than the ranges covered above.

7.4 Calculation of Results (time of earliest possible criticality)

Calculations varying all the input parameters showed the time to earliest possible criticality to be very sensitive to five of the parameters presented in Table 7.3-4: (1) dissolved iron limit, (2) the stainless steel corrosion rate, (3) the fraction of boron trapped in the solid iron oxide, (4) the exchange efficiency, (5) the drip rate.

The results are relatively insensitive to the carbon steel corrosion rate (since even the low corrosion rate has all the carbon steel oxidized within 10,000 years), so only the high value given in Section 7.3.4 will be used, to demonstrate conservatism.

The results are found to be extremely sensitive to trapped boron fraction if the dissolved iron limit is low. This is demonstrated by the alternative calculations with only a slightly larger range for the trapped boron fraction, presented in Section 7.4.2.

The calculation inputs and outputs are given in Attachment II.

7.4.1 Calculation of Earliest Time to Criticality

The calculations generally show the greatest sensitivity to the corrosion rate of borated stainless steel, so all calculations are presented for both high and low values of this parameter. The dependence on the other four parameters is demonstrated with two combination sets. For the first combination set four configurations are generated by selecting one parameter at a time to have its high value with the other three parameters having their low values. The results are given in Table 7.4-1. For the second combination set, six configurations are generated by selecting two parameters at a time to have high values, with the other two parameters having low values. The results are given in Table 7.4-2. It should be noted that the trapped boron fraction, f, is the only parameter which is negatively correlated with criticality, so its lower numerical value is actually its high value, as was indicated in Table 7.3-4.

The following observations on the results presented in Tables 7.4-1 and 7.4-2 are of interest:

- For all of the cases the remaining iron oxide is in excess of 5,300 kg, which is nearly all the iron in the intact basket. The boron remaining is less than 2 kg, which means that most of it has been removed. This is a consequence of the Fe solution limit, which keeps most of the iron in solid oxide, even at the high exchange rate.

- Under the worst case conditions: (1) waste package filling with water and remaining filled for tens of thousands of years (Assumption 4.3.1), (2) high value for both the drip rate (7.19 mm/yr, which is two orders of magnitude above the present value), and (3) high value for the exchange rate, the smallest time to criticality can be, 12,000 years following penetration of the waste package barriers. The simultaneous occurrence of these three conditions should be considered extremely unlikely.

Table 7.4-1. Times to earliest possible criticality with one parameter high

SS Corrosion rate (kg/yr)	Drip rate (mm/yr)	Exchange efficiency	f, Trapped boron fraction	Fe sol limit (kg)	High parameter	Earliest time to criticality (yr)
0.0544	0.53	0.01	0.02	0.021	f	1.35×10^5
0.163	0.53	0.01	0.02	0.021	f	1.22×10^5
0.0544	0.53	0.01	0.05	1.33	Fe sol	2.06×10^5
0.163	0.53	0.01	0.05	1.33	Fe sol	1.92×10^5
0.0544	7.19	0.01	0.05	0.021	Drip rate	4.21×10^4
0.163	7.19	0.01	0.05	0.021	Drip rate	2.16×10^4
0.0544	0.53	0.1	0.05	0.021	Exchg	4.58×10^4
0.163	0.53	0.1	0.05	0.021	Exchg	2.61×10^4

Table 7.4-2. Times to earliest possible criticality with two parameters high

SS Corrosion rate (kg/yr)	Drip rate (mm/yr)	Exchange efficiency	f, Trapped boron fraction	Fe sol limit (kg)	High parameters	Earliest time to criticality (yr)
0.0544	0.53	0.01	0.02	1.33	f, Fe sol	1.35×10^5
0.163	0.53	0.01	0.02	1.33	f, Fe sol	1.22×10^5
0.0544	7.19	0.01	0.02	0.021	f, Drip rate	3.67×10^4
0.163	7.19	0.01	0.02	0.021	f, Drip rate	1.62×10^4
0.0544	0.53	0.1	0.02	0.021	f, Exchg	3.84×10^4
0.163	0.53	0.1	0.02	0.021	f, Exchg	1.89×10^4
0.0544	7.19	0.01	0.05	1.33	Fe, Drip rate	4.16×10^4
0.163	7.19	0.01	0.05	1.33	Fe, Drip rate	2.14×10^4
0.0544	0.53	0.1	0.05	1.33	Fe, Exchg	4.53×10^4
0.163	0.53	0.1	0.05	1.33	Fe, Exchg	2.58×10^4
0.0544	7.19	0.1	0.05	0.021	Dr, Exchg	2.85×10^4
0.163	7.19	0.1	0.05	0.021	Dr, Exchg	1.20×10^4

- Although not directly apparent, some significant effect of lowering the Fe solubility limit when the trapped boron fraction is large can be inferred by comparing the last 2 lines of table 7.4.2 with the 2 lines immediately above. Comparing the times for the same stainless steel corrosion rates there is seen to be only a 50% decrease while increasing the drip rate by more than an order of magnitude. This limitation to a small decrease is due to the large decrease in the iron solubility limit (going from 1.33 kg to 0.021 kg) which keeps a significant amount of boron trapped in the oxide. This behavior is in contrast with the same change in parameters going from the first 2 lines of the table to the third and fourth lines. In this comparison the decrease is approximately an order of magnitude. The fundamental difference is that the trapped boron is very low so lowering the Fe solubility limit to slow the removal of the oxide has little effect. The influence of Fe solubility limit is more strongly demonstrated in the sensitivity study in the next Section.

7.4.2 Sensitivity Analysis: Extending the Range of the Trapped Boron Fraction

Increasing the value of trapped boron fraction only slightly above 0.05 will markedly increase the earliest time to criticality. With the same configuration selection scheme as was used for Tables 7.4-1 and 7.4-2, above, the range of values is changed to 0 to 0.055. The results are presented in Tables 7.4-3 and 7.4-4, below.

The following observations on the sensitivity results presented in Tables 7.4-3 and 7.4-4 are of interest:

- The earliest times to criticality for the f=0 cases show only a small decrease compared with the corresponding f=0.02 cases in Tables 7.3-1 and 7.3-2, indicating that f=0.02 does not trap enough boron in the oxide to prevent criticality.

- The last 4 lines of Table 7.4-3 show the striking effect of lowering the Fe solubility limit when the trapped boron fraction exceeds a threshold. This is in contrast with the first 2 lines of the table which also have the lower value of Fe solubility, but the trapped boron fraction is zero so there is little effect.

- Comparison of the last 2 lines in Table 7.4-4 with the 2 lines immediately above shows that only a slight change from f=0.050 to f=0.055 has reversed the relative dominance of drip rate and Fe solubility limit. Instead of a 50% decrease in earliest time to criticality when going from high Fe solubility limit and low drip rate to low Fe solubility limit and high drip rate, Table 7.4-4 shows nearly a 100% increase.

Table 7.4-3. Sensitivity to trapped boron fraction with one parameter high

SS Corrosion rate (kg/yr)	Drip rate (mm/yr)	Exchange efficiency	f, Trapped boron fraction	Fe sol limit (kg)	High parameter	Earliest time to criticality (yr)
0.0544	0.53	0.01	0	0.021	f	1.20×10^5
0.163	0.53	0.01	0	0.021	f	1.07×10^5
0.0544	0.53	0.01	0.055	1.33	Fe sol	6.61×10^5
0.163	0.53	0.01	0.055	1.33	Fe sol	5.64×10^5
0.0544	7.19	0.01	0.055	0.021	Drip rate	$>10^6$
0.163	7.19	0.01	0.055	0.021	Drip rate	$>10^6$
0.0544	0.53	0.1	0.055	0.021	Exchg	$>10^6$
0.163	0.53	0.1	0.055	0.021	Exchg	$>10^6$

Table 7.4-4. Sensitivity to trapped boron fraction with two parameters high

SS Corrosion rate (kg/yr)	Drip rate (mm/yr)	Exchange efficiency	f, Trapped boron fraction	Fe sol limit (kg)	High parameters	Earliest time to criticality (yr)
0.0544	0.53	0.01	0	1.33	f, Fe sol	1.19×10^5
0.163	0.53	0.01	0	1.33	f, Fe sol	1.07×10^5
0.0544	7.19	0.01	0	0.021	f, Drip rate	3.55×10^4
0.163	7.19	0.01	0	0.021	f, Drip rate	1.51×10^4
0.0544	0.53	0.1	0	0.021	f, Exchg	3.68×10^4
0.163	0.53	0.1	0	0.021	f, Exchg	1.73×10^4
0.0544	7.19	0.01	0.055	1.33	Fe, Drip rate	6.05×10^4
0.163	7.19	0.01	0.055	1.33	Fe, Drip rate	4.97×10^4
0.0544	0.53	0.1	0.055	1.33	Fe, Exchg	8.13×10^4
0.163	0.53	0.1	0.055	1.33	Fe, Exchg	6.73×10^4
0.0544	7.19	0.1	0.055	0.021	Dr, Exchg	3.18×10^5
0.163	7.19	0.1	0.055	0.021	Dr, Exchg	2.68×10^5

7.5 Criticality Consequences

The purpose of this section is to estimate the consequences of a criticality event, under the assumption that such an event does occur, and that it occurs at 15,000 years following emplacement. Furthermore, in order to support the maintenance of criticality for up to 10,000 years it is necessary to assume that the highest possible infiltration rate (10 mm/yr) does occur and can have, at most, a 10,000 year duration. These are worst case assumptions, and their justification is given in Assumption 4.3.37. The consequences of such a criticality event will be discussed in terms of the heat generated and the change in the radionuclide inventory of the waste package.

7.5.1 Estimated Power and Duration

The criticality scenarios discussed in the previous Sections detail a picture of a flooded waste package that is gradually approaching a critical condition ($k_{eff}=1$) as a result of positive reactivity insertions caused by a slow loss of boron and iron from the package interior. Once a WP reaches a k_{eff} of 1, continued small positive reactivity insertions will cause the power output of the WP to begin to slowly rise (i.e., a long reactor period). If the power exceeds a certain limit, the rate at which water is consequentially removed from the WP will exceed the rate of input, and the resulting water level drop will provide a negative reactivity insertion driving the WP back towards a subcritical condition. Conversely, if insufficient power is produced, the water level will be maintained and the exchange process discussed previously will continue to remove dissolved boron, thus providing a continued source of positive reactivity insertions until the point of equilibrium is achieved. The maximum steady state power can then be estimated by determining the power required to maintain the bulk WP water temperature at the point where water is removed at the same rate that it drips into the WP. The WP must produce sufficient power to raise the temperature of the incoming water to this equilibrium value, as well as account for heat losses to the environment by radiation and/or conduction. All calculations and unit conversions in this Section were performed using the MathCad v5.0+ with the worksheet provided in Attachment VII. Input data for the parameters discussed in this section is given in Section 4.1.

It is conservatively assumed that airflow is stagnant in a drift at the 15,000 year-plus time frame under consideration, and evaporation can be modeled as diffusion of water vapor into air. The first step is to obtain the diffusion coefficient for water into air. The following expression obtained from Ref. 5.14 provides an approximation for the diffusion coefficient as a function of temperature:

$$D(T) = [435.7 \cdot T^{3/2} \cdot (M_1^{-1} + M_2^{-1})^{1/2}]/(P_{atm} \cdot (V_1^{1/3} + V_2^{1/3}) \qquad \text{Eq. 7.5-1}$$

where,	$D(T)$	is the diffusion coefficient in cm^2/s at temperature T,
	T	is the temperature in K,
	P_{atm}	is the atmospheric pressure,
	V_1, V_2	are the molecular volumes of substances 1 and 2 (in this case water and air respectively) and,

M_1,M_2 are the molecular weights of substances 1 and 2 (water and air).

An additional factor of 0.056 cm^2/s has been added to values calculated by Eq. 7.5-1 to correspond with empirical measurements of the diffusion coefficient of water vapor into air at 8°C and 25°C.

With the diffusion coefficient determined, the volumetric flow rate of water out of the package due to evaporation is determined using the integrated form of Stefan's law (Ref. 5.14):

$$V_{evap}(T) = [(D(T)\cdot P_{atm}\cdot M_1\cdot A\cdot v(T))/(R_0\cdot T\cdot z)]\cdot \ln[(P_{atm} - p(T)\cdot RH)/(P_{atm} - p(T))] \quad \text{Eq. 7.5-2}$$

where,

$V_{evap}(T)$	is the volumetric evaporation rate,
$D(T)$	is the diffusion coefficient at temperature T,
T	is the temperature,
P_{atm}	is the atmospheric pressure,
$p(T)$	is the saturation pressure of water at temperature T,
R_0	is the Universal Gas Constant,
z	is the distance from the water surface to the bulk environment,
$v(T)$	is the specific volume of the water at temperature T,
A	is the surface area of the water in the WP,
RH	is the drift relative humidity, and
M_1	is the molecular weight of water.

The maximum rate of water dripping on a WP in TSPA-95 (Ref. 5.18) was approximately 1.9×10^5 cm^3/yr, and was assumed (in TSPA-95) to occur 50,000 years after emplacement. Using Eq. 7.5-2, the WP would have to produce sufficient power to maintain the water in the WP at a temperature of 57.4°C, as well as compensate for other mechanisms of heat loss, to match this drip rate. This indicates that evaporation alone will be sufficient to remove the incoming water, and bulk boiling will not occur.

It is assumed for this analysis that the WP configuration has a slightly negative moderator temperature coefficient, which also contributes to slowing rate of power increase such that a stable power level is gradually reached. This assumption is based on previous analyses of the ACD 21 PWR Uncanistered Fuel WP (Ref. 5.16) which indicate that the first 5% reduction in moderator density from that used in the calculation (sat. liq. at 27°C) will result in a negative reactivity insertion of approximately 10^{-2} $\Delta k/k$ for the criticality design basis fuel (Ref. 5.10). For comparison purposes, a 30°C increase results in only a 1% density reduction.

The amount of reactor heat dissipated by heating the incoming water, which is assumed to be at a temperature of 30°C, to a temperature of 57.4°C is given by the following expression:

$$q_{water} = [Cp(30°C)\cdot V_{drip}\cdot \Delta T]/v(30°C) \quad \text{Eq. 7.5-3}$$

where,

q_{water} is the heat input required to raise the water temperature 27.4°C,
V_{drip} is the rate of water dripping into the WP,
$Cp(30°C)$ is the specific heat of water at 30°C,
$\nu(30°C)$ is the specific gravity of water at 30°C, and
ΔT is the temperature increase (27.4°C).

Using Equation 7.5-3, only 0.677 W are required to raise the temperature of the water to the point where the evaporation rate equals the rate of influx.

Once at 57.4°C, the amount of power required to vaporize water at a rate of 1.9×10^5 cm^3/yr of water must also be accounted for. This is equal to the product of the heat of vaporization at 57.4°C, 2364.8 kJ/kg (linear interpolation from Ref. 5.15, Table A-3), the volume of water to be evaporated, 1.9×10^5 cm^3/yr, and the density of water at 57.4°C, 984.4 kg/m^3. Multiplying the above three values and performing the appropriate unit conversions yields an additional 14 W.

As stated above, additional heat losses will also occur due to radiation and/or conduction heat transfer to the local environment. The actual configuration of the drift thousands of years after emplacement cannot be defined sufficiently to allow a detailed heat transfer estimate. It is highly likely that a portion of the WP may be covered with rubble, possibly as a result of the gradual collapse of the drift, and both radiation and conduction mechanisms will be active. However, examination of ideal radiation-only and conduction-only systems should respectively provide an upper and lower bound on the heat loss from a WP with a bulk water temperature of 57.4°C. Heat losses due to radiation alone can be estimated by treating the WP and drift as a system of concentric cylinders, with the WP surface at 57.4°C, and the drift wall assumed to maintain a constant 30°C. The radiation heat transfer rate is then given by:

$$q_{rad} = [\sigma \cdot A_1 \cdot (T_1^4 - T_2^4)]/[\epsilon_1^{-1} + (A_1/A_2)(\epsilon_2^{-1} - 1)] \quad \text{(Ref. 5.14)} \qquad \text{Eq. 7.5-4}$$

where,

q_{rad} is the radiation heat transfer rate,
T_1 is the WP surface temperature,
T_2 is the drift wall temperature,
A_1 is the WP surface area,
A_2 is the drift surface area,
ϵ_1 is the emissivity of oxidized carbon steel,
ϵ_2 is the emissivity of tuff rock, and,
σ is the Stephan-Boltzman constant.

Using the above equation, radiation heat loss from a 57.4°C WP is estimated to be 3859 W. Again assuming the system of concentric cylinders and a drift wall temperature of 30°C, a WP entirely covered by crushed tuff would lose heat by conduction according to:

$$q_{cond} = [2\pi \cdot k \cdot L \cdot (T_1 - T_2)]/[\ln(d_2/d_1)] \quad \text{(Ref. 5.14)} \qquad \text{Eq. 7.5-5}$$

where,	q_{cond}	is the conduction heat transfer rate,
	k	is the average thermal conductivity of crushed tuff,
	L	is the WP outer length less that of the skirts,
	T_1	is the WP surface temperature,
	T_2	is the drift wall temperature,
	d_1	is the WP outer diameter; and,
	d_2	is the drift diameter.

Solving the above equation for a WP surface temperature of 57.4°C indicates that 504 W will be lost if all heat transfer occurs by conduction through crushed tuff. Assuming the more likely configuration of a WP covered half-way with rubble, the heat loss may be approximated (i.e., not specifically accounting for the radiation heat transfer between the rubble and the drift wall) by taking the mean of the above two extremes, 2.182 kW. Since the power dissipated in heating the water dripping in to 57.4°C and vaporizing it at that temperature has been shown to total less than 15 W, it is not added in this approximation.

The above power represents a conservative ideal condition because, in reality, there will be a number of feedback mechanisms which will act to disrupt the equilibrium. Some of these mechanisms include the decreases in the infiltration rate resulting from climatic cycles, the production of neutron absorbing fission products, the depletion of fissile nuclides, changes in moderator density, corrosion of the cladding or spacer grids (leading to consolidation of the fuel rods), and corrosion of the remainder of the WP barriers (leading to the formation of drainage holes). The combined effect of these mechanisms will likely limit any single WP criticality event to a relatively short duration, with criticality events reoccurring in the same WP in a cyclic pattern as long as the necessary conditions continue to recur. Therefore, use of a steady state power of 2.182 kW to estimate total burnup resulting from a long-term postclosure internal WP criticality should be a reasonable approximation to the cumulative effect of multiple pulses.

The overall duration of such a cyclic criticality is also dependent on some of the above-mentioned feedback mechanisms, primarily the continued availability of water, the ability of the WP to hold water, and the depletion of fissile nuclides. While the climate cycle period over the past 2 million years has been approximately 100,000 years, infiltration rates near the peak (which are required to maintain the steady state power level and water exchange rates discussed previously) may occur for only several thousand years (Ref. 5.18). Based on this information, a range of 1,000 year to 10,000 year durations has been evaluated, for the purposes of estimating the effects of criticality on radionuclide inventory. A 10,000 year criticality at a steady state power level of 2.182 kW yields an additional burnup of 7965 MWd for the SNF in the WP (817 MWd/MTU). Such long periods of steady state power production are expected to be conservative because of the cyclic nature of the criticality itself, the duration of the peak infiltration rates, and the expectation that the WP will have a much lower probability of being able to hold water by the time the next peak in infiltration returns.

7.5.2 Effects on the Radionuclide Inventory of the WP

To evaluate the effects of a criticality on the radionuclide inventory of a WP, the computer code ORIGEN-S was run using the criticality design basis fuel, and the steady state power of 2.182 kW discussed in Section 7.5.1 above. The criticality was assumed to occur after the fuel had aged/decayed for 15,000 years and was maintained at the above mentioned power for three durations: 1,000, 5,000 and 10,000 years. The output of these runs was the radionuclide inventory, in curies, at the times corresponding to the end of each criticality, and at fuel ages (time since reactor discharge) of 45,000 and 65,000 years. A fourth, decay-only case was run to determine the radionuclide inventories at the above times for fuel which did not experience a criticality event. The details of the ORIGEN-S calculations performed to obtain the radionuclide inventories for both decay-only and fission-plus-decay cases are reported in Ref. 5.4.

To provide a comparison between a WP which experienced a criticality, and one only decayed, 36 of the 39 isotopes in the TSPA-95 radionuclide inventory list (Ref. 5.18) were extracted from the ORIGEN-S output (Ref. 5.4). Comparisons of the activities of ^{36}Cl, ^{59}Ni, and ^{63}Ni were not made because the present ORIGEN-S analysis has not yet been extended to activation products. Differences were reported in terms of the percentage change in the activity of each radionuclide at each time, and the percentage change The calculations performed to determine the difference in radionuclide activities between the decay-only and criticality cases were performed using the Excel v5.0. The results are summarized in Tables 7.5-1, 7.5-2, and 7.5-3 for the 1,000 year, 5,000 year, and 10,000 year duration criticalities respectively.

Neutron activation of stable isotopes in the WP materials and water represents another potential source of radionuclides which may be produced during such a criticality. The ORIGEN-S output (Ref. 5.4) indicated that the total average neutron flux in the 2.182 kW WP was $\approx 2.9 \times 10^8$ neutrons/cm^{2}s, and that 10.9% of this flux was in the thermal part of the spectrum. ^{14}C and ^{36}Cl are two radionuclides in the TSPA-95 radionuclide inventory which may be produced from activation of trace elements in the water. ^{14}C is primarily produced by the ^{14}N(n,p) reaction and the ^{17}O(n,α) reaction, although much smaller quantities may also be produced by multiple neutron captures in ^{16}O (^{16}O(n,γ)$\rightarrow ^{17}$O(n,α)$\rightarrow ^{14}$C). The number density for ^{14}N in 57.4°C water in equilibrium with air at atmospheric pressure is given by the following expression:

$$N_{N14}=(A_{N14}\cdot\rho_w\cdot v_N\cdot P_{atm}\cdot N_a\cdot 2)/(M_w\cdot H_N) \qquad \text{Eq. 7.5-6}$$

where,		
	N_{N14}	is the number density of ^{14}N
	A_{N14}	is the abundance of ^{14}N,
	ρ_w	is the density of water at 57.4°C,
	v_N	is the volume fraction of N_2 in air,
	M_w	is the molecular weight of water,
	P_{atm}	is the air pressure,
	N_a	is Avogadro's Number, and,
	H_N	is Henry's Law solubility of N_2 in water at 57.4°C in

atm. N_2/(mole N_2/mole water).

This yields 4.35×10^{17} atoms of ^{14}N per cm^3 of water. The number density of ^{17}O in water is simply computed by:

$$N_{O17}=(A_{O17}\cdot\rho_w\cdot N_a)/M_w \qquad \text{Eq. 7.5-7}$$

where,

N_{O17} is the number density of ^{17}O,
A_{O17} is the abundance of ^{17}O,
ρ_w is the density of water at 57.4°C,
M_w is the molecular weight of water, and,
N_a is Avogadro's Number.

This yields 1.32×10^{19} ^{17}O atoms/cm^3. The amount of oxygen dissolved in the water is insignificant compared to that in the water itself, and has been neglected for this calculation. The above calculations and associated unit conversions (as well as those to follow in this section) were performed using the MathCad v5.0+ worksheet detailed in Attachment IX, and the inputs given in Section 4.1.

Given the above flux and thermal fraction, and assuming that the number density of ^{14}N and ^{17}O remains constant, the production rate of ^{14}C can be calculated as follows:

$$^{14}C=\lambda_{C14}\cdot(N_{N14}\cdot\sigma_{pN14}+N_{O17}\cdot\sigma_{\alpha O17})\cdot\phi\cdot f\cdot V_{WP} \qquad \text{Eq. 7.5-8}$$

where,

^{14}C is the production rate of ^{14}C,
λ_{C14} is the ^{14}C decay constant (ln2/half-life),
N_{N14} is the number density of ^{14}N,
N_{O17} is the number density of ^{17}O,
$\sigma_{\alpha O17}$ is the microscopic thermal cross section for the $^{17}O(n,\alpha)$ reaction,
σ_{pN14} is the microscopic thermal cross section for the $^{14}N(n,p)$ reaction,
ϕ is the average total neutron flux,
f is the fraction of the flux in the thermal part of the spectrum, and,
V_{WP} is the volume of water in the fully flooded WP.

Using the parameters given in Section 4.1.7, this yields 1.98 μCi of ^{14}C/yr of WP criticality, which is not contained by the cladding and may be available for immediate release from the WP. However, this production rate is almost six orders of magnitude below the NRC release limits for the site of 0.796 Ci of ^{14}C/yr (Ref. 5.18) and thus should have no impact on site performance.

Similarly, ^{36}Cl may be produced during the criticality by neutron activation of ^{35}Cl in the water. Chemical analyses of J-13 (Ref. 5.35) well water have found it to nominally contain 7.5 μg Cl^-/mL. However, evaporation of water from the WP would be expected to increase this concentration. Corrosion tests involving boiling J-13 well water, tuff rock, and stainless steel specimens found that the stable concentration of Cl^- had increased to 161 μg/mL after 1 year (Ref. 5.35). These values can be used to determine nominal and high ^{35}Cl number densities as follows:

$$N_{Cl35}=(C_{Cl}\cdot A_{Cl35}\cdot N_a)/M_{Cl} \qquad \text{Eq. 7.5-9}$$

where,	N_{Cl35}	is the number density of ^{35}Cl,
	A_{Cl35}	is the abundance of ^{35}Cl,
	C_{Cl}	is the concentration of Cl^- in the water,
	M_{Cl}	is the molecular weight of Cl, and,
	N_a	is Avogadro's Number.

Using the parameters given in Section 4.1.7, this yields a nominal value of 9.65×10^{16} atoms of ^{35}Cl/cm^3 or a high value of 2.07×10^{18} ^{36}Cl atoms/cm^3 if the high concentration is used. The production rate of ^{36}Cl can then be calculated by:

$$^{36}C=\lambda_{Cl36}\cdot(N_{Cl35}\cdot\sigma_{\gamma Cl35})\cdot\phi\cdot f\cdot V_{WP} \qquad \text{Eq. 7.5-10}$$

where,	^{36}Cl	is the production rate of ^{36}Cl,
	λ_{Cl36}	is the ^{36}Cl decay constant (ln2/half-life),
	N_{Cl35}	is the number density of ^{35}Cl,
	$\sigma_{\gamma Cl35}$	is the microscopic thermal cross section for the ^{35}Cl(n,γ) reaction,
	ϕ	is the average total neutron flux,
	f	is the fraction of the flux in the thermal part of the spectrum, and,
	V_{WP}	is the volume of water in the fully flooded WP.

This yields a nominal production rate of 0.04 μCi/yr of ^{36}Cl and a high rate of 0.86 μCi/yr. Both of these values are also several orders of magnitude below the NRC site release limits of 7.13 mCi/yr and should not impact site performance.

The overall effect of the criticality can be summarized by the percentage increase in the total curies for the 36 isotopes utilized in TSPA-95 immediately after the criticality ends and at later times. Table 7.5-4 below shows this comparison. The explicitly stated times are measured from emplacement. The duration of criticality times are relative to the start of criticality at 15,000 years, so the absolute (measured from emplacement) times at the end of criticality are determined by adding the duration of criticality to 15,000 years.

Table 7.5-1. Effects of 1,000 Year Criticality on the Radionuclide Inventory of a PWR Fuel Assembly

	16,000 yr				45,000 yr				65,000 yr			
	Act. (Ci) Critical	Act. (Ci) Decay Only	% Diff. Isotope	% Diff. Total	Act. (Ci) Critical	Act. (Ci) Decay Only	% Diff. Isotope	% Diff. Total	Act. (Ci) Critical	Act. (Ci) Decay Only	% Diff. Isotope	% Diff. Total
ac227	4.9e-003	4.3e-003	1.6e+001	4.9e-004	1.0e-002	1.0e-002	3.0e+000	5.6e-004	1.3e-002	1.3e-002	2.3e+000	9.3e-004
am241	2.6e+000	2.2e-003	1.2e+005	1.9e+000	2.0e-004	2.0e-004	-1.5e+000	-5.6e-006	3.9e-005	3.9e-005	-1.5e+000	-1.9e-006
am242m	2.0e-003	0.0e+000	N/A	1.4e-003	0.0e+000	0.0e+000	0.0e+000	0.0e+000	0.0e+000	0.0e+000	0.0e+000	0.0e+000
am243	4.8e-001	4.5e-001	7.2e+000	2.3e-002	3.1e-002	2.9e-002	7.2e+000	3.9e-003	4.8e-003	4.5e-003	7.2e+000	9.9e-004
c 14	4.9e-006	4.8e-006	2.5e+000	8.7e-008	1.5e-007	1.4e-007	2.8e+000	7.5e-009	1.3e-008	1.3e-008	2.3e+000	9.3e-010
cm244	1.7e-002	0.0e+000	N/A	1.2e-002	0.0e+000	0.0e+000	0.0e+000	0.0e+000	0.0e+000	0.0e+000	0.0e+000	0.0e+000
cm245	2.1e-003	2.1e-003	-1.4e+000	-2.2e-005	2.0e-004	2.0e-004	-1.5e+000	-5.6e-006	3.9e-005	3.9e-005	-1.5e+000	-1.9e-006
cm246	9.6e-005	8.8e-005	9.2e+000	5.8e-006	1.4e-006	1.3e-006	9.5e+000	2.3e-007	7.3e-008	6.7e-008	9.2e+000	1.9e-008
cs135	2.0e-001	2.0e-001	9.9e-001	1.4e-003	2.0e-001	2.0e-001	1.0e+000	3.8e-003	2.0e-001	2.0e-001	1.0e+000	6.2e-003
i129	8.8e-003	8.8e-003	4.5e-001	2.9e-005	8.8e-003	8.8e-003	4.5e-001	7.5e-005	8.8e-003	8.8e-003	3.4e-001	9.3e-005
nb 93m	3.5e-001	3.5e-001	5.8e-001	1.4e-003	3.4e-001	3.4e-001	2.9e-001	1.9e-003	3.4e-001	3.4e-001	2.9e-001	3.1e-003
nb 94	1.9e-005	1.4e-005	4.0e+001	4.0e-006	7.1e-006	5.0e-006	4.1e+001	3.9e-006	3.6e-006	2.5e-006	4.1e+001	3.2e-006
np237	3.8e-001	3.8e-001	2.6e-001	7.2e-004	3.8e-001	3.8e-001	2.6e-001	1.9e-003	3.8e-001	3.8e-001	2.7e-001	3.1e-003
pa231	4.9e-003	4.3e-003	1.6e+001	4.9e-004	1.0e-002	1.0e-002	3.0e+000	5.6e-004	1.3e-002	1.3e-002	1.6e+000	6.2e-004
pb210	8.0e-002	8.0e-002	0.0e+000	0.0e+000	2.1e-001	2.1e-001	4.7e-001	1.9e-003	2.8e-001	2.8e-001	7.1e-001	6.2e-003
pd107	2.6e-002	2.6e-002	3.8e-001	7.2e-005	2.6e-002	2.6e-002	3.8e-001	1.9e-004	2.6e-002	2.6e-002	7.7e-001	6.2e-004
pu238	2.9e+000	0.0e+000	N/A	2.1e+000	0.0e+000	0.0e+000	0.0e+000	0.0e+000	0.0e+000	0.0e+000	0.0e+000	0.0e+000
pu239	1.0e+002	1.0e+002	9.7e-001	7.2e-001	4.5e+001	4.5e+001	6.7e-001	5.6e-001	2.6e+001	2.5e+001	7.9e-001	6.2e-001
pu240	2.9e+001	2.8e+001	4.3e+000	8.7e-001	1.4e+000	1.3e+000	3.8e+000	9.4e-002	1.7e-001	1.6e-001	4.4e+000	2.2e-002
pu241	3.2e+000	2.1e-003	1.5e+005	2.3e+000	2.0e-004	2.0e-004	-1.5e+000	-5.6e-006	3.9e-005	3.9e-005	-1.5e+000	-1.9e-006
pu242	2.7e-001	2.7e-001	-3.7e-001	-7.2e-004	2.6e-001	2.6e-001	-3.9e-001	-1.9e-003	2.5e-001	2.5e-001	-4.0e-001	-3.1e-003
ra226	8.0e-002	8.0e-002	-1.3e-001	-7.2e-005	2.1e-001	2.1e-001	4.7e-001	1.9e-003	2.8e-001	2.8e-001	7.1e-001	6.2e-003
ra228	9.0e-008	9.0e-008	0.0e+000	0.0e+000	2.8e-007	2.8e-007	3.6e-001	1.9e-009	4.1e-007	4.1e-007	4.9e-001	6.2e-009
se 79	1.4e-001	1.4e-001	7.3e-001	7.2e-004	7.5e-002	7.5e-002	6.7e-001	9.4e-004	4.9e-002	4.9e-002	6.1e-001	9.3e-004
sm151	7.9e-001	0.0e+000	N/A	5.7e-001	0.0e+000	0.0e+000	0.0e+000	0.0e+000	0.0e+000	0.0e+000	0.0e+000	0.0e+000
sn126	1.3e-001	1.2e-001	8.1e-001	7.2e-004	1.0e-001	1.0e-001	0.0e+000	0.0e+000	8.9e-002	8.8e-002	4.5e-001	1.2e-003
tc 99	3.8e+000	3.7e+000	5.3e-001	1.4e-002	3.4e+000	3.4e+000	5.9e-001	3.8e-002	3.2e+000	3.2e+000	3.1e-001	3.1e-002
th229	1.1e-002	1.2e-002	-8.7e-001	-7.2e-005	5.1e-002	5.1e-002	0.0e+000	0.0e+000	7.8e-002	7.8e-002	0.0e+000	0.0e+000
th230	9.2e-002	9.2e-002	-2.2e-001	-1.4e-004	2.2e-001	2.2e-001	4.5e-001	1.9e-003	2.9e-001	2.9e-001	7.0e-001	6.2e-003
th232	9.0e-008	9.0e-008	0.0e+000	0.0e+000	2.8e-007	2.8e-007	3.6e-001	1.9e-009	4.1e-007	4.1e-007	4.9e-001	6.2e-009
u233	2.5e-002	2.5e-002	-8.0e-001	-1.4e-004	6.7e-002	6.7e-002	0.0e+000	0.0e+000	9.3e-002	9.3e-002	1.1e-001	3.1e-004
u234	6.7e-001	6.7e-001	9.0e-001	4.3e-003	6.3e-001	6.3e-001	9.6e-001	1.1e-002	6.1e-001	6.0e-001	1.0e+000	1.9e-002
u235	1.6e-002	1.6e-002	-6.4e-001	-7.2e-005	1.8e-002	1.8e-002	-5.6e-001	-1.9e-004	1.8e-002	1.8e-002	-5.4e-001	-3.1e-004
u236	1.3e-001	1.3e-001	7.9e-001	7.2e-004	1.3e-001	1.3e-001	0.0e+000	0.0e+000	1.4e-001	1.3e-001	7.5e-001	3.1e-003
u238	1.5e-001	1.5e-001	0.0e+000	0.0e+000	1.5e-001	1.5e-001	0.0e+000	0.0e+000	1.5e-001	1.5e-001	0.0e+000	0.0e+000
zr 93	3.5e-001	3.5e-001	5.8e-001	1.4e-003	3.4e-001	3.4e-001	2.9e-001	1.9e-003	3.4e-001	3.4e-001	2.9e-001	3.1e-003
36 Iso. Totals	1.5e+002	1.4e+002	8.5e+000	0.0e+000	5.4e+001	5.3e+001	7.3e-001	0.0e+000	3.3e+001	3.2e+001	7.3e-001	0.0e+000

Table 7.5-2. Effects of 5,000 Year Criticality on the Radionuclide Inventory of a PWR Fuel Assembly

	20,000 yr				45,000 yr				65,000 yr			
	Act. (Ci) Critical	Act. (Ci) Decay Only	% Diff. Isotope	% Diff. Total	Act. (Ci) Critical	Act. (Ci) Decay Only	% Diff. Isotope	% Diff. Total	Act. (Ci) Critical	Act. (Ci) Decay Only	% Diff. Isotope	% Diff. Total
Ac227	8.8e-003	5.2e-003	7.0e+001	3.1e-003	1.2e-002	1.0e-002	2.0e+001	3.8e-003	1.4e-002	1.3e-002	1.0e+001	4.0e-003
Am241	2.7e+000	1.6e-003	1.7e+005	2.3e+000	1.9e-004	2.0e-004	-7.5e+000	-2.8e-005	3.6e-005	3.9e-005	-7.4e+000	-9.0e-006
Am242m	2.4e-003	0.0e+000	N/A	2.0e-003	0.0e+000	0.0e+000	0.0e+000	0.0e+000	0.0e+000	0.0e+000	0.0e+000	0.0e+000
Am243	4.4e-001	3.1e-001	4.4e+001	1.1e-001	4.2e-002	2.9e-002	4.4e+001	2.4e-002	6.4e-003	4.5e-003	4.3e+001	6.0e-003
C 14	3.5e-006	3.0e-006	1.7e+001	4.3e-007	1.7e-007	1.4e-007	1.7e+001	4.5e-008	1.5e-008	1.3e-008	1.7e+001	6.8e-009
Cm244	1.6e-002	0.0e+000	N/A	1.3e-002	0.0e+000	0.0e+000	0.0e+000	0.0e+000	0.0e+000	0.0e+000	0.0e+000	0.0e+000
Cm245	1.4e-003	1.5e-003	-7.1e+000	-9.3e-005	1.9e-004	2.0e-004	-7.0e+000	-2.6e-005	3.6e-005	3.9e-005	-7.4e+000	-9.0e-006
Cm246	7.4e-005	4.9e-005	5.1e+001	2.1e-005	1.9e-006	1.3e-006	5.2e+001	1.2e-006	1.0e-007	6.7e-008	5.2e+001	1.1e-007
Cs135	2.1e-001	2.0e-001	4.4e+000	7.6e-003	2.1e-001	2.0e-001	4.5e+000	1.7e-002	2.1e-001	2.0e-001	4.5e+000	2.8e-002
I129	9.0e-003	8.8e-003	2.0e+000	1.5e-004	9.0e-003	8.8e-003	2.0e+000	3.4e-004	9.0e-003	8.8e-003	2.0e+000	5.6e-004
Nb 93m	3.5e-001	3.5e-001	2.0e+000	5.9e-003	3.5e-001	3.4e-001	2.0e+000	1.3e-002	3.5e-001	3.4e-001	2.1e+000	2.2e-002
Nb 94	4.1e-005	1.2e-005	2.5e+002	2.5e-005	1.8e-005	5.0e-006	2.5e+002	2.4e-005	8.9e-006	2.5e-006	2.5e+002	2.0e-005
Np237	3.8e-001	3.8e-001	1.0e+000	3.4e-003	3.8e-001	3.8e-001	1.1e+000	7.5e-003	3.8e-001	3.8e-001	1.3e+000	1.5e-002
Pa231	8.8e-003	5.2e-003	7.0e+001	3.1e-003	1.2e-002	1.0e-002	2.0e+001	3.8e-003	1.4e-002	1.3e-002	1.0e+001	4.0e-003
Pb210	1.0e-001	1.0e-001	-9.9e-001	-8.5e-004	2.2e-001	2.1e-001	2.3e+000	9.4e-003	2.9e-001	2.8e-001	3.6e+000	3.1e-002
Pd107	2.7e-002	2.6e-002	1.9e+000	4.2e-004	2.7e-002	2.6e-002	1.9e+000	9.4e-004	2.7e-002	2.6e-002	2.3e+000	1.9e-003
Pu238	3.0e+000	0.0e+000	N/A	2.5e+000	0.0e+000	0.0e+000	0.0e+000	0.0e+000	0.0e+000	0.0e+000	0.0e+000	0.0e+000
Pu239	9.6e+001	9.2e+001	3.6e+000	2.8e+000	4.7e+001	4.5e+001	3.8e+000	3.2e+000	2.6e+001	2.5e+001	4.0e+000	3.1e+000
Pu240	2.3e+001	1.9e+001	2.6e+001	4.1e+000	1.7e+000	1.3e+000	2.6e+001	6.4e-001	2.0e-001	1.6e-001	2.6e+001	1.3e-001
Pu241	2.6e+000	1.5e-003	1.7e+005	2.2e+000	1.9e-004	2.0e-004	-7.5e+000	-2.8e-005	3.6e-005	3.9e-005	-7.4e+000	-9.0e-006
Pu242	2.7e-001	2.7e-001	-1.1e+000	-2.5e-003	2.5e-001	2.6e-001	-1.2e+000	-5.6e-003	2.5e-001	2.5e-001	-1.6e+000	-1.2e-002
Ra226	1.0e-001	1.0e-001	-9.9e-001	-8.5e-004	2.2e-001	2.1e-001	2.8e+000	1.1e-002	2.9e-001	2.8e-001	3.9e+000	3.4e-002
Ra228	1.1e-007	1.1e-007	0.0e+000	0.0e+000	2.8e-007	2.8e-007	1.4e+000	7.5e-009	4.2e-007	4.1e-007	1.7e+000	2.2e-008
Se 79	1.3e-001	1.3e-001	3.2e+000	3.4e-003	7.7e-002	7.5e-002	3.1e+000	4.3e-003	5.1e-002	4.9e-002	3.1e+000	4.6e-003
Sm151	8.0e-001	0.0e+000	N/A	6.8e-001	0.0e+000	0.0e+000	0.0e+000	0.0e+000	0.0e+000	0.0e+000	0.0e+000	0.0e+000
Sn126	1.2e-001	1.2e-001	2.5e+000	2.5e-003	1.0e-001	1.0e-001	2.0e+000	3.8e-003	9.1e-002	8.8e-002	2.5e+000	6.8e-003
Tc 99	3.8e+000	3.7e+000	2.2e+000	6.8e-002	3.5e+000	3.4e+000	2.1e+000	1.3e-001	3.3e+000	3.2e+000	1.9e+000	1.9e-001
Th229	1.6e-002	1.6e-002	-6.1e-001	-8.5e-005	5.1e-002	5.1e-002	-3.9e-001	-3.8e-004	7.8e-002	7.8e-002	1.3e-001	3.1e-004
Th230	1.1e-001	1.1e-001	-8.8e-001	-8.5e-004	2.3e-001	2.2e-001	2.7e+000	1.1e-002	3.0e-001	2.9e-001	3.8e+000	3.4e-002
Th232	1.1e-007	1.1e-007	0.0e+000	0.0e+000	2.8e-007	2.8e-007	1.4e+000	7.5e-009	4.2e-007	4.1e-007	1.7e+000	2.2e-008
U233	3.1e-002	3.1e-002	-1.9e+000	-5.1e-004	6.7e-002	6.7e-002	-1.5e-001	-1.9e-004	9.3e-002	9.3e-002	3.2e-001	9.3e-004
U234	6.9e-001	6.6e-001	5.3e+000	3.0e-002	6.6e-001	6.3e-001	5.3e+000	6.2e-002	6.3e-001	6.0e-001	5.2e+000	9.6e-002
U235	1.6e-002	1.6e-002	-1.9e+000	-2.5e-004	1.8e-002	1.8e-002	-1.1e+000	-3.8e-004	1.8e-002	1.8e-002	-1.6e+000	-9.3e-004
U236	1.3e-001	1.3e-001	1.6e+000	1.7e-003	1.4e-001	1.3e-001	2.2e+000	5.6e-003	1.4e-001	1.3e-001	2.2e+000	9.3e-003
U238	1.5e-001	1.5e-001	0.0e+000	0.0e+000	1.5e-001	1.5e-001	0.0e+000	0.0e+000	1.5e-001	1.5e-001	0.0e+000	0.0e+000
Zr 93	3.5e-001	3.5e-001	2.0e+000	5.9e-003	3.5e-001	3.4e-001	2.0e+000	1.3e-002	3.5e-001	3.4e-001	2.1e+000	2.2e-002
36 Iso. Totals	1.4e+002	1.2e+002	1.5e+001	0.0e+000	5.5e+001	5.3e+001	4.2e+000	0.0e+000	3.3e+001	3.2e+001	3.7e+000	0.0e+000

Table 7.5-3. Effects of 10,000 Year Criticality on the Radionuclide Inventory of a PWR Fuel Assembly

	25,000 yr				45,000 yr				65,000 yr			
	Act. (Ci) Critical	Act. (Ci) Decay Only	% Diff. Isotope	% Diff. Total	Act. (Ci) Critical	Act. (Ci) Decay Only	% Diff. Isotope	% Diff. Total	Act. (Ci) Critical	Act. (Ci) Decay Only	% Diff. Isotope	% Diff. Total
Ac227	1.4e-002	6.3e-003	1.2e+002	8.0e-003	1.5e-002	1.0e-002	4.9e+001	9.2e-003	1.6e-002	1.3e-002	2.4e+001	9.6e-003
Am241	2.1e+000	1.1e-003	2.0e+005	2.2e+000	1.7e-004	2.0e-004	-1.4e+001	-5.5e-005	3.4e-005	3.9e-005	-1.5e+001	-1.8e-005
Am242m	1.9e-003	0.0e+000	N/A	2.0e-003	0.0e+000	0.0e+000	0.0e+000	0.0e+000	0.0e+000	0.0e+000	0.0e+000	0.0e+000
Am243	4.1e-001	1.9e-001	1.1e+002	2.2e-001	6.3e-002	2.9e-002	1.1e+002	6.3e-002	9.5e-003	4.5e-003	1.1e+002	1.6e-002
C14	2.4e-006	1.6e-006	4.8e+001	8.0e-007	2.1e-007	1.4e-007	4.9e+001	1.3e-007	1.9e-008	1.3e-008	4.8e+001	1.9e-008
Cm244	1.5e-002	0.0e+000	N/A	1.6e-002	0.0e+000	0.0e+000	0.0e+000	0.0e+000	0.0e+000	0.0e+000	0.0e+000	0.0e+000
Cm245	8.8e-004	1.0e-003	-1.4e+001	-1.5e-004	1.7e-004	2.0e-004	-1.4e+001	-5.5e-005	3.4e-005	3.9e-005	-1.5e+001	-1.8e-005
Cm246	5.2e-005	2.4e-005	1.2e+002	2.9e-005	2.8e-006	1.3e-006	1.2e+002	2.8e-006	1.5e-007	6.7e-008	1.2e+002	2.5e-007
Cs135	2.2e-001	2.0e-001	8.4e+000	1.7e-002	2.2e-001	2.0e-001	9.0e+000	3.4e-002	2.2e-001	2.0e-001	8.5e+000	5.3e-002
I129	9.2e-003	8.8e-003	4.1e+000	3.7e-004	9.2e-003	8.8e-003	4.1e+000	6.8e-004	9.2e-003	8.8e-003	4.0e+000	1.1e-003
Nb 93m	3.6e-001	3.4e-001	4.1e+000	1.4e-002	3.6e-001	3.4e-001	4.1e+000	2.6e-002	3.5e-001	3.4e-001	3.8e+000	4.0e-002
Nb 94	7.4e-005	1.0e-005	6.4e+002	6.5e-005	3.7e-005	5.0e-006	6.4e+002	6.1e-005	1.9e-005	2.5e-006	6.4e+002	5.0e-005
Np237	3.9e-001	3.8e-001	2.1e+000	8.2e-003	3.9e-001	3.8e-001	2.1e+000	1.5e-002	3.8e-001	3.8e-001	2.4e+000	2.8e-002
Pa231	1.4e-002	6.3e-003	1.2e+002	8.0e-003	1.5e-002	1.0e-002	4.9e+001	9.2e-003	1.6e-002	1.3e-002	2.4e+001	9.6e-003
Pb210	1.3e-001	1.3e-001	-7.9e-001	-1.0e-003	2.2e-001	2.1e-001	4.7e+000	1.9e-002	3.1e-001	2.8e-001	1.1e+001	9.9e-002
Pd107	2.7e-002	2.6e-002	3.8e+000	1.0e-003	2.7e-002	2.6e-002	3.8e+000	1.9e-003	2.7e-002	2.6e-002	4.2e+000	3.4e-003
Pu238	3.1e+000	0.0e+000	N/A	3.1e+000	0.0e+000	0.0e+000	0.0e+000	0.0e+000	0.0e+000	0.0e+000	0.0e+000	0.0e+000
Pu239	8.7e+001	8.0e+001	8.6e+000	7.0e+000	4.9e+001	4.5e+001	8.9e+000	7.5e+000	2.8e+001	2.5e+001	9.1e+000	7.1e+000
Pu240	1.8e+001	1.1e+001	6.9e+001	7.7e+000	2.2e+000	1.3e+000	6.8e+001	1.7e+000	2.7e-001	1.6e-001	6.9e+001	3.4e-001
Pu241	2.1e+000	1.0e-003	2.1e+005	2.2e+000	1.7e-004	2.0e-004	-1.4e+001	-5.5e-005	3.4e-005	3.9e-005	-1.5e+001	-1.8e-005
Pu242	2.6e-001	2.7e-001	-2.6e+000	-7.1e-003	2.5e-001	2.6e-001	-2.7e+000	-1.3e-002	2.4e-001	2.5e-001	-2.8e+000	-2.2e-002
Ra226	1.3e-001	1.3e-001	-7.9e-001	-1.0e-003	2.2e-001	2.1e-001	4.7e+000	1.9e-002	3.1e-001	2.8e-001	1.1e+001	9.9e-002
Ra228	1.5e-007	1.5e-007	6.8e-001	1.0e-009	2.8e-007	2.8e-007	2.2e+000	1.1e-008	4.2e-007	4.1e-007	2.9e+000	3.7e-008
Se 79	1.2e-001	1.1e-001	6.1e+000	7.1e-003	7.9e-002	7.5e-002	6.3e+000	8.8e-003	5.2e-002	4.9e-002	6.3e+000	9.6e-003
Sm151	8.1e-001	0.0e+000	N/A	8.2e-001	0.0e+000	0.0e+000	0.0e+000	0.0e+000	0.0e+000	0.0e+000	0.0e+000	0.0e+000
Sn126	1.2e-001	1.2e-001	5.1e+000	6.1e-003	1.1e-001	1.0e-001	4.9e+000	9.4e-003	9.3e-002	8.8e-002	5.0e+000	1.4e-002
Tc 99	3.8e+000	3.6e+000	4.1e+000	1.5e-001	3.5e+000	3.4e+000	4.1e+000	2.6e-001	3.3e+000	3.2e+000	3.8e+000	3.7e-001
Th229	2.3e-002	2.3e-002	-1.7e+000	-4.1e-004	5.1e-002	5.1e-002	-1.2e+000	-1.1e-003	7.8e-002	7.8e-002	-1.3e-001	-3.1e-004
Th230	1.4e-001	1.4e-001	0.0e+000	0.0e+000	2.3e-001	2.2e-001	5.0e+000	2.1e-002	3.1e-001	2.9e-001	7.3e+000	6.5e-002
Th232	1.5e-007	1.5e-007	6.8e-001	1.0e-009	2.8e-007	2.8e-007	2.2e+000	1.1e-008	4.2e-007	4.1e-007	2.9e+000	3.7e-008
U233	3.7e-002	3.9e-002	-3.1e+000	-1.2e-003	6.7e-002	6.7e-002	-6.0e-001	-7.5e-004	9.3e-002	9.3e-002	3.2e-001	9.3e-004
U234	7.2e-001	6.5e-001	1.1e+001	7.4e-002	6.9e-001	6.3e-001	1.1e+001	1.3e-001	6.6e-001	6.0e-001	1.1e+001	2.0e-001
U235	1.6e-002	1.6e-002	-3.6e+000	-6.1e-004	1.7e-002	1.8e-002	-2.8e+000	-9.4e-004	1.8e-002	1.8e-002	-2.7e+000	-1.5e-003
U236	1.4e-001	1.3e-001	3.1e+000	4.1e-003	1.4e-001	1.3e-001	4.5e+000	1.1e-002	1.4e-001	1.3e-001	4.5e+000	1.9e-002
U238	1.5e-001	1.5e-001	0.0e+000	0.0e+000	1.5e-001	1.5e-001	0.0e+000	0.0e+000	1.5e-001	1.5e-001	0.0e+000	0.0e+000
Zr 93	3.6e-001	3.4e-001	4.1e+000	1.4e-002	3.6e-001	3.4e-001	4.1e+000	2.6e-002	3.5e-001	3.4e-001	3.8e+000	4.0e-002
36 Iso. Total	1.2e+002	9.8e+001	2.4e+001	0.0e+000	5.8e+001	5.3e+001	9.9e+000	0.0e+000	3.5e+001	3.2e+001	8.5e+000	0.0e+000

Table 7.5-4. Percentage Increase in Total Curies of the 36 TSPA-95 Isotopes

Duration of Criticality	Percent Increase at End of Criticality	Percent Increase at 45,000 years	Percent Increase at 65,000 years
1,000 years	8.5% (16k yrs.)	0.73%	0.73%
5,000 years	15% (20k yrs.)	4.2%	3.7%
10,000 years	24% (25k yrs.)	9.9%	8.5%

8. Conclusions -

In compliance with the M&O Quality Administrative Procedures, the design results presented in this document should not be used for procurement, fabrication, or construction unless properly identified, tracked as TBV, and controlled by the appropriate procedures.

The purpose of this analysis was to evaluate the criticality potential of the range of possible degraded mode configurations. From the calculations performed in this analysis, it can be concluded that:

- The earliest time to criticality is strongly dependent on a number of parameters which are presently the subject of significant uncertainty: (1) the ability of the WP to hold sufficient quantities of moderator for long periods of time (which may be affected by several factors, including corrosion of the WP bottom, the balance between evaporation and drip rates, and the buildup of moderator excluding oxides and mineral deposits), (2) the fraction of boron trapped in the solid iron oxide, (3) the stainless steel corrosion rate, (4) the upper limit for dissolved iron in the waste package water, (5) the efficiency of exchanging water between a filled waste package and the external environment, and (6) the drip rate.

- For a trapped boron fraction significantly larger than 0.05, the result will be very sensitive to the iron solubility limit, because there can be enough boron trapped in the solid oxide to prevent criticality, and the iron solubility limit will determine how fast this oxide can be removed.

- Trapping of the boron from the stainless steel in the solid iron oxide remaining after corrosion of the stainless steel will significantly increase the time to earliest criticality, particularly at anything but the highest rate of package flushing. Once combined with the probability of the WP being able to hold water, which decreases as a function of time, a limit on the time frame for internal criticality concerns may be established.

- For very small values of the trapped boron fraction, the dominant parameters are generally the stainless steel corrosion rate, the drip rate, and the exchange rate. The exception is for low values of the drip rate and exchange rate; the earliest time to criticality will be insensitive to the borated stainless steel corrosion rate because the time is much longer than the time to corrode the borated stainless steel even at the lower corrosion rate.

- For a WP which achieves criticality, the consequences measured in curies of increased inventory of radionuclides will increase with increasing criticality duration. For the longest likely duration (10,000 years) the increase in curies of the 36 nuclides of greatest interest to Performance Assessment will be approximately 24% (with respect to the same SNF decayed to the same time) immediately after the ending of criticality and less than 10% 40,000 years later. Even these small percentages are stated overly-conservative because they are with respect to the criticality design basis fuel which has a burnup of only 20,000 MWd/MTU. Typical PWR fuel will have more than twice this burnup from its reactor history, and therefore have twice as large decay radiation at any time of comparison. For such fuel the percentage increases in curies would be less than half the values calculated here.

From the results of this analysis it is recommended that future studies should:

- Consider relevant design modifications:
    - Examine the possibility of thickening the borated stainless steel plates to reduce the ratio of surface area to volume, thereby decreasing the kg/yr corrosion rate, for the same micron/yr corrosion rate.

- Incorporate the results of ongoing materials investigations, including
    - Quantify the boride trapping in the iron oxide, and study the metallurgy of boride formation and the rate of boride dissolution.
    - Record observations regarding the integrity of the oxide corrosion products during future corrosion testing of carbon steels and borated stainless steels.

- Refine the analysis to evaluate certain physical effects neglected in the present approximation:
    - WP corrosion model with a unique characterization of penetration of the bottom, distinguishing between before and after penetrationfrom the top.
    - The filling retardation effects of evaporation.
    - The moderator exclusion effects of mineral buildup.

9. Attachments -

List of Attachments

Attachment	Description	Date	Number of Pages
I	Listing of model program with detailed output	3/26/96	7
II	Input and output files for calculation of results	3/20/96	5
III	MathCad calculation of k_{eff} regression	3/15/96	3
IV	Solubility of Iron From Waste Package Internals	3/21/96	7
V	Calculation details of package drain times, with program listing	3/25/96	3
VI	MathCad calculations of circulation parameters	3/27/96	7
VII	MathCad calculation of steady state criticality power output	3/27/96	13
VIII	MathCad calculation of internal areas and volumes	3/27/96	7
IX	MathCad calculation of activation products	3/27/96	5

Listing of model program with detailed output.

This program was used to calculate earliest possible times to criticality (Tables 7.4-1,2,3,4)

```
/*deltasd.c  This program computes the concentrations of boron and Fe, which are decreasing
with time as a result of corrosion processes and flushing of a waste package filled with water.
The program numerically integrates a set of first order linear differential rate equations defining
the corrosion processes. At each time step it also computes the value of keff as a linear function
of remaining boron and iron.  If the value is greater than a threshold (presently coded as 0.91) the
program will stop.  Othewise it will continue to run until it reaches a minimum concentration of
iron or until it reaches 1 million years.   When the concentration of either steel reaches zero it
may overshoot to a negative value.  The steel concentration is easily corrected to zero, but a
special takeout accounting must correct for the extra addition into the oxide pool caused by the
fictitious negative steel removed.

The program reads input from a file "deltasd.dat" which can contain any number of cases, with
one input line per case.

Output is printed to 2 files: "deltasd.out" which provides a detailed listing of the amounts of iron
at each 1000 year time interval, and "deltasd.log" which lists the relevant parameters at the
completion of each case. */


#include <stdio.h>
#include <stdlib.h>
#include <math.h>
#define TINT 10    //Time step in years for numerical integration
#define PI 2*asin(1) //Value of π
float mfec0=(float)3514.0,      //Initial mass of iron in carbon steel (kg)
    mfes0=(float)1858.0,    //Initial mass of total metals in stainless steel (kg)
    mbs0=(float)30.47,  //Initial mass of boron in stainless steel (kg)
    mbtot,        //Total mass of boron as a function of time
         mfeo,            //Mass of iron oxide
    mfeon,        //Updated value of iron oxide mass
    mfetot,       //Total mass of iron
    nus,         //Stainless steel corrosion rate (input, kg/yr)
    nuc,            //Carbon steel corrosion rate (input, kg/yr)
    rho0,             //Initial flushing rate (computed directly from input, per year)
    rho,             //Actual flushing rate (computed from rho0 according to specified
//time dependence, which is assumed constant in this study)
    s;          //Iron solubility limit (input, kg)
```

```
void main()
{long int t,          //Timekeeping
    tt,          //Time to start flushing, zero in cases for this analysis
    finished,    //variable to test whether each case is finished
    tcr,         //Time at which earliest criticality occurs
    tcyc=50000;        //Period for cyclic flushing time (not used in this analysis)
    int i,            //Dummy variable for testing input status
    count=0;       //Counts number of cases started
float alph,           //Ratio of boron mass to total stainless steel mass
    x,           //Temporary variable
    ex,          //Exchange efficiency (input)
    dr,          //Drip rate (input, mm/yr)
    mbcr,            //Total boron at time of criticality
    mfecr,           //Total iron at time of criticalityy
    keff,           //keff computed from linear regression function
    mfec,            //mass of Fe remaining in carbon steel
    mfecn,           //Updated value of mass of carbon steel (Fe)
    mfes,           //mass of Fe remaining in stainless steel
    mfesn,           //Update value of mass of Fe (equivalent) remaining in stainless
    mbs,         //mass of boron remaining in stainless steel
    mbsn,            //Updated mass of boron remaining in stainless steel
    f,           //Fraction of boron trapped in iron oxide
    mbot,            //Mass of boron trapped in iron oxide as a function of time
    mbotn,        //Updated mass of boron trapped in iron oxide as a function of time
    mbosol,       //Mass of boron in solution as a function of time
    mbosoln;      //Updated mass of boron in solution as a function of time
FILE *fin,                    //Input file pointer
    *fout,           //Detailed output file
    *flog,           //Log output file
    *ferr;           //File for reporting non-standard conditions
char buff[100];        //Dummy variable for read-through of input file header
fin=fopen("deltasd.dat","r");
fout=fopen("deltasd.out","w");
flog =fopen("deltasd.log","w");
ferr=fopen("junk.out","w");
fgets(buff,99,fin);  //Dummy read through data file header line
//Following instruction reads one input case and defines the start of the basic processing loop.
while((i=fscanf(fin, "%f %f %f %f %f %f %ld",&nus,&nuc,&dr,&ex,&f,&s,&tt))!=EOF)
 {printf("read data %d\n",count++);        //Print loop/case count on screen
 fprintf(fout,"nus=%f nuc=%f dr=%f ex=%f f=%f s=%f tt=%ld\n",
              nus,nuc,dr,ex,f,s,tt);  //print out input data in header for detailed listing
 rho0=dr*ex*.005479;       //The constant factor is
```

```
//concentration_fac*horiz_area*(meters/mm)/water_vol according to the              //calculation
sequence for flush/exchange rate given in Section 7.3.5
 fprintf(fout,"%7s%8s%8s%9s%8s%8s%8s%8s%8s\n","Time","B Stl","Tr B Ox",
      "B sltn","Tot B","Tot Fe","Cs Fe","Ss Fe","Oxide"); //Column headers for output file
 t=0;          //The following are initializations for each case loop
 finished=0;
 mbot=0;
 mbotn=0;
 mbosol=0;
 mbosoln=0;
 mfeo=0;
 mfeon=0;
 mbs=mbs0;
 mbsn=mbs;
 mfec=mfec0;
 mfecn=mfec;
 mfes=mfes0;
 mfesn=mfes;
 alph=mbs0/(mfes0+mbs0);
 mfetot=mfec+mfes+mfeo;
 while((mfetot>rho*s)&&(finished==0)&&(t<1000000)) //Start time step loop;
              // Loop until criticality or time limit (1000000 yrs)
  {if(t<tt) rho=0;     //No exchange before designated start; this study always inputs tt=0
  else   //rho=.1*rho0+.45*rho0*(1-cos(PI*t/tcyc)); Used for cyclic infiltration
        //rates, not in this study
    rho=rho0;     //rho will be the variable used in the calculations
  //Iron oxide balance
  mfeon=mfeo+nus*TINT*(mfes>0?1:0)*(1-alph)+nuc*TINT*(mfec>0?1:0)-rho*s*TINT;
  x=rho*TINT;
  if(x>1)mbosoln=0; //Entire volume exchanged in TINT; TINT chosen to prevent this.
  else   //Dissolved boron balance
    mbosoln=mbosol*(1-x)+(1-f)*nus*TINT*alph*(mbs>0?1:0)
              +rho*s*TINT*mbot/mfeon;
                   //Trapped boron balance
  mbotn=mbot+nus*TINT*alph*f*(mbs>0?1:0)-rho*s*TINT*mbot/mfeon;
  if(mfec>0)mfecn=mfec-nuc*TINT;  //Carbon steel balance
  if(mfes>0)mfesn=mfes-nus*TINT*(1-alph);  //Stainless steel Fe balance
  if(mbs>0)mbsn=mbs-nus*TINT*alph;         //Stainless steel B balance
  if(mfecn<0)
   {mfeon+=mfecn;              //Takeout for carbon steel overshoot
   mfecn=0;}
  if(mfesn<0)
```

```
   {mfeon+=mfesn;          //Takeout for stainless steel iron overshoot
   mfesn=0;}
  if(mbsn<0)
   {mbotn+=mbsn;           //Takeout for stainless steel boron overshoot
   mbsn=0;}
  if(mbotn<0)
   {mbosoln+=mbotn;                //Takeout for trapped boron overshoot
   mbotn=0;}
  if(mbosoln<0) mbosoln=0;
  mfec=mfecn;
  mfes=mfesn;
  mbs=mbsn;
  mbot=mbotn;
  mbosol=mbosoln;
  mfeo=mfeon; //Don't bother testing for mfeo<0 since it can't happen
  t+=TINT;
  mbtot=mbs+mbot+mbosol; //Compute total boron
  mfetot=mfec+mfes+mfeo+s;  //Compute total iron
  if(mfes>0) keff=1.026-2.42e-5*mfetot-.00645*mbtot; //Compute keff
  else keff=1.0675-2.213e-5*mfetot-.02363*mbtot;
  if(keff>.91) //Test keff against criticality threshold
    {finished=1; //Finished if threshold is exceeded
    tcr=t;           //Assign criticality time
    mfecr=mfetot; //Assign total iron
    mbcr=mbtot;} //Assign total boron
  if(t%1000==0)    //Print if time is multiple of 1000 years
   fprintf(fout,"%7ld%8.2f%8.5f%9.1e%8.3f%8.1f%8.1f%8.1f%8.1f\n",
     t,mbs,mbot,mbosol,mbtot,mfetot,mfec,mfes,mfeo);}//End timestep loop
 if(finished==1)                          //Print at end of each case
  {fprintf(fout,"first criticality at %ld  Fe=%f  B=%f\n\n\n",
     tcr,mfecr,mbcr);
  fprintf(flog,"nus=%f  nuc=%f  dr=%f ex=%f f=%f  s=%f  tt=%ld\n",
             nus,nuc,dr,ex,f,s,tt);
  fprintf(flog,"first criticality at %ld  Fe=%f  B=%f\n\n",
             tcr,mfecr,mbcr);}
 else                                     //Alternate case print if no criticality
  {fprintf(fout,"No criticality after %ld years\n\n\n",t);
  fprintf(flog,"nus=%f  nuc=%f  dr=%f  ex=%f f=%f  s=%f  tt=%ld\n",
             nus,nuc,dr,ex,f,s,tt);
  fprintf(flog,"no criticality at %ld  Fe=%f  B=%f\n\n",t,mfecr,mbcr);}
 } //End case loop
} //End program
```

Input file for verification case

```
nus    nuc   dr   ex   f    s     tt
.0544  1.65  .53  .01  .02  .021  0
```

Output file for verification case

```
nus=0.054400 nuc=1.650000 dr=0.530000 ex=0.010000 f=0.020000 s=0.021000 tt=0
   Time    B Stl Tr B Ox   B sltn    Tot B   Tot Fe    Cs Fe    Ss Fe    Oxide
   1000    29.59 0.01755 8.5e-001   30.458   5372.0   1864.0   1804.5   1703.5
   2000    28.71 0.03511 1.7e+000   30.421   5372.0    214.0   1750.9   3407.0
   3000    27.84 0.05266 2.5e+000   30.361   5372.0      0.0   1697.4   3674.6
   4000    26.96 0.07022 3.2e+000   30.278   5372.0      0.0   1643.9   3728.1
   5000    26.08 0.08777 4.0e+000   30.173   5372.0      0.0   1590.4   3781.6
   6000    25.20 0.10533 4.7e+000   30.046   5372.0      0.0   1536.8   3835.1
   7000    24.33 0.12288 5.4e+000   29.898   5371.9      0.0   1483.3   3888.6
   8000    23.45 0.14044 6.1e+000   29.730   5371.9      0.0   1429.8   3942.1
   9000    22.57 0.15799 6.8e+000   29.542   5371.9      0.0   1376.2   3995.6
  10000    21.69 0.17555 7.5e+000   29.334   5371.9      0.0   1322.7   4049.2
  11000    20.81 0.19310 8.1e+000   29.108   5371.9      0.0   1269.2   4102.7
  12000    19.94 0.21066 8.7e+000   28.864   5371.9      0.0   1215.7   4156.2
  13000    19.06 0.22821 9.3e+000   28.602   5371.9      0.0   1162.1   4209.7
  14000    18.18 0.24577 9.9e+000   28.323   5371.9      0.0   1108.6   4263.2
  15000    17.30 0.26332 1.0e+001   28.028   5371.8      0.0   1055.1   4316.7
  16000    16.43 0.28087 1.1e+001   27.716   5371.8      0.0   1001.6   4370.3
  17000    15.55 0.29843 1.2e+001   27.389   5371.8      0.0    948.0   4423.8
  18000    14.67 0.31598 1.2e+001   27.046   5371.8      0.0    894.5   4477.3
  19000    13.79 0.33353 1.3e+001   26.689   5371.8      0.0    841.0   4530.8
  20000    12.91 0.35109 1.3e+001   26.317   5371.8      0.0    787.5   4584.3
  21000    12.04 0.36864 1.4e+001   25.931   5371.8      0.0    733.9   4637.8
  22000    11.16 0.38620 1.4e+001   25.531   5371.8      0.0    680.4   4691.3
  23000    10.28 0.40375 1.4e+001   25.119   5371.8      0.0    626.9   4744.9
  24000     9.40 0.42130 1.5e+001   24.693   5371.8      0.0    573.4   4798.4
  25000     8.53 0.43886 1.5e+001   24.255   5371.8      0.0    519.9   4851.9
  26000     7.65 0.45641 1.6e+001   23.805   5371.8      0.0    466.3   4905.4
  27000     6.77 0.47396 1.6e+001   23.344   5371.8      0.0    412.8   4958.9
  28000     5.89 0.49152 1.6e+001   22.871   5371.8      0.0    359.3   5012.4
  29000     5.02 0.50907 1.7e+001   22.387   5371.8      0.0    305.8   5066.0
  30000     4.14 0.52662 1.7e+001   21.892   5371.7      0.0    252.3   5119.5
  31000     3.26 0.54418 1.8e+001   21.386   5371.7      0.0    198.7   5173.0
  32000     2.38 0.56173 1.8e+001   20.871   5371.7      0.0    145.2   5226.5
  33000     1.50 0.57928 1.8e+001   20.345   5371.7      0.0     91.7   5280.0
  34000     0.63 0.59684 1.9e+001   19.810   5371.7      0.0     38.2   5333.5
  35000     0.00 0.60393 1.9e+001   19.267   5371.7      0.0      0.0   5371.7
  36000     0.00 0.60393 1.8e+001   18.733   5371.7      0.0      0.0   5371.7
  37000     0.00 0.60393 1.8e+001   18.214   5371.7      0.0      0.0   5371.7
  38000     0.00 0.60393 1.7e+001   17.710   5371.7      0.0      0.0   5371.7
  39000     0.00 0.60393 1.7e+001   17.220   5371.7      0.0      0.0   5371.7
  40000     0.00 0.60393 1.6e+001   16.744   5371.7      0.0      0.0   5371.7
  41000     0.00 0.60393 1.6e+001   16.282   5371.7      0.0      0.0   5371.7
  42000     0.00 0.60393 1.5e+001   15.834   5371.7      0.0      0.0   5371.7
  43000     0.00 0.60393 1.5e+001   15.398   5371.7      0.0      0.0   5371.7
  44000     0.00 0.60393 1.4e+001   14.974   5371.7      0.0      0.0   5371.7
  45000     0.00 0.60393 1.4e+001   14.563   5371.7      0.0      0.0   5371.7
  46000     0.00 0.60393 1.4e+001   14.163   5371.7      0.0      0.0   5371.7
  47000     0.00 0.60393 1.3e+001   13.775   5371.7      0.0      0.0   5371.7
```

```
 48000    0.00 0.60393 1.3e+001  13.398  5371.7     0.0     0.0 5371.7
 49000    0.00 0.60393 1.2e+001  13.032  5371.7     0.0     0.0 5371.7
 50000    0.00 0.60393 1.2e+001  12.676  5371.7     0.0     0.0 5371.7
 51000    0.00 0.60393 1.2e+001  12.330  5371.7     0.0     0.0 5371.7
 52000    0.00 0.60393 1.1e+001  11.995  5371.7     0.0     0.0 5371.7
 53000    0.00 0.60393 1.1e+001  11.669  5371.7     0.0     0.0 5371.7
 54000    0.00 0.60393 1.1e+001  11.352  5371.7     0.0     0.0 5371.7
 55000    0.00 0.60393 1.0e+001  11.044  5371.7     0.0     0.0 5371.7
 56000    0.00 0.60393 1.0e+001  10.745  5371.7     0.0     0.0 5371.7
 57000    0.00 0.60393 9.9e+000  10.455  5371.7     0.0     0.0 5371.7
 58000    0.00 0.60393 9.6e+000  10.173  5371.7     0.0     0.0 5371.7
 59000    0.00 0.60393 9.3e+000   9.899  5371.7     0.0     0.0 5371.7
 60000    0.00 0.60393 9.0e+000   9.633  5371.7     0.0     0.0 5371.7
 61000    0.00 0.60393 8.8e+000   9.375  5371.7     0.0     0.0 5371.7
 62000    0.00 0.60393 8.5e+000   9.124  5371.7     0.0     0.0 5371.7
 63000    0.00 0.60393 8.3e+000   8.880  5371.7     0.0     0.0 5371.7
 64000    0.00 0.60393 8.0e+000   8.643  5371.7     0.0     0.0 5371.7
 65000    0.00 0.60393 7.8e+000   8.413  5371.7     0.0     0.0 5371.7
 66000    0.00 0.60393 7.6e+000   8.189  5371.7     0.0     0.0 5371.7
 67000    0.00 0.60393 7.4e+000   7.972  5371.7     0.0     0.0 5371.7
 68000    0.00 0.60393 7.2e+000   7.761  5371.7     0.0     0.0 5371.7
 69000    0.00 0.60393 7.0e+000   7.556  5371.7     0.0     0.0 5371.7
 70000    0.00 0.60393 6.8e+000   7.357  5371.7     0.0     0.0 5371.7
 71000    0.00 0.60393 6.6e+000   7.164  5371.7     0.0     0.0 5371.7
 72000    0.00 0.60393 6.4e+000   6.976  5371.7     0.0     0.0 5371.7
 73000    0.00 0.60393 6.2e+000   6.794  5371.7     0.0     0.0 5371.7
 74000    0.00 0.60393 6.0e+000   6.617  5371.7     0.0     0.0 5371.7
 75000    0.00 0.60393 5.8e+000   6.444  5371.7     0.0     0.0 5371.7
 76000    0.00 0.60393 5.7e+000   6.277  5371.7     0.0     0.0 5371.7
 77000    0.00 0.60393 5.5e+000   6.115  5371.7     0.0     0.0 5371.7
 78000    0.00 0.60393 5.4e+000   5.957  5371.7     0.0     0.0 5371.7
 79000    0.00 0.60393 5.2e+000   5.804  5371.7     0.0     0.0 5371.7
 80000    0.00 0.60393 5.1e+000   5.655  5371.7     0.0     0.0 5371.7
 81000    0.00 0.60393 4.9e+000   5.510  5371.7     0.0     0.0 5371.7
 82000    0.00 0.60393 4.8e+000   5.370  5371.7     0.0     0.0 5371.7
 83000    0.00 0.60393 4.6e+000   5.234  5371.7     0.0     0.0 5371.7
 84000    0.00 0.60393 4.5e+000   5.101  5371.7     0.0     0.0 5371.7
 85000    0.00 0.60393 4.4e+000   4.972  5371.7     0.0     0.0 5371.7
 86000    0.00 0.60393 4.2e+000   4.847  5371.7     0.0     0.0 5371.7
 87000    0.00 0.60393 4.1e+000   4.726  5371.7     0.0     0.0 5371.7
 88000    0.00 0.60393 4.0e+000   4.608  5371.7     0.0     0.0 5371.7
 89000    0.00 0.60393 3.9e+000   4.493  5371.7     0.0     0.0 5371.7
 90000    0.00 0.60393 3.8e+000   4.382  5371.7     0.0     0.0 5371.7
 91000    0.00 0.60393 3.7e+000   4.274  5371.7     0.0     0.0 5371.7
 92000    0.00 0.60393 3.6e+000   4.169  5371.7     0.0     0.0 5371.7
 93000    0.00 0.60393 3.5e+000   4.067  5371.7     0.0     0.0 5371.7
 94000    0.00 0.60393 3.4e+000   3.968  5371.7     0.0     0.0 5371.7
 95000    0.00 0.60393 3.3e+000   3.871  5371.7     0.0     0.0 5371.7
 96000    0.00 0.60393 3.2e+000   3.778  5371.7     0.0     0.0 5371.7
 97000    0.00 0.60393 3.1e+000   3.687  5371.7     0.0     0.0 5371.7
 98000    0.00 0.60393 3.0e+000   3.599  5371.7     0.0     0.0 5371.7
 99000    0.00 0.60393 2.9e+000   3.513  5371.7     0.0     0.0 5371.7
100000    0.00 0.60393 2.8e+000   3.430  5371.7     0.0     0.0 5371.7
101000    0.00 0.60393 2.7e+000   3.349  5371.7     0.0     0.0 5371.7
102000    0.00 0.60393 2.7e+000   3.270  5371.7     0.0     0.0 5371.7
103000    0.00 0.60393 2.6e+000   3.194  5371.7     0.0     0.0 5371.7
```

```
 104000     0.00 0.60393 2.5e+000   3.120  5371.7      0.0      0.0  5371.7
 105000     0.00 0.60393 2.4e+000   3.048  5371.7      0.0      0.0  5371.7
 106000     0.00 0.60393 2.4e+000   2.978  5371.7      0.0      0.0  5371.7
 107000     0.00 0.60393 2.3e+000   2.910  5371.7      0.0      0.0  5371.7
 108000     0.00 0.60393 2.2e+000   2.844  5371.7      0.0      0.0  5371.7
 109000     0.00 0.60393 2.2e+000   2.780  5371.7      0.0      0.0  5371.7
 110000     0.00 0.60393 2.1e+000   2.717  5371.7      0.0      0.0  5371.7
 111000     0.00 0.60393 2.1e+000   2.657  5371.7      0.0      0.0  5371.7
 112000     0.00 0.60393 2.0e+000   2.598  5371.7      0.0      0.0  5371.7
 113000     0.00 0.60393 1.9e+000   2.541  5371.7      0.0      0.0  5371.7
 114000     0.00 0.60393 1.9e+000   2.486  5371.7      0.0      0.0  5371.7
 115000     0.00 0.60393 1.8e+000   2.432  5371.7      0.0      0.0  5371.7
 116000     0.00 0.60393 1.8e+000   2.379  5371.7      0.0      0.0  5371.7
 117000     0.00 0.60393 1.7e+000   2.329  5371.7      0.0      0.0  5371.7
 118000     0.00 0.60393 1.7e+000   2.279  5371.7      0.0      0.0  5371.7
 119000     0.00 0.60393 1.6e+000   2.231  5371.7      0.0      0.0  5371.7
 120000     0.00 0.60393 1.6e+000   2.185  5371.7      0.0      0.0  5371.7
 121000     0.00 0.60393 1.5e+000   2.139  5371.7      0.0      0.0  5371.7
 122000     0.00 0.60393 1.5e+000   2.095  5371.7      0.0      0.0  5371.7
 123000     0.00 0.60393 1.4e+000   2.053  5371.7      0.0      0.0  5371.7
 124000     0.00 0.60393 1.4e+000   2.011  5371.7      0.0      0.0  5371.7
 125000     0.00 0.60393 1.4e+000   1.971  5371.7      0.0      0.0  5371.7
 126000     0.00 0.60393 1.3e+000   1.932  5371.7      0.0      0.0  5371.7
 127000     0.00 0.60393 1.3e+000   1.894  5371.7      0.0      0.0  5371.7
 128000     0.00 0.60393 1.3e+000   1.857  5371.7      0.0      0.0  5371.7
 129000     0.00 0.60393 1.2e+000   1.821  5371.7      0.0      0.0  5371.7
 130000     0.00 0.60393 1.2e+000   1.786  5371.7      0.0      0.0  5371.7
 131000     0.00 0.60393 1.1e+000   1.752  5371.7      0.0      0.0  5371.7
 132000     0.00 0.60393 1.1e+000   1.720  5371.7      0.0      0.0  5371.7
 133000     0.00 0.60393 1.1e+000   1.688  5371.7      0.0      0.0  5371.7
 134000     0.00 0.60393 1.1e+000   1.657  5371.7      0.0      0.0  5371.7
first criticality at 134730  Fe=5371.716309  B=1.634483
```

Input and output files for calculation of results.

For Table 7.4-1

Input file: 1bad.dat 3/20/96 1:44pm

```
nus   nuc   dr   ex   f   s    tt
.0544 1.65  .53  .01 .02 .021  0
.163  1.65  .53  .01 .02 .021  0
.0544 1.65  .53  .01 .05 1.33  0
.163  1.65  .53  .01 .05 1.33  0
.0544 1.65  7.19 .01 .05 .021  0
.163  1.65  7.19 .01 .05 .021  0
.0544 1.65  .53  .10 .05 .021  0
.163  1.65  .53  .10 .05 .021  0
```

Output file: 1bad.log 3/20/96 1:42pm

```
nus=0.054400 nuc=1.650000 dr=0.530000 ex=0.010000 f=0.020000 s=0.021000 tt=0
first criticality at 134730 Fe=5371.716309 B=1.634483

nus=0.163000 nuc=1.650000 dr=0.530000 ex=0.010000 f=0.020000 s=0.021000 tt=0
first criticality at 121700 Fe=5371.854980 B=1.634171

nus=0.054400 nuc=1.650000 dr=0.530000 ex=0.010000 f=0.050000 s=1.330000 tt=0
first criticality at 205990 Fe=5363.217773 B=1.642480

nus=0.163000 nuc=1.650000 dr=0.530000 ex=0.010000 f=0.050000 s=1.330000 tt=0
first criticality at 191840 Fe=5364.198730 B=1.641558

nus=0.054400 nuc=1.650000 dr=7.190000 ex=0.010000 f=0.050000 s=0.021000 tt=0
first criticality at 42070 Fe=5371.711426 B=1.634466

nus=0.163000 nuc=1.650000 dr=7.190000 ex=0.010000 f=0.050000 s=0.021000 tt=0
first criticality at 21580 Fe=5371.790039 B=1.634101

nus=0.054400 nuc=1.650000 dr=0.530000 ex=0.100000 f=0.050000 s=0.021000 tt=0
first criticality at 45750 Fe=5371.712891 B=1.634295

nus=0.163000 nuc=1.650000 dr=0.530000 ex=0.100000 f=0.050000 s=0.021000 tt=0
first criticality at 26110 Fe=5371.851563 B=1.634238
```

For Table 7.4-2

```
Input file: 2bad.dat   3/20/96   1:55pm
nus    nuc   dr  ex  f    s    tt
.0544  1.65  .53  .01  .02  1.33  0
.163   1.65  .53  .01  .02  1.33  0
.0544  1.65  7.19 .01  .02  .021  0
.163   1.65  7.19 .01  .02  .021  0
.0544  1.65   .53  .1  .02  .021  0
.163   1.65   .53  .1  .02  .021  0
.0544  1.65  7.19 .01  .050  1.33   0
.163   1.65  7.19 .01  .050  1.33   0
.0544  1.65  .53   .1 .050  1.33   0
.163   1.65  .53   .1 .050  1.33   0
.0544  1.65  7.19  .1 .050  021    0
.163   1.65  7.19  .1 .050  .021   0
```

```
Output file: 2bad.log   3/20/96   1:65 pm
nus=0.054400  nuc=1.650000  dr=0.530000 ex=0.010000 f=0.020000  s=1.330000  tt=0
first criticality at 134560  Fe=5366.705566  B=1.639052

nus=0.163000  nuc=1.650000  dr=0.530000 ex=0.010000 f=0.020000  s=1.330000  tt=0
first criticality at 121550  Fe=5367.630859  B=1.638149

nus=0.054400  nuc=1.650000  dr=7.190000 ex=0.010000 f=0.020000  s=0.021000  tt=0
first criticality at 36630  Fe=5371.711426  B=1.631306

nus=0.163000  nuc=1.650000  dr=7.190000 ex=0.010000 f=0.020000  s=0.021000  tt=0
first criticality at 16240  Fe=5371.790039  B=1.631034

nus=0.054400  nuc=1.650000  dr=0.530000 ex=0.100000 f=0.020000  s=0.021000  tt=0
first criticality at 38360  Fe=5371.712891  B=1.631643

nus=0.163000  nuc=1.650000  dr=0.530000 ex=0.100000 f=0.020000  s=0.021000  tt=0
first criticality at 18860  Fe=5371.851563  B=1.632715

nus=0.054400  nuc=1.650000  dr=7.190000 ex=0.010000 f=0.050000  s=1.330000  tt=0
first criticality at 41620  Fe=5350.931641  B=1.653565

nus=0.163000  nuc=1.650000  dr=7.190000 ex=0.010000 f=0.050000  s=1.330000  tt=0
first criticality at 21360  Fe=5362.100586  B=1.643093
```

```
nus=0.054400  nuc=1.650000  dr=0.530000 ex=0.100000 f=0.050000  s=1.330000  tt=0
first criticality at 45250  Fe=5355.360352  B=1.649592

nus=0.163000  nuc=1.650000  dr=0.530000 ex=0.100000 f=0.050000  s=1.330000  tt=0
first criticality at 25840  Fe=5363.080078  B=1.642268

nus=0.054400  nuc=1.650000  dr=7.190000 ex=0.100000 f=0.050000  s=21.000000  tt=0
first criticality at 28450  Fe=3039.489990  B=6.573341

nus=0.163000  nuc=1.650000  dr=7.190000 ex=0.100000 f=0.050000  s=0.021000  tt=0
first criticality at 12000  Fe=5371.093262  B=1.634312
```

For Table 7.4-3

Input file: 1sbad.dat 3/20/96 1:47pm

```
nus   nuc    dr  ex    f     s    tt
.0544  1.65   .53  .01    0  .021  0
.163   1.65   .53  .01    0  .021  0
.0544  1.65   .53  .01   .055  1.33   0
.163   1.65   .53  .01   .055  1.33   0
.0544  1.65   7.19 .01   .055 .021   0
.163   1.65   7.19 .01   .055 .021   0
.0544  1.65   .53  .1   .055  .021  0
.163   1.65   .53  .1   .055  .021  0
```

Output file: 1sbad.log 3/20/96 1:49pm

```
nus=0.054400  nuc=1.650000  dr=0.530000 ex=0.010000 f=0.000000  s=0.021000  tt=0
first criticality at 119540  Fe=5371.716309  B=1.634217

nus=0.163000  nuc=1.650000  dr=0.530000 ex=0.010000 f=0.000000  s=0.021000  tt=0
first criticality at 106690  Fe=5371.854980  B=1.634337

nus=0.054400  nuc=1.650000  dr=0.530000 ex=0.010000 f=0.055000  s=1.330000  tt=0
first criticality at 661280  Fe=5340.986816  B=1.663308

nus=0.163000  nuc=1.650000  dr=0.530000 ex=0.010000 f=0.055000  s=1.330000  tt=0
first criticality at 563690  Fe=5346.041992  B=1.658573

nus=0.054400  nuc=1.650000  dr=7.190000  ex=0.010000 f=0.055000  s=0.021000  tt=0
no criticality at 1000000  Fe=5346.041992  B=1.658573
```

```
nus=0.163000  nuc=1.650000  dr=7.190000  ex=0.010000 f=0.055000  s=0.021000  tt=0
no criticality at 1000000  Fe=5346.041992  B=1.658573

nus=0.054400  nuc=1.650000  dr=0.530000  ex=0.100000 f=0.055000  s=0.021000  tt=0
no criticality at 1000000  Fe=5346.041992  B=1.658573

nus=0.163000  nuc=1.650000  dr=0.530000  ex=0.100000 f=0.055000  s=0.021000  tt=0
no criticality at 1000000  Fe=5346.041992  B=1.658573
```

For Table 7.4-4

Input file: 2sbad.dat   3/20/96   1:50pm

```
nus    nuc    dr  ex    f     s    tt
.0544  1.65   .53  .01   0    1.33  0
.163   1.65   .53  .01   0  1.33   0
.0544  1.65   7.19 .01   0    .021   0
.163   1.65   7.19 .01   0    .021   0
.0544  1.65    .53  .1   0   .021   0
.163   1.65    .53  .1   0   .021    0
.0544  1.65   7.19 .01  .055  1.33    0
.163   1.65   7.19 .01  .055  1.33    0
.0544  1.65   .53   .1 .055   1.33    0
.163   1.65   .53   .1 .055  1.33   0
.0544  1.65   7.19   .1 .055   .021    0
.163   1.65   7.19  .1 .055  .021    0
```

Output file: 2sbad.log   3/20/96 1:51pm

```
nus=0.054400  nuc=1.650000  dr=0.530000 ex=0.010000 f=0.000000  s=1.330000  tt=0
first criticality at 119450  Fe=5367.443359  B=1.638494

nus=0.163000  nuc=1.650000  dr=0.530000 ex=0.010000 f=0.000000  s=1.330000  tt=0
first criticality at 106620  Fe=5368.359863  B=1.637663

nus=0.054400  nuc=1.650000  dr=7.190000 ex=0.010000 f=0.000000  s=0.021000  tt=0
first criticality at 35500  Fe=5371.711426  B=1.633551

nus=0.163000  nuc=1.650000  dr=7.190000 ex=0.010000 f=0.000000  s=0.021000  tt=0
first criticality at 15130  Fe=5371.790039  B=1.630845
```

```
nus=0.054400  nuc=1.650000  dr=0.530000 ex=0.100000 f=0.000000  s=0.021000  tt=0
first criticality at 36830  Fe=5371.712891  B=1.633362

nus=0.163000  nuc=1.650000  dr=0.530000 ex=0.100000 f=0.000000  s=0.021000  tt=0
first criticality at 17360  Fe=5371.851563  B=1.631060

nus=0.054400  nuc=1.650000  dr=7.190000 ex=0.010000 f=0.055000  s=1.330000  tt=0
first criticality at 60530  Fe=5340.774902  B=1.663501

nus=0.163000  nuc=1.650000  dr=7.190000 ex=0.010000 f=0.055000  s=1.330000  tt=0
first criticality at 49650  Fe=5346.905762  B=1.657764

nus=0.054400  nuc=1.650000  dr=0.530000 ex=0.100000 f=0.055000  s=1.330000  tt=0
first criticality at 81320  Fe=5341.270508  B=1.663038

nus=0.163000  nuc=1.650000  dr=0.530000 ex=0.100000 f=0.055000  s=1.330000  tt=0
first criticality at 67270  Fe=5346.896484  B=1.657773

nus=0.054400  nuc=1.650000  dr=7.190000 ex=0.100000 f=0.055000  s=0.021000  tt=0
first criticality at 317670  Fe=5340.955078  B=1.663337

nus=0.163000  nuc=1.650000  dr=7.190000 ex=0.100000 f=0.055000  s=0.021000  tt=0
first criticality at 268070  Fe=5346.086426  B=1.658531
```

TRIVARIATE REGRESSION FOR k_{eff} AS A FUNCTION OF Fe AND B MASS REMAINING IN THE WP BASKET

Load Data $\quad \mathrm{DATA} := \mathrm{READPRN}(\mathrm{kdata}_{\mathrm{prn}})$

Case 1: Compoisite of All 17 Data Points

$i := 0 .. 16$

Set Up A and y matricies

$A_{i,0} := 1 \qquad A_{i,1} := \mathrm{DATA}_{i,0} \qquad A_{i,2} := \mathrm{DATA}_{i,1} \qquad y_i := \mathrm{DATA}_{i,2}$

Solve for λ vector

$$\lambda := \left(A^T \cdot A\right)^{-1} \cdot A^T \cdot y \qquad \lambda = \begin{bmatrix} 0.98908 \\ -1.31641 \cdot 10^{-5} \\ -0.00679 \end{bmatrix} \qquad y^{<1>} := A \cdot \lambda$$

Calculate R^2

$j := 0 .. 2$

$$M_{0,j} := \frac{\sum_{i=0}^{16} A_{i,j}}{17} \qquad M = \begin{pmatrix} 1 & 3.884 \cdot 10^3 & 4.694 \end{pmatrix}$$

$my := M \cdot \lambda$

$$Rsq := 1 - \frac{\sum_{i=0}^{16} \left(y_{i,0} - y_{i,1}\right)^2}{\sum_{i=0}^{16} \left(y_{i,0} - my\right)^2} \qquad Rsq = 0.536$$

k_{eff}

y =

	calc	fit
	0	1
0	0.851	0.846
1	0.917	0.873
2	0.857	0.877
3	0.88	0.89
4	0.887	0.897
5	0.908	0.911
6	0.944	0.938
7	0.928	0.906
8	0.913	0.902
9	0.89	0.896
10	0.979	0.934
11	0.941	0.924
12	0.902	0.913
13	0.872	0.903
14	0.947	0.941
15	0.909	0.931
16	0.879	0.92

DATA =

	Fe (kg)	B(kg)	k_{eff}
	0	1	2
0	$2.978 \cdot 10^3$	15.25	0.851
1	929	15.25	0.917
2	$4.608 \cdot 10^3$	7.625	0.857
3	$3.572 \cdot 10^3$	7.625	0.88
4	$5.399 \cdot 10^3$	3.05	0.887
5	$4.392 \cdot 10^3$	3.05	0.908
6	$2.271 \cdot 10^3$	3.05	0.944
7	$6.283 \cdot 10^3$	0	0.928
8	$6.283 \cdot 10^3$	0.6	0.913
9	$6.283 \cdot 10^3$	1.5	0.89
10	$4.188 \cdot 10^3$	0	0.979
11	$4.188 \cdot 10^3$	1.5	0.941
12	$4.188 \cdot 10^3$	3.05	0.902
13	$4.188 \cdot 10^3$	4.55	0.872
14	$2.094 \cdot 10^3$	3.05	0.947
15	$2.094 \cdot 10^3$	4.55	0.909
16	$2.094 \cdot 10^3$	6.1	0.879

Case 2: First Seven Data Points - Partial Basket

$i := 0..6$

Set Up A and y matricies

$A1_{i,0} := 1$ $A1_{i,1} := DATA_{i,0}$ $A1_{i,2} := DATA_{i,1}$ $y1_i := DATA_{i,2}$

Solve for λ vector

$\lambda := \left(A1^T \cdot A1\right)^{-1} \cdot A1^T \cdot y1$ $\lambda = \begin{bmatrix} 1.02613 \\ -2.42204 \cdot 10^{-5} \\ -0.00645 \end{bmatrix}$ $y1^{<1>} := A1 \cdot \lambda$

$$y1 = \begin{array}{c} k_{eff} \\ \begin{array}{cc} \text{calc} & \text{fit} \end{array} \\ \begin{bmatrix} 0.851 & 0.856 \\ 0.917 & 0.905 \\ 0.857 & 0.865 \\ 0.88 & 0.89 \\ 0.887 & 0.876 \\ 0.908 & 0.9 \\ 0.944 & 0.951 \end{bmatrix} \end{array}$$

Calculate R²

$j := 0..2$

$M1_{0,j} := \dfrac{\sum_{i=0}^{6} A1_{i,j}}{7}$ $M1 = \left(1 \quad 3.45 \cdot 10^3 \quad 7.843\right)$ $my1 := M1 \cdot \lambda$

$Rsq := 1 - \dfrac{\sum_{i=0}^{6} \left(y1_{i,0} - y1_{i,1}\right)^2}{\sum_{i=0}^{6} \left(y1_{i,0} - my1\right)^2}$ $Rsq = 0.912$

Case 3: Last 10 Data Points - Assemblies Touching

$i := 7 .. 16$

Set Up A and y matricies

$A2_{i-7,0} := 1 \qquad A2_{i-7,1} := DATA_{i,0} \qquad A2_{i-7,2} := DATA_{i,1} \qquad y2_{i-7} := DATA_{i,2}$

Solve for λ vector

$$\lambda := \left(A2^{T} \cdot A2\right)^{-1} \cdot A2^{T} \cdot y2 \qquad \lambda = \begin{bmatrix} 1.0675 \\ -2.21316 \cdot 10^{-5} \\ -0.02363 \end{bmatrix} \qquad y2^{<1>} := A2 \cdot \lambda$$

k_{eff}

y2 =

	calc 0	fit 1
0	0.928	0.928
1	0.913	0.914
2	0.89	0.893
3	0.979	0.975
4	0.941	0.939
5	0.902	0.903
6	0.872	0.867
7	0.947	0.949
8	0.909	0.914
9	0.879	0.877

Calculate R^2

$j := 0 .. 2$

$$M2_{0,j} := \frac{\sum_{i=0}^{9} A2_{i,j}}{10} \qquad M2 = \begin{pmatrix} 1 & 4.188 \cdot 10^{3} & 2.49 \end{pmatrix} \qquad my2 := M2 \cdot \lambda$$

$$Rsq := 1 - \frac{\sum_{i=0}^{9} \left(y2_{i,0} - y2_{i,1}\right)^{2}}{\sum_{i=0}^{9} \left(y2_{i,0} - my2\right)^{2}} \qquad Rsq = 0.992$$

SOLUBILITY OF IRON FROM WASTE PACKAGE INTERNALS

This attachment describes a method for predicting the solubility of iron. Dissolution of iron is of interest because one type of waste package for spent nuclear fuel that is currently being considered includes substantial quantities of iron-base materials in the basket.

One of the postulated scenarios is that the container will fill with water. Such filling would require that both the outer and inner containment barriers fail by corrosion. If the containment barriers fail on the top but remain intact on the bottom, water could drip in through the openings and accumulate in the container. (If the bottom of the container also corrodes and perforates, water would not accumulate.) The interior of the container may also be acidified by radiolysis. Removal of iron atoms from the waste package by dissolution and washout, however, requires not only corrosion of the iron but dissolution as well.

When iron-base materials are exposed to water, they are expected to corrode. The anodic half-reaction is

$$Fe(s) \rightarrow Fe^{++} + 2e^{-} \quad . \tag{1}$$

The cathodic half-reactions may be

$$O_2 + 2H_2O + 4e^{-} \rightarrow 4OH^{-} \tag{2}$$

if dissolved oxygen is present or

$$2H^{+} + 2e^{-} \rightarrow H_2 \quad . \tag{3}$$

The latter reaction is fast in acid solution but slow in neutral or alkaline solutions. These corrosion reactions are documented by Shreir (L. L. Shreir, editor, *Corrosion*, 2nd ed., vol. 1, *Metal Environment Reactions*, (Newnes-Butterworths, London, 1976), p. 3:4).

Despite the appearance of the oxidation half-reactions, the products of corrosion are normally solids, not ions. The overall corrosion reactions might be represented as

$$Fe(s) + 2H_2O \rightarrow Fe(OH)_2(s) + H_2 \quad . \tag{4}$$

If conditions are sufficiently oxidizing, additional oxidation may occur and the overall reaction might be written as

$$Fe(s) + 3H_2O \rightarrow Fe(OH)_3(s) + \tfrac{3}{2}H_2 \quad . \tag{5}$$

or

$$Fe(s) + \tfrac{1}{2}H_2O + \tfrac{3}{4}O_2 \rightarrow FeOOH(s) \tag{6}$$

Formation of the divalent corrosion product ($Fe(OH)_2$) would be expected under reducing conditions and formation of the trivalent corrosion products ($Fe(OH)_3$ and FeOOH) would be expected under oxidizing conditions. The level of hydration is immaterial because water will be present in excess. Depending on the oxygen supply, the conditions may be either reducing or oxidizing. Both cases are treated below.

The current assumption about water chemistry is that water that may drip onto a waste package will be similar to J-13 well water. The composition of this water is given in the *Preliminary Near-Field Environment Report* (UCRL-LR-107476, April 1993, vol. 2, p. 38). Here the mean value of pH is given as 7.41 and the mean value of alkalinity as HCO_3^- is 128.9 mg/L. From the atomic masses of the elements, this is found to be 0.0021 molar. (Because of the variability in composition, additional decimal places would be insignificant.) Carbonate has ionization equilibria as follows:

$$H_2CO_3(aq) = HCO_3^- + H^+ \qquad \log_{10}K = -6.3 \tag{7}$$

$$HCO_3^- = CO_3^{--} + H^+ \qquad \log_{10}K = -10.3 \ . \tag{8}$$

In addition, water itself dissociates to a small extent:

$$H_2O = H^+ + OH^- \qquad \log_{10}K = -14.0 \tag{9}$$

The equilibrium constants are from Stumm and Morgan (Werner Stumm and James J. Morgan, *Aquatic Chemistry: An Introduction Emphasizing Chemical Equilibrium in Natural Waters* (John Wiley and Sons, New York, 1981, p. 246). According to UCRL-LR-107476 (loc. cit.), J-13 water contains other dissolved species, most of which are present in small concentrations. The exceptions are Na (sic) and Si (sic). Sodium will be present as Na^+ because NaOH is a strong base and will be completely dissociated. Silicon will be present as H_4SiO_4 because silicic acid is a very weak acid and is essentially unionized for $pH < 8.5$ (Stumm and Morgan, op. cit., p. 541). Since silicic acid does not react to release or consume hydrogen ions under the pH values of interest, its presence may be neglected.

To represent J-13 water accurately, the concentration of Na^+ may be adjusted to provide agreement in pH. In such a calculation, six species should be included: Na^+, H^+, OH^-, $H_2CO_3(aq)$, HCO_3^-, and CO_3^{--}. The six equations that must be satisified are

$$[H^+] = 10^{-7.41} \tag{10}$$

$$[H_2CO_3(aq)] + [HCO_3^-] + [CO_3^{--}] = 0.0021 \tag{11}$$

$$\frac{[H^+][HCO_3^-]}{[H_2CO_3(aq)]} = 10^{-6.3} \tag{12}$$

$$\frac{[H^+][CO_3^{--}]}{[HCO_3^-]} = 10^{-10.3} \tag{13}$$

$$[H^+][OH^-] = 10^{-14.0} \tag{14}$$

$$[H^+] + [Na^+] = [HCO_3^-] + 2[CO_3^{--}] + [OH^-] \tag{15}$$

These equations use the bracket notation of aqueous chemistry: [X] is the concentration of solute species X. The standard state for each solute species is taken so that the thermodynamic activity is numerically equal to the molarity of the species for dilute solutions. The activities of the solvent and solid phases are taken to be 1. Equations 10 and 11 result from the measured values of pH and alkalinity as HCO_3^- cited above. Equations 12 through 14 result from equations 7 through 9 above. Equation 15 represents the requirement that the net electrical charge of the solution must be zero.

The solution to these equations is (approximately)

$[Na^+] = 1.95 \times 10^{-3}$
$[H^+] = 3.89 \times 10^{-8}$
$[OH^-] = 2.57 \times 10^{-7}$
$[H_2CO_3(aq)] = 1.51 \times 10^{-4}$
$[HCO_3^-] = 1.95 \times 10^{-3}$
$[CO_3^{--}] = 2.51 \times 10^{-6}$.

The value of $[Na^+]$ is in good agreement with that in the *Preliminary Near-Field Environment Report*, which is 45.8 mg/L or 1.99×10^{-3} molar. The precision of the values is larger than is justified by the accuracy of the data; this is to allow for more accurate checking of results.

A waste package partially filled with water will contain humid air and will have a radiation field that can cause radiolytic production of nitric acid, HNO_3. Nitric acid is a strong acid, that is, it dissociates in water to H^+ and NO_3^-. In view of the limited amounts of nitric acid that are expected to be produced in a waste package, it is reasonable to suppose that the concentration of acid for water in the waste package will be no larger than 0.01 molar.

For dissolution of $Fe(OH)_2$, Stumm and Morgan (op. cit., p. 241) give the reaction

$$Fe(OH)_2(s) + 2H^+ = Fe^{++} + 2H_2O \qquad \log_{10}K = 12.85 \ , \tag{16}$$

where K is the equilibrium constant. The Fe^{++} ions may also form other species:

$$Fe^{++} + H_2O = FeOH^+ + H^+ \qquad \log_{10}K = -9.5 \tag{17}$$

$$Fe^{++} + 2H_2O = HFeO_2^- + 3H^+ \qquad \log_{10}K = -30.95 \tag{18}$$

The equilibrium constant for equation 17 is Stumm and Morgan (ibid.), and the equilibrium constant for equation 18 is obtained by combining equation 16 (reversed) with the following equation:

$$Fe(OH)_2(s) = H^+ + HFeO_2^- \qquad \log_{10}K = -18.1 \tag{19}$$

The equilibrium constant for equation 19 is deduced from a Pourbaix (potential-pH) diagram given by Jones (Denny A. Jones, *Principles and Prevention of Corrosion* (Macmillan, New York, 1992, p. 60)). Jones's datum is that for reducing water, $Fe(OH)_2(s)$ is in equilibrium with 10^{-6} molar $HFeO_2^-$ at pH = 12.1. Under these conditions, $[H^+] = 10^{-12.1}$ and $[HFeO_2^-] = 10^{-6}$. Since $Fe(OH)_2(s)$ is present as a solid, its activity is 1 and thus $K = 10^{-18.1}$. Aqueous, unionized $Fe(OH)_2$ is apparently never present in significant concentrations. Since the various reactions above involve H^+ ions, the distribution of iron among solid $Fe(OH)_2$ and the aqueous species will depend on the pH. Equally important is that redistribution of the species will also influence the pH.

In treating the dissolution of $Fe(OH)_2$ in J-13 water in the presence of nitric acid, the treatment should include ten dissolved species: Na^+, H^+, OH^-, $H_2CO_3(aq)$, HCO_3^-, CO_3^{--}, NO_3^-, Fe^{++}, $FeOH^+$, and $HFeO_2^-$. Because HNO_3 is a strong acid, it can be assumed to be fully dissociated, so the concentration of NO_3^- will be equal to the concentration of added acid. The following equations may be solved to determine the concentrations of the various species:

$$[Na^+] = 0.00195 \tag{20}$$

$$[NO_3^-] = 0.01 \tag{21}$$

$$\frac{[Fe^{++}]}{[H^+]^2} = 10^{12.85} \tag{22}$$

$$\frac{[FeOH^+][H^+]}{[Fe^{++}]} = 10^{-9.5} \tag{23}$$

$$\frac{[HFeO_2^-][H^+]^3}{[Fe^{++}]} = 10^{-30.95} \tag{24}$$

$$2[Fe^{++}] + [FeOH^{+}] + [H^{+}] + [Na^{+}] = [HFeO_2^{-}] + [OH^{-}] + [NO_3^{-}] + [HCO_3^{-}] + 2[CO_3^{--}] \tag{25}$$

Equation 20 results from the sodium concentration obtained from calculations for J-13 water. Equation 21 results from the postulated amount of nitric acid. Equations 22 through 24 are derived from equations 16 through 18, respectively. Equation 25 represents the requirement for electrical neutrality. In addition, equations 11 through 14 apply.

The solution to these equations is (approximately)

$[Na^+] = 1.95 \times 10^{-3}$
$[H^+] = 2.66 \times 10^{-8}$
$[OH^-] = 3.77 \times 10^{-7}$
$[H_2CO_3(aq)] = 1.05 \times 10^{-4}$
$[HCO_3^-] = 1.99 \times 10^{-3}$
$[CO_3^{--}] = 3.76 \times 10^{-6}$
$[NO_3^-] = 1.00 \times 10^{-2}$
$[Fe^{++}] = 4.99 \times 10^{-3}$
$[FeOH^+] = 5.95 \times 10^{-5}$
$[HFeO_2^-] = 2.99 \times 10^{-11}$.

The total concentration of iron is thus 5.05×10^{-3} molar for reducing conditions with 0.01 molar nitric acid in J-13.

For dissolution of iron under reducing conditions without added acid, the same equations apply except that equation 21 must be changed to set the concentration of nitrate to zero. The solution to these modified equations is (approximately)

$[Na^+] = 1.95 \times 10^{-3}$
$[H^+] = 3.36 \times 10^{-9}$
$[OH^-] = 2.97 \times 10^{-6}$
$[H_2CO_3(aq)] = 1.38 \times 10^{-5}$
$[HCO_3^-] = 2.06 \times 10^{-3}$
$[CO_3^{--}] = 3.06 \times 10^{-5}$
$[NO_3^-] = 0$
$[Fe^{++}] = 8.01 \times 10^{-5}$
$[FeOH^+] = 7.53 \times 10^{-6}$
$[HFeO_2^-] = 2.36 \times 10^{-10}$.

The total concentration of iron is thus 8.77×10^{-5} molar for reducing conditions without acid in J-13. (The values given above are rounded from a more precise solution.)

FeOOH. Stumm and Morgan (op. cit., p. 241) give the following equations for dissolution of amorphous FeOOH:

$$\mathrm{FeOOH(s)} + 3\mathrm{H}^+ = \mathrm{Fe}^{+++} + 2\mathrm{H_2O} \qquad \log_{10}K = 2.5 \tag{26}$$

$$\mathrm{Fe}^{+++} + \mathrm{H_2O} = \mathrm{FeOH}^{++} + \mathrm{H}^+ \qquad \log_{10}K = -2.19 \tag{27}$$

$$\mathrm{Fe}^{+++} + 2\mathrm{H_2O} = \mathrm{Fe(OH)}_2^+ + 2\mathrm{H}^+ \qquad \log_{10}K = -5.67 \tag{28}$$

$$\mathrm{Fe}^{+++} + 3\mathrm{H_2O} = \mathrm{Fe(OH)_3(aq)} + 3\mathrm{H}^+ \qquad \log_{10}K < -12 \tag{29}$$

$$\mathrm{Fe}^{+++} + 4\mathrm{H_2O} = \mathrm{Fe(OH)}_4^- + 4\mathrm{H}^+ \qquad \log_{10}K = -21.6 \tag{30}$$

A treatment of the dissolution of FeOOH in the presence of a strong acid should include twelve dissolved species: $\mathrm{Na^+}$, $\mathrm{H^+}$, $\mathrm{OH^-}$, $\mathrm{H_2CO_3(aq)}$, $\mathrm{HCO_3^-}$, $\mathrm{CO_3^{--}}$, $\mathrm{NO_3^-}$, $\mathrm{Fe^{+++}}$, $\mathrm{FeOH^{++}}$, $\mathrm{Fe(OH)_2^+}$, $\mathrm{Fe(OH)_3(aq)}$, and $\mathrm{Fe(OH)_4^-}$. The applicable equations that can be used to determining the concentrations of the various species are equations 11 through 14, 20, and 21 plus the following six equations:

$$\frac{[\mathrm{Fe}^{+++}]}{[\mathrm{H}^+]^3} = 10^{2.5} \tag{31}$$

$$\frac{[\mathrm{FeOH}^{++}][\mathrm{H}^+]}{[\mathrm{Fe}^{+++}]} = 10^{-2.19} \tag{32}$$

$$\frac{[\mathrm{Fe(OH)}_2^+][\mathrm{H}^+]^2}{[\mathrm{Fe}^{+++}]} = 10^{-5.67} \tag{33}$$

$$\frac{[\mathrm{Fe(OH)_3(aq)}][\mathrm{H}^+]^3}{[\mathrm{Fe}^{+++}]} = 10^{-12} \tag{34}$$

$$\frac{[\mathrm{Fe(OH)}_4^-][\mathrm{H}^+]^4}{[\mathrm{Fe}^{+++}]} = 10^{-21.6} \tag{35}$$

$$\begin{aligned} 3[\mathrm{Fe}^{+++}] + 2[\mathrm{FeOH}^{++}] + [\mathrm{Fe(OH)}_2^+] + [\mathrm{H}^+] + [\mathrm{Na}^+] &= \\ [\mathrm{Fe(OH)}_4^-] + [\mathrm{NO}_3^-] + [\mathrm{OH}^-] + [\mathrm{HCO}_3^-] + 2[\mathrm{CO}_3^{--}] \end{aligned} \tag{36}$$

In equation 34, the equilibrium constant was taken to be 10^{-12}. The value has little effect on the results because $[Fe(OH)_3(aq)]$ is always small. Since this species is electrically neutral, its concentration has no effect on the charge density of the solution.

The solution to these equations is (approximately)

$[Na^+] = 1.95 \times 10^{-3}$
$[H^+] = 7.43 \times 10^{-3}$
$[OH^-] = 1.35 \times 10^{-12}$
$[H_2CO_3(aq)] = 2.10 \times 10^{-3}$
$[HCO_3^-] = 1.42 \times 10^{-7}$
$[CO_3^{--}] = 9.56 \times 10^{-16}$
$[NO_3^-] = 1.00 \times 10^{-2}$
$[Fe^{+++}] = 1.30 \times 10^{-4}$
$[FeOH^{++}] = 1.13 \times 10^{-4}$
$[Fe(OH)_2^+] = 5.02 \times 10^{-6}$
$[Fe(OH)_3(aq)] = 3.16 \times 10^{-10}$
$[Fe(OH)_4^-] = 1.07 \times 10^{-17}$.

The total concentration of iron is thus 2.47×10^{-4} molar for oxidizing conditions with 0.01 molar nitric acid in J-13. (The values given above are rounded from a more precise solution.)

For dissolution of iron under reducing conditions without added acid, the same equations apply except that equation 21 must again be changed to set the concentration of nitrate to zero. The solution to these modified equations is (approximately)

$[Na^+] = 1.95 \times 10^{-3}$
$[H^+] = 3.88 \times 10^{-8}$
$[OH^-] = 2.58 \times 10^{-7}$
$[H_2CO_3(aq)] = 1.51 \times 10^{-4}$
$[HCO_3^-] = 1.95 \times 10^{-3}$
$[CO_3^{--}] = 2.51 \times 10^{-6}$
$[NO_3^-] = 0$
$[Fe^{+++}] = 1.85 \times 10^{-20}$
$[FeOH^{++}] = 3.07 \times 10^{-15}$
$[Fe(OH)_2^+] = 2.62 \times 10^{-11}$
$[Fe(OH)_3(aq)] = 3.16 \times 10^{-10}$
$[Fe(OH)_4^-] = 2.05 \times 10^{-12}$.

The total concentration of iron is thus 3.45×10^{-10} molar for oxidizing conditions without acid in J-13. (The values given above are rounded from a more precise solution.)

Program listing and calculation details for package drain times.

```
/* leak.c  Calculates the time to reduce the water level in the waste  package to zero.  Both
laminar and turbulent formulas are calculated,  but only the lower one is used at any given
integration step.  This is more conservative than simply using a Reynolds number criterion, but the
Reynolds number is also computed for comparison.

The program runs multiple cases by reading one input line for each case and stopping at EOF*/

#include <stdio.h>
#include <math.h>
#include <stdlib.h>
#define PI 2*asin(1)            //Value of π
#define T 3600*24*365           //Number of seconds in a year
#define Tinv 1/3600/24/365   //Reciprocal of seconds in a year

void main()
{float hi,        //Height of water above bottom of package (input, meters)
        l,        //length of drainage hole (input, mm)
        r,        //radius of drainage hole (input, mm)
        dh,       //integration step (input, meters)
        rp=(float).711, //inner radius of package, meters
        il=(float)4.665, //inner length of package, meters
        f=(float).08,  //friction factor
        g=(float)9.8, //acceleration due to gravity
        mu=(float)8.01e-4, //viscosity of water at 30°C
        rho=(float)995.72,    //density of water (kg/cubic meter) at 30°C
        q,              //volumetric flow rate, computed selected from one of the following
        qturb,          //volumetric flow rate, computed by turbulent formula
        qlam,           //volumetric flow rate, computed by laminar formula
        qtot=0,         //cumulated volume drained
        ttot=0,         //cumulated time taken to drain
        re,             //reynolds number, computed by formula
        h,              //height of water as a function of time
        alpha=(float).653; //Voidspace fraction in waste package
int count=0;            //Counter of cases run
char buffer[100];     //Dummy for readthrough of header
FILE *fin,*fout,*flog;
fin=fopen("leak.dat","r");
fout=fopen("leak.out","w");
flog=fopen("leak.log","a");
fgets(buffer,99,fin);  //readthrough header line
```

```
while(fscanf(fin,"%f %f %f %f",&hi,&l,&r,&dh)!=EOF) //read data, start of processing loop
                                                     //for each case
{ fprintf(fout,"\n\nHin=%f  Hole len=%f  Radius=%f  Height step=%f\n",
    hi,l,r,dh);
 l/=1000;                       //Convert mm to meters
 r/=1000;
fprintf(fout,"%11s%11s%11s%11s%11s%11s%11s\n",
  "Time","Height","Reynolds","Vol rate","Vol out","Turb rate","Lam Rate");
for(h=hi;h>0;h-=dh)  //Basic integration loop, decrementing h until it is zero
 {re=2*r*rho*sqrt(g*h*r/f/l)/mu;  //computation of Reynolds number
 qturb=2*PI*r*r*sqrt(g*h*r/f/l);  //turbulent flow derived from eq 8.32 of Ref. 5.21
 qlam=PI*pow(r,4)*rho*(h/l+1)/8/mu;  //laminar flow derived from eq 8.13c of Ref. 5.21
 q=__min(qturb,qlam);             //selection of minimum
 qtot+=alpha*2*il*sqrt(rp*rp-(rp-h)*(rp-h))*dh; //increment of total outflow for this step
 ttot+=alpha*2*il*sqrt(rp*rp-(rp-h)*(rp-h))*dh/q*Tinv; //increment of total time for this step
 fprintf(fout,"%11g%11.2f%11g%11g%11g%11g%11g\n",
   ttot,h,re,q*T,qtot,qturb*T,qlam*T);}
fprintf(flog,"len=%f  radius=%f  aspect=%f  Time=%f\n",1000*l,1000*r,l/r/2,ttot);}}}
```

Input file "leak.dat" 3/16/96

```
hi       len(mm) rad(mm)     dh
1.422      2      .2         .05
1.422     1       .05        .05
```

```
Output file "leak.out"  3/25/96
Hin=1.422000  Hole len=2.000000  Radius=0.200000  Height step=0.050000
       Time     Height   Reynolds   Vol rate    Vol out  Turb rate   Lam Rate
          0       1.42    2075.31    17.5376          0    33.0799    17.5376
 0.00471497       1.37     2038.5    16.9219   0.079786    32.4931    16.9219
  0.0115075       1.32    2001.01    16.3061   0.190545    31.8956    16.3061
   0.019988       1.27     1962.8    15.6903   0.323607    31.2866    15.6903
  0.0299782       1.22    1923.84    15.0745   0.474204    30.6655    15.0745
  0.0413825       1.17    1884.07    14.4587   0.639096    30.0316    14.4587
  0.0541496       1.12    1843.44    13.8429    0.81583     29.384    13.8429
  0.0682565       1.07     1801.9    13.2271    1.00242    28.7218    13.2271
  0.0837005       1.02    1759.37    12.6113    1.19719     28.044    12.6113
   0.100496       0.97     1715.8    11.9956    1.39866    27.3494    11.9956
   0.118671       0.92    1671.08    11.3798    1.60549    26.6367    11.3798
    0.13827       0.87    1625.14     10.764    1.81645    25.9044     10.764
   0.159351       0.82    1577.86    10.1482    2.03039    25.1507    10.1482
   0.181988       0.77    1529.12     9.5324    2.24617    24.3738     9.5324
   0.206276       0.72    1478.77    8.91662    2.46274    23.5713    8.91662
   0.232329       0.67    1426.65    8.30083      2.679    22.7405    8.30083
    0.26029       0.62    1372.55    7.68504    2.89388    21.8781    7.68504
   0.290337       0.57    1316.23    7.06925    3.10629    20.9804    7.06925
   0.322691       0.52    1257.38    6.45346    3.31509    20.0424    6.45346
   0.357634       0.47    1195.65    5.83768    3.51907    19.0584    5.83768
    0.39553       0.42    1130.55    5.22189    3.71696    18.0207    5.22189
   0.436863       0.37    1061.46     4.6061    3.90735    16.9194     4.6061
   0.482297       0.32    987.554    3.99031    4.08864    15.7414    3.99031
```

```
     0.532785          0.27     907.648     3.37452     4.25901     14.4677     3.37452
     0.589778          0.22     819.992     2.75873     4.41624     13.0705     2.75873
     0.655691          0.17     721.768     2.14295     4.55749     11.5048     2.14295
      0.73513          0.12     607.873     1.52716     4.67881     9.68936     1.52716
     0.839339          0.07     466.982     0.91137     4.77378     7.44358     0.91137
      1.02021          0.02     258.135    0.295582     4.82724     4.11461    0.295582


Hin=1.422000  Hole len=1.000000  Radius=0.050000  Height step=0.050000
         Time        Height   Reynolds    Vol rate     Vol out   Turb rate    Lam Rate
      1.02021          1.42    366.866    0.136917     4.82724     1.46194    0.136917
      1.62416          1.37    360.359    0.132106     4.90703     1.43601    0.132106
      2.49426          1.32    353.731    0.127295     5.01779      1.4096    0.127295
      3.58062          1.27    346.978    0.122484     5.15085     1.38268    0.122484
      4.86041          1.22     340.09    0.117673     5.30144     1.35524    0.117673
      6.32141          1.17    333.059    0.112862     5.46634     1.32722    0.112862
      7.95706          1.12    325.877    0.108052     5.64307      1.2986    0.108052
      9.76442          1.07    318.534    0.103241     5.82966     1.26934    0.103241
      11.7432          1.02    311.016   0.0984299     6.02443     1.23938   0.0984299
      13.8952          0.97    303.313   0.0936191      6.2259     1.20868   0.0936191
      16.2241          0.92    295.409   0.0888082     6.43273     1.17719   0.0888082
      18.7357          0.87    287.287   0.0839974     6.64369     1.14482   0.0839974
      21.4373          0.82    278.929   0.0791865     6.85763     1.11152   0.0791865
      24.3386          0.77    270.313   0.0743757     7.07342     1.07718   0.0743757
      27.4517          0.72    261.413   0.0695648     7.28998     1.04171   0.0695648
      30.7915          0.67    252.199    0.064754     7.50624       1.005    0.064754
      34.3763          0.62    242.635   0.0599432     7.72112    0.966885   0.0599432
       38.229          0.57    232.678   0.0551323     7.93353    0.927209   0.0551323
      42.3782          0.52    222.276   0.0503215     8.14233    0.885758   0.0503215
      46.8604          0.47    211.363   0.0455106     8.34631    0.842269   0.0455106
      51.7225          0.42    199.855   0.0406998      8.5442    0.796409   0.0406998
      57.0273          0.37    187.642   0.0358889     8.73459    0.747741   0.0358889
      62.8609          0.32    174.577   0.0310781     8.91588    0.695677   0.0310781
       69.347          0.27    160.451   0.0262672     9.08625    0.639388   0.0262672
      76.6749          0.22    144.955   0.0214564     9.24348    0.577639   0.0214564
      85.1605          0.17    127.592   0.0166455     9.38473    0.508445   0.0166455
      95.4114          0.12    107.458   0.0118347     9.50605    0.428213   0.0118347
      108.933          0.07    82.5515  0.00702386     9.60102    0.328963  0.00702386
      133.091          0.02    45.6322  0.00221301     9.65448    0.181842  0.00221301
```

OXYGEN DIFFUSION CALCULATION

REFERENCES (For Information Only)

5.14 J.P. Holman, "Heat Transfer," 7th Edition, McGraw-Hill Publishing Company, New York, 1990.
5.15 M.J. Moran, H.N. Shapiro, "Fundamentals of Engineering Thermodynamics," John Wiley & Sons, 1988.
5.26 J.H. Perry, "Chemical Engineers Handbook," Third Edition, McGraw-Hill Publishing Company, New York, 1950.
5.17 R.C. Weast, "CRC Handbook of Chemistry and Physics," 66th Edition, Boca Raton, FL, 1985 .
5.6 "AUCF WP Design (21 PWR) Tube Design" Sketches, CRWMS M&O, BBAA00000-01717-2100-16000 thru 16022, REV00A.
5.7 "Characteristics of Potential Repository Wastes," U.S. Department of Energy, DOW/RW-0184-R1 Volume 1, July 1992.
5.27 L.S. Darken, R.W. Gurry, "Physical Chemistry of Metals," McGraw-Hill Publishing Company, 1953.
5.28 F.P. Incropera, D.P. DeWitt, "Introduction to Heat Transfer," John Wiley & Sons, 1985.
5.19 "Final Design Package, Babcock & Wilcox, BR-100 100 Ton Rail/Barge Spent Fuel Shipping Cask," DI# 51-1203400-01, November 1991.
5.29. M.R. Lindeburg, "EIT Reference Manual - 8th Edition," Professional Publications, Inc. Belmont, CA, 1992.
5.30 LWR Radiological PC Database version 1.1, CRWMS M&O, CSCI A0000000-02268-1200-20003, 1991.

MATHCAD UNITS DEFINITION

$kg := 1M$

$g := 10^{\ 3}\cdot kg$

$kmol := mole\cdot 10^{3}$

$s := 1T$

$min := 60\cdot s$

$hr := 60\cdot min$

$day := 24\cdot hr$

$wk := 7\cdot day$

$yr := 365\cdot day$

$m := 1L$

$cm := 10^{-2}\cdot m$

$mm := 10^{\ 3}\cdot m$

$C := 1K$

$N := kg\cdot\frac{m}{s^2}$

$J := N\cdot m$

$kJ := 10^{3}\cdot J$

$Pa := \frac{N}{m^2}$

$MPa := 10^{6}\cdot Pa$

$bars := 10^{5}\cdot Pa$

$atm := 1.0132\cdot 10^{5}\cdot Pa$

21 PWR UNCANISTERED FUEL WP PHYSICAL PARAMETERS

WP Inner Diameter $ID := 1.422 \cdot m$ Ref. 5.6

WP Inner Length $IL := 4.665 \cdot m$ Ref. 5.6

Vol. of one PWR SNF Assembly $VSNF := 0.0807 \cdot m^3$ Ref. 5.19; B&W Mark B

Vol. of New 21 UCF WP Basket Assembly (tubes, SS-B plates, & structural members)

$VBAS := 8.731 \cdot 10^8 \cdot mm^3$ $VBAS = 8.731 \cdot 10^{-1} \cdot m^3$ Ref 5.6 Determined using Pro-Engineer, which is the software used to create the sketches

Total volume occupied by all internal structures (basket & fuel)

$VINT := VBAS + 21 \cdot VSNF$ $VINT = 2.568 \cdot m^3$

Total WP interior void space

$$VOID := \frac{\pi \cdot ID^2}{4} \cdot IL - VINT \qquad VOID = 4.841 \cdot m^3$$

Waste Package Tube Opening

$WPTUBEheight := 228.5 \cdot mm$

WATER SURFACE AREA AS A FUNCTION OF HEIGHT

Table App. 16.C from Ref. 5.29 which contains this relationship is read into CircArea and a function is defined to interpolate from this table to deterimine the wetted perimeter given the water height.

$CircArea := READPRN(circarea_{prn})$ $WettedPerimeter := cspline\left(CircArea^{<0>}, CircArea^{<2>}\right)$

$$Wet(h) := interp\left(WettedPerimeter, CircArea^{<0>}, CircArea^{<2>}, \frac{h}{ID}\right) \cdot ID$$

IB inner circumference wetted

The free surface area at the water line is then defined by the following function.

$$FreeSurf(h) := ID \cdot \sin\left(\frac{Wet(h)}{ID}\right) \cdot IL$$

LOAD IN STEAM TABLES AND WATER VISCOSITY INFORMATION

Read in sat. pressure and sat. liq. specific volume columns from temperature based steam table from Table A-2 of Ref. 5.15. Temperatures are in °C, Presures in bars, and Specific Volumes in cc/g

$$\mathrm{SteamTable} := \mathrm{READPRN}(\mathrm{steamtab}_{\mathrm{prn}})$$

Define vectors of second derivative coefficients using cubic spline function.

$$\mathrm{PSAT} := \mathrm{cspline}\left(\mathrm{SteamTable}^{\langle 0\rangle}, \mathrm{SteamTable}^{\langle 1\rangle}\right)$$

$$\mathrm{SPVOL} := \mathrm{cspline}\left(\mathrm{SteamTable}^{\langle 0\rangle}, \mathrm{SteamTable}^{\langle 2\rangle}\right)$$

Set up functions for interpolating pressure and specific volume as a function of the temperature

$$p(T) := \mathrm{interp}\left(\mathrm{PSAT}, \mathrm{SteamTable}^{\langle 0\rangle}, \mathrm{SteamTable}^{\langle 1\rangle}, T\right)\cdot \mathrm{bars}$$

$$\upsilon(T) := \mathrm{interp}\left(\mathrm{SPVOL}, \mathrm{SteamTable}^{\langle 0\rangle}, \mathrm{SteamTable}^{\langle 2\rangle}, T\right)\cdot \frac{\mathrm{cm}^3}{\mathrm{g}}$$

Water Density as a function of Temperature

$$\rho(T) := \frac{1}{\upsilon(T)}$$

Similarly, the viscosity and specific heat of saturated liquid water as a function of temperature is shown in the TempVisc matrix to the right, and was obtained from Table A-9 of Ref. 5.14.

As above, the vectors of the second derivative coefficients are defined using the cubic spline function

$$\mathrm{Viscosity} := \mathrm{cspline}\left(\mathrm{TempVisc}^{\langle 0\rangle}, \mathrm{TempVisc}^{\langle 1\rangle}\right) \qquad \mathrm{SpHeat} := \mathrm{cspline}\left(\mathrm{TempVisc}^{\langle 0\rangle}, \mathrm{TempVisc}^{\langle 2\rangle}\right)$$

Next, the function for interpolating viscosity as a function of the temperature is defined

$$\mu(T) := \left(\mathrm{interp}\left(\mathrm{Viscosity}, \mathrm{TempVisc}^{\langle 0\rangle}, \mathrm{TempVisc}^{\langle 1\rangle}, T\right)\right)\cdot \frac{\mathrm{kg}}{\mathrm{m}\cdot \mathrm{s}}$$

$$\mathrm{Cp}(T) := \left(\mathrm{interp}\left(\mathrm{SpHeat}, \mathrm{TempVisc}^{\langle 0\rangle}, \mathrm{TempVisc}^{\langle 2\rangle}, T\right)\right)\cdot \frac{\mathrm{kJ}}{\mathrm{kg}\cdot \mathrm{K}}$$

Viscosity and Specific Heat of Sat. Liquid Water as a function of Temperature (C) from Ref. 5.14.

$$\mathrm{TempVisc} := \begin{array}{ccc} \text{Temp} & \mu & \text{Cp} \\ (^{\circ}\text{C}) & \text{kg/m-s} & \text{kJ/kg-}^{\circ}\text{C} \\ \hline 26.67 & 8.6\cdot 10^{-4} & 4.179 \\ 32.22 & 7.65\cdot 10^{-4} & 4.174 \\ 37.78 & 6.82\cdot 10^{-4} & 4.174 \\ 43.33 & 6.16\cdot 10^{-4} & 4.174 \\ 48.89 & 5.62\cdot 10^{-4} & 4.174 \\ 54.44 & 5.13\cdot 10^{-4} & 4.179 \\ 60 & 4.71\cdot 10^{-4} & 4.179 \end{array}$$

THERMAL PROPERTIES OF PWR CRITICALITY DESIGN BASIS FUEL

From Ref. 5.30 for 3% initial enrichment, 20MWd/MTU

$$\mathrm{PWRHEAT} := \begin{bmatrix} 13.26 \\ 9.95 \\ 6.22 \\ 2.38 \\ 0.831 \end{bmatrix} \cdot \frac{\mathrm{watt}}{\mathrm{tonne}} \qquad \mathrm{PWRAGE} := \begin{bmatrix} 5000 \\ 10000 \\ 20000 \\ 50000 \\ 100000 \end{bmatrix}$$

Mass of uranium in a B&W 15x15 SNF assembly $\mathrm{MTUpSNF} := 0.464 \cdot \mathrm{tonne}$ (Ref.5.7)

Active length of a B&W 15x15 SNF assembly $\mathrm{PWRactleng} := 141.8 \cdot \mathrm{in}$ (Ref.5.7)

Width of one side of a B&W 15x15 SNF assembly $\mathrm{PWRwidth} := 8.54 \cdot \mathrm{in}$ (Ref.5.7)

MISC. INFORMATION

Universal Gas Constant $R_0 := 8315 \cdot \frac{\mathrm{J}}{\mathrm{kmol} \cdot \mathrm{K}}$ Ref. 5.14

Atm. Pressure $\mathrm{PATM} := 1.0132 \cdot 10^{5} \cdot \mathrm{Pa}$ Ref. 5.15

	Atomic Volume	Molecular Weight	
Water	$V_1 := 18.8$	$M_1 := 18.02$	From Ref. 5.14
Air	$V_2 := 29.9$	$M_2 := 28.97$	
O_2	$V_3 := 7.4$	$M_3 := 2 \cdot 15.99$	

Acceleration of Gravity $\mathrm{gr} := 9.807 \cdot \frac{\mathrm{m}}{\mathrm{s}^2}$ Ref.5.15

Volume Fraction O_2 in Air $\mathrm{Vo2} := 0.209$ Ref. 5.17

Henry's Law Solubility of O_2 in 30°C Water $\mathrm{hO2} := 4.75 \cdot 10^{4} \cdot \frac{\mathrm{atm}}{\mathrm{mole}}$ Ref. 5.26

Properties of Sat. Water at 32C

Coefficient of Thermal Expansion $\beta := 320.6 \cdot 10^{-6} \cdot \mathrm{K}^{-1}$ Ref.5.28

Thermal Conductivity $k := 0.620 \cdot \frac{\mathrm{watt}}{\mathrm{m} \cdot \mathrm{K}}$ Ref.5.28

Thermal Diffusivity $\alpha := \frac{k}{\rho(31.85) \cdot \mathrm{Cp}(31.85)}$

$\alpha = 1.493 \cdot 10^{-7} \cdot \mathrm{m}^2 \cdot \mathrm{sec}^{-1}$

Kinematic Viscosity $\nu := \frac{\mu(31.85)}{\rho(31.85)}$ $\nu = 7.748 \cdot 10^{-7} \cdot \mathrm{m}^2 \cdot \mathrm{sec}^{-1}$

Diffusion Coefficient for Oxygen into Water at 20°C (Ref. 5.26; only value available) $\mathrm{Dox} := 1.8 \cdot 10^{-9} \cdot \frac{\mathrm{m}^2}{\mathrm{s}}$

OXYGEN DIFFUSION WITH CONVECTION IN WP

$i := 0..4$

Convection and Diffusion in WP filled to half way between the top row and the top of the package

Area of 1 side of an assembly times three assemblies on top row $A := 3 \cdot \mathrm{PWRactleng} \cdot \mathrm{PWRwidth}$

Half the height between the top row and the inside surface of the inner barrier $L := \dfrac{82.9 \cdot \mathrm{mm}}{2}$

Heat of three fuel assemblies as a function of time $3 \cdot \mathrm{PWRHEAT} \cdot \mathrm{MTUpSNF} = \begin{pmatrix} 1.846 \cdot 10^{1} \\ 1.385 \cdot 10^{1} \\ 8.658 \\ 3.313 \\ 1.157 \end{pmatrix} \cdot \mathrm{watt}$

Temperature Difference Between the two surfaces assuming planar conduction through water (divided by 4 because assembly has 4 sides)

$$\Delta T_i := \frac{\mathrm{PWRHEAT}_i \cdot 3 \cdot \mathrm{MTUpSNF} \cdot L}{4 \cdot k \cdot A} \qquad \Delta T = \begin{pmatrix} 1.316 \cdot 10^{-1} \\ 9.877 \cdot 10^{-2} \\ 6.174 \cdot 10^{-2} \\ 2.362 \cdot 10^{-2} \\ 8.249 \cdot 10^{-3} \end{pmatrix} \cdot K$$

Calculate Rayleigh Number

$$Ra_i := \frac{gr \cdot \beta \cdot \Delta T_i \cdot L^3}{\alpha \cdot \nu} \qquad Ra = \begin{pmatrix} 2.548 \cdot 10^{5} \\ 1.912 \cdot 10^{5} \\ 1.195 \cdot 10^{5} \\ 4.574 \cdot 10^{4} \\ 1.597 \cdot 10^{4} \end{pmatrix}$$

Per Ref. 5.28, circulation occurs in geometries similar to the space above the top row if Ra > 1708. This is the case for at least the first 100,000 years if the WP is flooded.

To estimate the circulation time for the water above the top row, assume that all heat transfer occurs by heating the fluid to the temperature of the hot surface, then moving the fluid to the cold surface and chilling it there. The circulation time for this process is given by:

$$q = h \cdot A \cdot \Delta T = \frac{Cp \cdot \Delta T \cdot \rho \cdot A \cdot L}{\tau}$$

Simplifying yields,

$$\tau = \frac{Cp \cdot \rho \cdot L}{h}$$

To estimate the convection heat transfer coefficient, first calculate the Prandtl Number

$$Pr := \frac{\nu}{\alpha} \qquad Pr = 5.191$$

Aspect Ratio

$$AR := \frac{\left(\frac{A}{PWRactleng}\right)}{L} \qquad AR = 1.57 \cdot 10^{1}$$

Finally, the heat transfer coefficient can be determined from the following empirical correlation given in Eq. 9.40 of Ref. 5.28.

$$h_i := 0.42 \cdot \left(Ra_i\right)^{\frac{1}{4}} \cdot Pr^{0.012} \cdot AR^{-0.3} \cdot \frac{k}{L}$$

$$h = \begin{bmatrix} 6.302 \cdot 10^{1} \\ 5.866 \cdot 10^{1} \\ 5.216 \cdot 10^{1} \\ 4.102 \cdot 10^{1} \\ 3.153 \cdot 10^{1} \end{bmatrix} \cdot kg \cdot sec^{-3} \cdot K^{-1}$$

Circulation Time for Cell

$$\tau_i := \frac{Cp(31.85) \cdot \rho(31.85) \cdot L}{h_i}$$

$$\tau = \begin{bmatrix} 2.732 \cdot 10^{3} \\ 2.935 \cdot 10^{3} \\ 3.301 \cdot 10^{3} \\ 4.197 \cdot 10^{3} \\ 5.46 \cdot 10^{3} \end{bmatrix} \cdot sec$$

Assume the time spent at surface is half of circulation time

$$tc_i := \frac{\tau_i}{2}$$

Diffusion surface area for a half full package

$Af := \mathrm{FreeSurf}(ID - L)$

$Af = 2.231 \cdot m^2$

Saturation Concentration of Oxygen at Surface of Water

$$Csat := \frac{PATM \cdot Vo2}{hO2} \cdot \frac{M_3}{M_1} \cdot \rho(30)$$

$Csat = 7.775 \cdot 10^{-3} \cdot kg \cdot m^{-3}$

Oxygen Supply Rate For Half Full Package

(Ref. 5.27)

$$OXh_i := \frac{Af \cdot Csat \cdot 2 \cdot \sqrt{Dox \cdot tc_i}}{tc_i \cdot \sqrt{\pi}}$$

$$OXh = \begin{bmatrix} 7.086 \cdot 10^{-1} \\ 6.836 \cdot 10^{-1} \\ 6.446 \cdot 10^{-1} \\ 5.717 \cdot 10^{-1} \\ 5.012 \cdot 10^{-1} \end{bmatrix} \cdot kgyr^{-1}$$

ESTIMATE OF MAX POWER PRODUCED BY A STEADY STATE CRITICALITY IN AN AUCF WP

REFERENCES (For Information Only)

5.6 "AUCF WP Design (21 PWR) Tube Design" Sketches, CRWMS M&O, BBAA00000-01717-2100-16000 thru 16022, REV00A.
5.14 J.P. Holman, Heat Transfer, 7th Edition, 1990.
5.15 M.J. Moran, H.N. Shapiro, "Fundamentals of Engineering Thermodynamics," John Wiley & Sons, 1988.
5.16 "UCF Waste Package Criticality Analysis," BBAA0000-01717-0200-0005 Rev 00B, 1996.
5.17 CRC Handbook, 66th Edition, page F-45.
5.18 "Total System Performance Assessment - 1995: An Evaluation of the Potential Yucca Mountain Repository", B00000000-01717-2200-00136, Rev. 00, August 1995.
5.19 "Final Design Package, Babcock & Wilcox, BR-100 100 Ton Rail/Barge Spent Fuel Shipping Cask," DI# 51-1203400-01, November 1991.
5.29. M.R. Lindeburg, "EIT Reference Manual - 8th Edition," Professional Publications, Inc. Belmont, CA, 1992.
5.31 "Emplacement Scale Thermal Evaluations of Large and Small WP Designs (SCPB: N/A)," CRWMS M&O BB0000000-01717-0200-00009, REV 00, 12/18/95.
5.32 "Waste Package/Engineered Barrier Segment Conceptual Design Report," CRWMS M&O, BBA000000-01717-5705-00006 REV 00A, October 24, 1995.
5.37 "Spatial Distribution of Potential Near Surface Moisture Flux at Yucca Mountain," High Level Radioactive Waste Management: Proceedings of the Fifth Annual International Conference, ANS & ASCE, pgs 2352-2358, May 1994.
5.38 "Rainfall and Net Infiltration Probabilities for Future Climate Conditions at Yucca Mountain," High Level Radioactive Waste Management: Proceedings of the Fourth Annual International Conference, ANS & ASCE, pgs 112-121, May 1993.

MATHCAD UNITS DEFINITION

$kg := 1M$

$g := 10^{-3} \cdot kg$

$kmol := mole \cdot 10^{3}$

$s := 1T$

$min := 60 \cdot s$

$hr := 60 \cdot min$

$day := 24 \cdot hr$

$wk := 7 \cdot day$

$yr := 365 \cdot day$

$m := 1L$

$cm := 10^{-2} \cdot m$

$mm := 10^{-3} \cdot m$

$N := kg \cdot \frac{m}{s^{2}}$

$J := N \cdot m$

$kJ := 10^{3} \cdot J$

$Pa := \frac{N}{m^{2}}$

$MPa := 10^{6} \cdot Pa$

$bars := 10^{5} \cdot Pa$

INPUT

WP Inner Diameter $ID := 1.422 \cdot m$ Ref. 5.6 WP Outer Diameter $OD := 1.662 \cdot m$ Ref. 5.6

WP Inner Length $IL := 4.665 \cdot m$ Ref. 5.6 WP Outer Length minus skirts $OL := (5.335 - .450) \cdot m$ Ref. 5.6

Vol. of one PWR SNF Assembly $VSNF := 0.0807 \cdot m^3$ Ref. 5.19 ; B&W Mark B

Vol. of New 21 UCF WP Basket Assembly (tubes, SS-B plates, & structural members)

$VBAS := 8.7309204 \cdot 10^8 \cdot mm^3$ $VBAS = 0.9 \cdot m^3$ Ref 5.6 Determined using Pro-Engineer

Total volume occupied by all internal structures (basket & fuel)

$VINT := VBAS + 21 \cdot VSNF$ $VINT = 2.6 \cdot m^3$

Total WP interior void space

$VOID := \frac{\pi \cdot ID^2}{4} \cdot IL - VINT$ $VOID = 4.8 \cdot m^3$

LOAD IN STEAM TABLES AND OTHER PROPERTIES OF WATER

Read in sat. pressure and sat. liq. specific volume columns from temperature based steam table from Table A-2 of Ref. 5.15. Temperatures are in °C, Presures in bars, and Specific Volumes in cc/g

$$\mathrm{SteamTable} := \mathrm{READPRN}(\mathrm{steamtab}_{\mathrm{prn}})$$

Define vectors of second derivative coefficients using cubic spline function.

$$\mathrm{PSAT} := \mathrm{cspline}\left(\mathrm{SteamTable}^{\langle 0\rangle}, \mathrm{SteamTable}^{\langle 1\rangle}\right)$$

$$\mathrm{SPVOL} := \mathrm{cspline}\left(\mathrm{SteamTable}^{\langle 0\rangle}, \mathrm{SteamTable}^{\langle 2\rangle}\right)$$

Set up functions for interpolating pressure and specific volume as a function of the temperature

$$p(T) := \mathrm{interp}\left(\mathrm{PSAT}, \mathrm{SteamTable}^{\langle 0\rangle}, \mathrm{SteamTable}^{\langle 1\rangle}, T\right)\cdot \mathrm{bars}$$

$$\upsilon(T) := \mathrm{interp}\left(\mathrm{SPVOL}, \mathrm{SteamTable}^{\langle 0\rangle}, \mathrm{SteamTable}^{\langle 2\rangle}, T\right)\cdot \frac{\mathrm{cm}^3}{\mathrm{g}} \qquad \rho(T) := \frac{1}{\upsilon(T)}$$

Viscosity and Specific Heat of Sat. Liquid Water as a function of Temperature (C) from Ref. 5.14.

$$\mathrm{TempVisc} := \begin{array}{ccc} \text{Temp (°C)} & \mu \text{ kg/m-s} & \text{Cp kJ/kg-K} \\ \left[\begin{array}{ccc} 21.11 & 9.8\cdot 10^{-4} & 4.179 \\ 26.67 & 8.6\cdot 10^{-4} & 4.179 \\ 32.22 & 7.65\cdot 10^{-4} & 4.174 \\ 37.78 & 6.82\cdot 10^{-4} & 4.174 \\ 43.33 & 6.16\cdot 10^{-4} & 4.174 \\ 48.89 & 5.62\cdot 10^{-4} & 4.174 \\ 54.44 & 5.13\cdot 10^{-4} & 4.179 \\ 60 & 4.71\cdot 10^{-4} & 4.179 \end{array}\right] \end{array}$$

Similarly, the viscosity and specific heat of saturated liquid water as a function of temperature is shown in the TempVisc matrix to the right, and was obtained from Table A-9 of Ref. 5.14.

As above, the vectors of the second derivative coefficients are defined using the cubic spline function

$$\mathrm{Viscosity} := \mathrm{cspline}\left(\mathrm{TempVisc}^{\langle 0\rangle}, \mathrm{TempVisc}^{\langle 1\rangle}\right) \qquad \mathrm{SpHeat} := \mathrm{cspline}\left(\mathrm{TempVisc}^{\langle 0\rangle}, \mathrm{TempVisc}^{\langle 2\rangle}\right)$$

Next, the function for interpolating viscosity as a function of the temperature (C) is defined

$$\mu(t) := \left(\mathrm{interp}\left(\mathrm{Viscosity}, \mathrm{TempVisc}^{\langle 0\rangle}, \mathrm{TempVisc}^{\langle 1\rangle}, t\right)\right)\cdot \frac{\mathrm{kg}}{\mathrm{m}\cdot \mathrm{s}}$$

$$\mathrm{Cp}(T) := \left(\mathrm{interp}\left(\mathrm{SpHeat}, \mathrm{TempVisc}^{\langle 0\rangle}, \mathrm{TempVisc}^{\langle 2\rangle}, T\right)\right)\cdot \frac{\mathrm{kJ}}{\mathrm{kg}\cdot \mathrm{K}}$$

MISC. OTHER INFORMATION

Drift Diameter $\mathrm{DriftD} := 5 \cdot \mathrm{m}$

Stephan-Boltzman Constant $\sigma := 5.669 \cdot 10^{-8} \cdot \frac{\mathrm{watt}}{\mathrm{m}^2 \cdot \mathrm{K}^4}$ (Ref. 5.14)

Carbon Steel Emissivity $\varepsilon 1 := 0.80$ (Ref. 5.31, A516 oxidized)

Drift Wall Emissivity $\varepsilon 2 := 0.85$ (Ref. 5.31, TSw2)

Thermal Conductivity of Crushed tuff $\mathrm{kct} := 0.66 \cdot \frac{\mathrm{watt}}{\mathrm{m} \cdot \mathrm{K}}$

Estimates of thermal conductivity for crushed TSw2 tuff range from 0.58 to 0.74 W/m-K (Ref 5.32). The middle of this range was used for this analysis.

Acceleration of gravity $\mathrm{gr} := 9.80665 \cdot \frac{\mathrm{m}}{\mathrm{s}^2}$ (Ref. 5.15)

Relative Humidity $\mathrm{RH} := 0.96$

(Per Ref. 5.18 83MTU/acre RH history, RH is constant at this value after approx. 6600 years.)

Evaporation Area $\mathrm{Area} := 3 \cdot \mathrm{m}^2$

Universal Gas Constant $R_0 := 8315 \cdot \frac{\mathrm{J}}{\mathrm{kmol} \cdot \mathrm{K}}$ (Ref. 5.14)

Atm. Pressure $\mathrm{PATM} := 1.0132 \cdot 10^5 \cdot \mathrm{Pa}$ (Ref. 5.15)

	Atomic Volume	Molecular Weight (g/mole)	
Water	$V_1 := 18.8$	$M_1 := 18.02$	From Ref. 5.15
Air	$V_2 := 29.9$	$M_2 := 28.97$	
O_2	$V_3 := 7.4$	$M_3 := 2 \cdot 16.00$	

TSPA-95 Model Parameters (Ref. 5.18)

Climate Cycle Period (years) $\tau := 100000$ Concentration Factor $\mathrm{CF} := 4$

		Low Infiltration Scenario	*High Infiltration Scenario*
Minimum Infiltration Rate	*Lower Bound*	$\mathrm{LlImin} := .01 \cdot \frac{\mathrm{mm}}{\mathrm{yr}}$	$\mathrm{HlImin} := .5 \cdot \frac{\mathrm{mm}}{\mathrm{yr}}$
	Mean	$\mathrm{LmImin} := .03 \cdot \frac{\mathrm{mm}}{\mathrm{yr}}$	$\mathrm{HmImin} := 1.25 \cdot \frac{\mathrm{mm}}{\mathrm{yr}}$
	Upper Bound	$\mathrm{LuImin} := .05 \cdot \frac{\mathrm{mm}}{\mathrm{yr}}$	$\mathrm{HuImin} := 2 \cdot \frac{\mathrm{mm}}{\mathrm{yr}}$
Cycle Peak Multiplier	*Lower Bnd*	$\mathrm{lFGM} := 1$	
	Mean	$\mathrm{mFGM} := 3$	Same
	Upper Bnd	$\mathrm{uFGM} := 5$	

MODERATOR DENSITY CHANGE EFFECTS ON k_{eff} FROM ACD(R) UCF DESIGN ANALYSIS

(100% Density is that for sat. liq. water at 300K)   (Ref. 5.16)

	Intact w/ No Boron	Degraded w/ No Boron
100% Density	$I100 := 1.0079$	$C100 := 1.018$
98% Density	$I98 := 1.0044$	$C98 := 1.0152$
95% Density	$I95 := .9959$	$C95 := 1.0085$
90% Density	$I90 := .987$	
80% Density	$I80 := .9705$	

% Negative Reactivity Insertion as A function of Moderator Density Change

5% Changes	3% Changes	2% Changes
$\frac{I95 - I100}{I95} \cdot 100 = -1.2$	$\frac{I95 - I98}{I95} \cdot 100 = -0.9$	$\frac{I98 - I100}{I98} \cdot 100 = -0.3$
$\frac{C95 - C100}{C95} \cdot 100 = -0.9$	$\frac{C95 - C98}{C95} \cdot 100 = -0.7$	$\frac{C98 - C100}{C98} \cdot 100 = -0.3$
$\frac{I90 - I95}{I90} \cdot 100 = -0.9$		

The WP would slowly approach a keff of 1.0 as the water level rises. Criticality calcs for degraded AUCF WP design indicate that k_{eff} approaches the peak once the water level rises above the third row of assemblies for certain configurations. For a collapsed basket, this is approximately at the centerline of the WP. Ideally, given such a slow reactivity insertion, the power level of the resulting WP "reactor" would gradually increase to the point that equilibrium was maintained with the incoming water (i.e., just the amount of power required to remove the incoming water but maintain the water level at the height required for $k_{eff} = 1.0$.

FLOW RATE OF WATER ONTO WASTE PACKAGE

Infiltration Rate

The simple model for change in infiltration rate as a function of time due to climate cycles is the same as that that detailed in Chapter 7 of TSPA-95 with a few minor differences. One minor difference is that the nature/shape of the cycle has been taken to be sinusoidal rather than triangular as in TSPA-95. This change was made because it was felt that a sinusoidal shape would more realistically represent natural processes.

For both models, there are three parameters which must be defined, the cycle period (τ), the minimum infiltration rate for the cycle (Imin), and the maximum infiltration rate for the cycle (Imax) which is a multiple of (Imin). The multiplier was uniformly distributed between 1 and 5. These distribution parameters were selected because Ref. 5.38 indicated that during the last glacial maximum the annual precipitation rate was 2.5 times that of the present.

For determining the minimum infiltration rate, TSPA-95 had two scenarios: a low infiltration scenario where Imin was uniformly distributed between 0.01 and 0.05 mm/yr, and a high infiltration scenario where Imin was uniformly distributed between 0.5 and 2 mm/yr. The former (low infiltration) values bound the current day average infiltration rate of 0.025 mm/yr for the rock units immediately above and in the area surrounding the repository as reported in Ref. 5.37. The basic assumption for the low infiltration scenario is that percolation flow occurs predominantly in the vertical direction. The high infiltration scenario assumes that there is some lateral flow due to the sloping nature of the rock units, and factors in the average higher infiltration rate of 1 mm/yr for the Paintbrush tuff outcropping immediately to the north of the repository block, as reported in Ref 5.37

For TSPA-95, the cycle period (τ) was fixed at 100,000 years (peak infiltration at 50,000 years). The form of the model for this is shown below

Infiltration Rate as a Function of Time,
Minimum Infiltration Rate, and Cycle Peak

$$\mathrm{qinf}(t,\mathrm{Imin},\mathrm{FGM}) := \left[\mathrm{Imin} + \left(\frac{\mathrm{FGM}\cdot\mathrm{Imin} - \mathrm{Imin}}{2}\right)\cdot\left(1 - \cos\left(\frac{2\cdot\pi\cdot t}{\tau}\right)\right)\right]$$

Drip Rate onto WPs from Flowing Fractures

The drip rate of water onto a package beneath a flowing fracture (qdrip) is taken to be a function of qinf, as given in TSPA-95 figures 7.3-7 and 7.3-8 for low and high infiltration respectively. This simple relationship was developed for use with RIP in TSPA-95 and is based on thermo-hydrologic process-level model simulations conducted using FEHM. For this model, some amount of dripping flow occured if the saturated matrix conductivity was less than the infiltration flux. This linear relationship between qinf and qdrip has been input into the DRIP matrix and a function for linearly interpolating qdrip is created.

$$\begin{array}{c} \text{qinf} \quad \text{qdrip} \\ \text{(mm/yr)} \end{array}$$

$$\mathrm{DRIP} := \begin{bmatrix} 0.01 & 0.0004 \\ 0.02 & 0.0014 \\ 0.03 & 0.0028 \\ 0.04 & 0.0046 \\ 0.05 & 0.0066 \\ 0.5 & 0.22 \\ 1.0 & 0.53 \\ 1.5 & 0.9 \\ 2.0 & 1.27 \end{bmatrix}$$

$$\mathrm{qdrip}(t,\mathrm{Imin},\mathrm{FGM}) := \mathrm{linterp}\left(\mathrm{DRIP}^{<0>},\mathrm{DRIP}^{<1>},\mathrm{qinf}(t,\mathrm{Imin},\mathrm{FGM})\cdot \mathrm{yr}\cdot \mathrm{mm}^{-1}\right)\cdot\frac{\mathrm{mm}}{\mathrm{yr}}$$

$$q(i) := \mathrm{linterp}\left(\mathrm{DRIP}^{<0>},\mathrm{DRIP}^{<1>},i\cdot \mathrm{mm}^{-1}\cdot \mathrm{yr}\right)\cdot\frac{\mathrm{mm}}{\mathrm{yr}}$$

Flow of Infiltrating Water Onto a WP by Fracture Network Concentration

The TSPA 95 corrosion models did not incorporate a "weeps" model of fracture flow onto a WP. Instead, aqueous conditions were assumed once drift relative humidity reached the 85-95% range. However, the radionuclide transport part of TSPA-95 did include a weeps model, although it was not specifically named as such. This model assumed that infiltrating water is focused onto a point over the WP by a fracture network covering a specified collection area. The collection area is defined as a multiple of the physical cross-sectional area of the emplaced WP interior as viewed from above. For TSPA-95 this "concentration factor was uniformly distributed between 0 and 4. The peak concentration factor of 4 will be used here.

Cross-Sectional Area of WP $\mathrm{WPAREA} := \mathrm{ID}\cdot\mathrm{IL}$

$\mathrm{WPAREA} = 6.6\cdot \mathrm{m}^2$

Flow Rate of Water Onto WP $\mathrm{FR}(t,\mathrm{Imin},\mathrm{FGM}) := \mathrm{qdrip}(t,\mathrm{Imin},\mathrm{FGM})\cdot\mathrm{WPAREA}\cdot\mathrm{CF}$

For the TSPA 95 Low (L) and High (H) Infiltration Scenarios (Ref. 5.18), the minimum, maximum, and mean values for the flow rate of water onto the WP at the 50,000 year full glacial maximum are as follows :

$\mathrm{Lminflow} := \mathrm{FR}(50000, \mathrm{LlImin}, \mathrm{lFGM})$ $\mathrm{Lminflow} = 1.1\cdot 10^{1}\cdot \mathrm{cm}^{3}\cdot \mathrm{yr}^{-1}$

$\mathrm{Lmeanflow} := \mathrm{FR}(50000, \mathrm{LmImin}, \mathrm{mFGM})$ $\mathrm{Lmeanflow} = 6.8\cdot 10^{2}\cdot \mathrm{cm}^{3}\cdot \mathrm{yr}^{-1}$

$\mathrm{Lmaxflow} := \mathrm{FR}(50000, \mathrm{LuImin}, \mathrm{uFGM})$ $\mathrm{Lmaxflow} = 2.7\cdot 10^{3}\cdot \mathrm{cm}^{3}\cdot \mathrm{yr}^{-1}$

$t := 10000, 12000 .. 100000$

$\mathrm{Hminflow} := \mathrm{FR}(50000, \mathrm{HlImin}, \mathrm{lFGM})$ $\mathrm{Hminflow} = 5.8\cdot 10^{3}\cdot \mathrm{cm}^{3}\cdot \mathrm{yr}^{-1}$

$\mathrm{Hmeanflow} := \mathrm{FR}(50000, \mathrm{HmImin}, \mathrm{mFGM})$ $\mathrm{Hmeanflow} = 6.8\cdot 10^{4}\cdot \mathrm{cm}^{3}\cdot \mathrm{yr}^{-1}$

$\mathrm{Hmaxflow} := \mathrm{FR}(50000, \mathrm{HuImin}, \mathrm{uFGM})$ $\mathrm{Hmaxflow} = 1.9\cdot 10^{5}\cdot \mathrm{cm}^{3}\cdot \mathrm{yr}^{-1}$

High Infiltration Scenario Maximum Flow Rates Onto WP

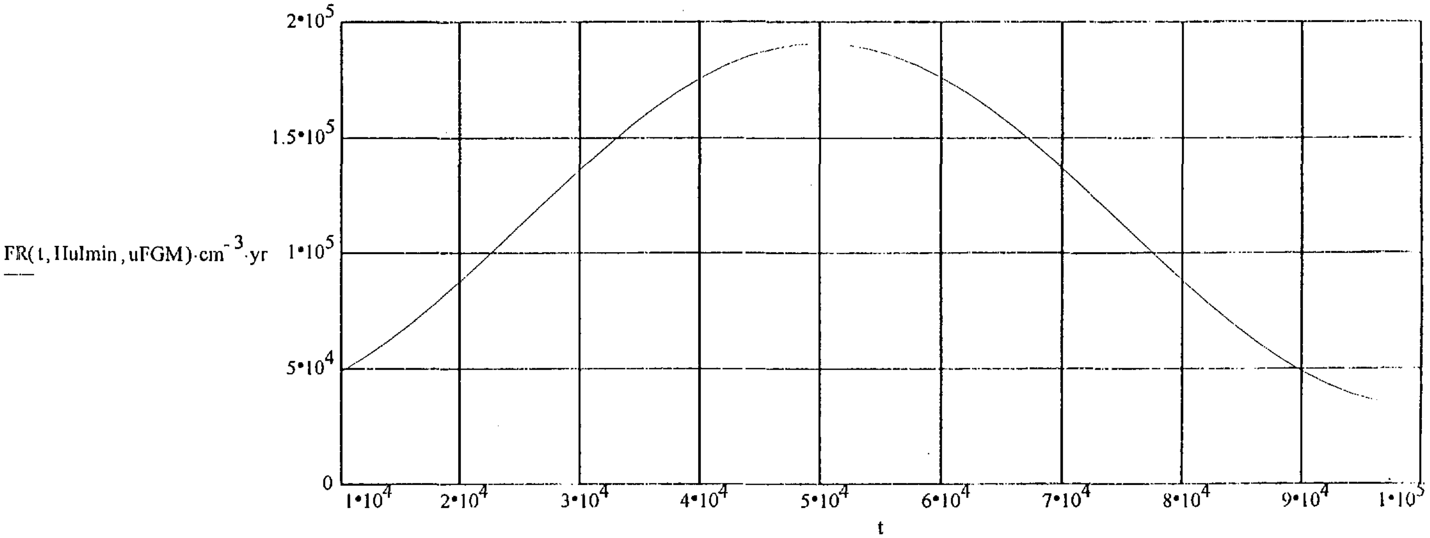

WP Fill Times for Various Infiltration Rates and Filling Efficiencies

$q\left(.01\cdot\frac{mm}{yr}\right) = 4\cdot 10^{-4}\cdot\frac{mm}{yr}$ $\quad q\left(.1\cdot\frac{mm}{yr}\right) = 3\cdot 10^{-2}\cdot\frac{mm}{yr}$ $\quad q\left(1\cdot\frac{mm}{yr}\right) = 0.5\cdot\frac{mm}{yr}$ $\quad q\left(10\cdot\frac{mm}{yr}\right) = 7.2\cdot\frac{mm}{yr}$

$$\mathrm{FillTime}(i,f) := \frac{\mathrm{VOID}}{q(i)\cdot \mathrm{CF}\cdot \mathrm{WPAREA}\cdot f}$$

Infiltration Rate	Filling Eff. = 1	Filling Eff. = 0.1	Filling Eff. = 0.01
.01 mm/yr	$\mathrm{FillTime}\left(.01\cdot\frac{mm}{yr},1\right) = 4.6\cdot 10^{5}\cdot yr$	$\mathrm{FillTime}\left(.01\cdot\frac{mm}{yr},0.1\right) = 4.6\cdot 10^{6}\cdot yr$	$\mathrm{FillTime}\left(.01\cdot\frac{mm}{yr},0.01\right) = 4.6\cdot 10^{7}\cdot yr$
.1 mm/yr	$\mathrm{FillTime}\left(.1\cdot\frac{mm}{yr},1\right) = 6\cdot 10^{3}\cdot yr$	$\mathrm{FillTime}\left(.1\cdot\frac{mm}{yr},0.1\right) = 6\cdot 10^{4}\cdot yr$	$\mathrm{FillTime}\left(.1\cdot\frac{mm}{yr},0.01\right) = 6\cdot 10^{5}\cdot yr$
1 mm/yr	$\mathrm{FillTime}\left(1\cdot\frac{mm}{yr},1\right) = 3.4\cdot 10^{2}\cdot yr$	$\mathrm{FillTime}\left(1\cdot\frac{mm}{yr},0.1\right) = 3.4\cdot 10^{3}\cdot yr$	$\mathrm{FillTime}\left(1\cdot\frac{mm}{yr},0.01\right) = 3.4\cdot 10^{4}\cdot yr$
10 mm/yr	$\mathrm{FillTime}\left(10\cdot\frac{mm}{yr},1\right) = 2.5\cdot 10^{1}\cdot yr$	$\mathrm{FillTime}\left(10\cdot\frac{mm}{yr},0.1\right) = 2.5\cdot 10^{2}\cdot yr$	$\mathrm{FillTime}\left(10\cdot\frac{mm}{yr},0.01\right) = 2.5\cdot 10^{3}\cdot yr$

EVAPORATION THROUGH BREACH HOLES IN TOP OF PACKAGE

As airflow is stagnant in a drift, evaporation will be modeled as diffusion of water vapor into air. First, the diffusion coefficient must be determined. In Ref. 5.14 Holman provides the following formula for approximating the diffusion coefficient as a function of temperature for water into air at atmospheric pressure:

$$D(T) := 435.7 \cdot \frac{(T + 273.15)^{\frac{3}{2}}}{PATM \cdot Pa^{-1} \cdot \left[(V_1)^{\frac{1}{3}} + (V_2)^{\frac{1}{3}} \right]^2} \cdot \sqrt{\frac{1}{M_1} + \frac{1}{M_2}} \cdot \frac{cm^2}{s}$$

For Water into Air, at atmospheric pressure and 8C the above yields: $D(8) = 0.183 \cdot sec^{-1} \cdot cm^2$

Ref. 5.17 gives 0.239 at 8C for a difference of $.239 - .183 = 0.056$

For 25C the above equation gives 0.2 and Ref. 5.14 Table A-8 gives 0.256 for a difference of $.256 - .2 = 0.056$

Since the equation is consistently low by the same amount, a correction factor of 0.056 will be added to bring the equation into agreement with available experimental data. With simplification, this yields

$$D(T) := D(T) + 0.056 \cdot \frac{cm^2}{s}$$

From Holman p.606, the volume flow rate out due to evaporation at temperature T is given by,

$$Vevap(T) := \frac{Area \cdot \upsilon(T) \cdot D(T) \cdot PATM \cdot M_1 \cdot \frac{kg}{kmol}}{R_0 \cdot (T + 273.15) \cdot K \cdot (.058 \cdot ID)} \cdot \ln\left(\frac{PATM - p(T) \cdot RH}{PATM - p(T)} \right)$$

$\text{Lminflow} = 1.1 \cdot 10^{1} \cdot cm^{3} \cdot yr^{-1}$ $\qquad \text{Vevap}(30) = 3.8 \cdot 10^{4} \cdot yr^{-1} \cdot cm^{3}$

$\text{Lmeanflow} = 6.8 \cdot 10^{2} \cdot cm^{3} \cdot yr^{-1}$ $\qquad \text{Vevap}(30) = 3.8 \cdot 10^{4} \cdot yr^{-1} \cdot cm^{3}$

$\text{Lmaxflow} = 2.7 \cdot 10^{3} \cdot cm^{3} \cdot yr^{-1}$ $\qquad \text{Vevap}(30) = 3.8 \cdot 10^{4} \cdot yr^{-1} \cdot cm^{3}$

$\text{Hminflow} = 5.8 \cdot 10^{3} \cdot cm^{3} \cdot yr^{-1}$ $\qquad \text{Vevap}(30) = 3.8 \cdot 10^{4} \cdot yr^{-1} \cdot cm^{3}$

$\text{Hmeanflow} = 6.8 \cdot 10^{4} \cdot cm^{3} \cdot yr^{-1}$ $\qquad \text{Vevap}(40) = 6.9 \cdot 10^{4} \cdot yr^{-1} \cdot cm^{3}$

$\text{Hmaxflow} = 1.9 \cdot 10^{5} \cdot cm^{3} \cdot yr^{-1}$ $\qquad \text{Vevap}(57.4) = 1.9 \cdot 10^{5} \cdot yr^{-1} \cdot cm^{3}$

Assume heat losses from WP are entirely due to radiation, and treat WP and drift as concentric cylinders.

1D Estimate of Radiation Heat Transfer Losses for a WP at T°C and a Drift Wall at 30°C

Drift Area $\qquad$ WP Area

$A2 := \pi \cdot \text{DriftD} \cdot OL \qquad A1 := \pi \cdot OD \cdot OL$

$A2 = 7.7 \cdot 10^{1} m^{2} \qquad A1 = 2.6 \cdot 10^{1} m^{2} \qquad T2 := (30 + 273.15) \cdot K$

Shape Factor equals one because the WP sees only the drift wall

$$\text{qrad}(T) := \frac{\sigma \cdot \left[((T + 273.15) \cdot K)^{4} - T2^{4} \right] \cdot A1}{\frac{1}{\varepsilon 1} + \left(\frac{A1}{A2} \right) \cdot \left(\frac{1}{\varepsilon 2} - 1 \right)}$$

From Ref. 5.14 Equation 8-43

$\text{qrad}(57.4) = 3.859 \cdot 10^{3} \cdot watt$

Assume heat transfer losses are entirely from conduction through crushed tuff, possibly because WP has become buried as the drift roof collapses over time. The temperature at what used to be the drift wall is still assumed to be 30°C.

$$\mathrm{qcond}(T) := 2\cdot\pi\cdot \mathrm{kct}\cdot \mathrm{OL}\cdot\frac{(T+273.15)\cdot K - 303.15\cdot K}{\ln\left[\frac{\frac{\mathrm{DriftD}}{2}}{\left(\frac{\mathrm{OD}}{2}\right)}\right]}$$

$$\mathrm{qcond}(57.4) = 5.04\cdot 10^{2}\cdot \mathrm{watt}$$

The above two values represent upper and lower bounds, respectively. The more likely configuration will be a partially covered WP with both radiation and conduction heat transfer mechanisms contributing to heat removal. For this analysis, it will be assumed that half of the WP is covered, and that the heat removed is the average of the conduction and radiation values.

$$q(T) := \frac{\mathrm{qcond}(T) + \mathrm{qrad}(T)}{2}$$

$$q(57.4) = 2.182\cdot 10^{3}\cdot \mathrm{kg}\cdot \mathrm{m}^{2}\cdot \mathrm{sec}^{-3}$$

Heat of Vaporization

$$2364.8\cdot\frac{\mathrm{kJ}}{\mathrm{kg}}\cdot 1.9\cdot 10^{5}\cdot\frac{\mathrm{cm}^{3}}{\mathrm{yr}}\cdot\rho(57.4) = 14.025\cdot \mathrm{watt}$$

For Low Infiltration Scenarios, package never fills because water evaporates quicker than it is supplied

For the High Infiltration Scenario the power level is that required to maintain equilibrium with the maximum flow rate of water entering the WP. Radiation heat transfer only yields the most conservative result, followed by power levels for half-radiation, half-conduction, and all conduction.

If criticality occurs when water is at 30°C (after 100,000 years) then the process of heating the water would cause a density change of:

$$\frac{\rho(57.4)-\rho(30)}{\rho(57.4)}\cdot 100 = -1.1$$

This will cause a minor negative reactivity insertion as temperature increases which should, at the least, lengthen the period.

AUCF WP INTERNAL VOLUMES AND MASSES FOR INTACT AND DEGRADED CRITICALITY CALCULATIONS

REFERENCES (For Information Only)

5.5 "Material Compositions and Number Densities for Neutronics Calculations, (SCPB: N/A)," CRWMS M&O, BBA000000-01717-0200-00002, REV 00, 1/2/96.

5.6 "AUCF WP Design (21 PWR) Tube Design" Sketches, CRWMS M&O, BBAA00000-01717-2100-16000 thru 16022, REV00A.

5.17 R.C. Weast, "CRC Handbook of Chemistry and Physics," 66th Edition, Boca Raton, FL, 1985 .

5.19 "Final Design Package, Babcock & Wilcox, BR-100 100 Ton Rail/Barge Spent Fuel Shipping Cask," FCF DI# 51-1203400-01, November 1991.

5.33 "Nuclides and Isotopes," Fourteenth Edition, General Electric Company, 1989.

MATHCAD UNITS DEFINITION

$g := 1M$ $m := 1L$

$kg := 10^{3} \cdot g$ $mm := 10^{-3} \cdot m$ $cm := 10^{\ 2} \cdot m$ $\mu m := 10^{-6} \cdot m$ $b := 10^{\ 24} \cdot cm^{2}$

INPUT

WP Physical Dimmensions

WP Inner Diameter $ID := 1.422 \cdot m$ (Ref. 5.6)

Vol. of one PWR SNF Assembly $VSNF := 0.0807 \cdot m^3$ (Ref. 5.19)

WP Inner Length $IL := 4.665 \cdot m$ (Ref. 5.6)

Vol. of 21PWR AUCF WP Basket Assembly (tubes, SS-B plates, & structural members)

$VBAS := 8.7309204 \cdot 10^8 \cdot mm^3$ $VBAS = 0.873 \cdot m^3$ (Determined using Pro-Engineer, which was used to produce Ref. 5.6)

Vol. of 21 PWR AUCF WP Carbon Steel Tube (Ref. 5.6)

$VTUBE := \left[(238.5 \cdot mm)^2 - (228.5 \cdot mm)^2\right] \cdot 4575 \cdot mm$ $VTUBE = 2.137 \cdot 10^7 \cdot mm^3$ $21 \cdot VTUBE = 0.449 \cdot m^3$

Vol. of Borated SS Basket Plates (Ref. 5.6)

$VSHORT := (730 \cdot mm \cdot 1134 \cdot mm - 2 \cdot 7 \cdot mm \cdot 567 \cdot mm) \cdot 7 \cdot mm$ $VAPLATE := (1221 \cdot mm \cdot 1134 \cdot mm - 4 \cdot 7 \cdot mm \cdot 567 \cdot mm) \cdot 7 \cdot mm$

$VBPLATE := (1221 \cdot mm \cdot 1134 \cdot mm - 4 \cdot 7 \cdot mm \cdot 567 \cdot mm) \cdot 7 \cdot mm$ $VPLATES := (4 \cdot VSHORT + 2 \cdot VAPLATE + 2 \cdot VBPLATE) \cdot 4$

$VPLATES = 0.245 \cdot m^3$

Vol. of Carbon Steel Guides & Stifeners

$VGUIDES := VBAS - 21 \cdot VTUBE - VPLATES$ $VGUIDES = 0.179 \cdot m^3$

WP Material Properties (Ref. 5.5 unless otherwise noted)

	Weight Fractions for A516 Carbon Steel	Weight Fractions for Borated 316 Stainless Steel (SS316B6A)	Atomic Mass (Ref. 5.33)
Fe	$fFeCS := .98535$	$fFeSS := .60445$	$AMFe := 55.847 \cdot \frac{g}{mole}$
B		$fBSS := .00288 + .01312$	
Cr		$fCrSS := .19$	
Ni		$fNiSS := .135$	
Mn	$fMnCS := .009$	$fMnSS := .02$	
Mo		$fMoSS := .025$	
N		$fNSS := .001$	
S	$fSCS := .00035$	$fSSS := .0003$	
Si	$fSiCS := .00275$	$fSiSS := .0075$	
P	$fPCS := .00035$	$fPSS := .00045$	
C	$fCCS := .0022$	$fCSS := .0003$	
O			$AMO := 15.9994 \cdot \frac{g}{mole}$

Density of Carbon Steel	$\rho CS := 7.832 \cdot \frac{g}{cm^3}$	(Ref. 5.5)
Density of Borated SS (SS316B6A)	$\rho SS := 7.77 \cdot \frac{g}{cm^3}$	(Ref. 5.5)
Density of Iron Oxide	$\rho Fe2O3 := 5.24 \cdot \frac{g}{cm^3}$	(Ref. 5.17)

CALCULATIONS

Calculation of Volumes

Total interior volume of empty WP (no basket or fuel)

$\mathrm{VEMPTY} := \frac{\pi \cdot \mathrm{ID}^2}{4} \cdot \mathrm{IL}$ $\mathrm{VEMPTY} = 7.409 \cdot \mathrm{m}^3$

Total volume occupied by all internal structures (basket & fuel)

$\mathrm{VINT} := \mathrm{VBAS} + 21 \cdot \mathrm{VSNF}$ $\mathrm{VINT} = 2.568 \cdot \mathrm{m}^3$

Total WP interior void space

$\mathrm{VOID} := \frac{\pi \cdot \mathrm{ID}^2}{4} \cdot \mathrm{IL} - \mathrm{VINT}$ $\mathrm{VOID} = 4.841 \cdot \mathrm{m}^3$

Total volume occupied by carbon steel tubes

$21 \cdot \mathrm{VTUBE} = 0.449 \cdot \mathrm{m}^3$

Void Space Fraction

$\frac{\mathrm{VOID}}{\mathrm{VEMPTY}} = 0.653$

Total WP interior void space with no basket material left $\mathrm{VOIDNB} := \mathrm{VOID} + \mathrm{VBAS}$ $\mathrm{VOIDNB} = 5.714 \cdot \mathrm{m}^3$

Calculation of Surface Areas

Total Surface Area of All Carbon Steel Tubes $\frac{2 \cdot 21 \cdot \mathrm{VTUBE}}{5 \cdot \mathrm{mm}} = 179.468 \cdot \mathrm{m}^2$

Total Surface Area of One Carbon Steel Tube $\frac{2 \cdot \mathrm{VTUBE}}{5 \cdot \mathrm{mm}} = 8.546 \cdot \mathrm{m}^2$

Total Surface Area of All Stainless Steel Plates $\frac{2 \cdot \mathrm{VPLATES}}{7 \cdot \mathrm{mm}} = 70.036 \cdot \mathrm{m}^2$

Calculation of Masses

	Total Mass	Total Mass of Fe	Total Mass of Mn	Total Mass of B	Total Mass of Cr	Total Mass of Ni	Total Mass of Mo
	$MT := 21 \cdot VTUBE \cdot \rho CS$	$mtFe := MT \cdot fFeCS$	$mtMn := MT \cdot fMnCS$				
TUBES	$MT = 3.514 \cdot 10^{3} \cdot kg$	$mtFe = 3.46 \cdot 10^{3} \cdot kg$	$mtMn = 31.63 \cdot kg$				
	$MP := VPLATES \cdot \rho SS$	$mpFe := MP \cdot fFeSS$	$mpMn := MP \cdot fMnSS$	$mpB := MP \cdot fBSS$	$mpCr := MP \cdot fCrSS$	$mpNi := MP \cdot fNiSS$	$mpMo := MP \cdot fMoSS$
PLATES	$MP = 1.905 \cdot 10^{3} \cdot kg$	$mpFe = 1.15 \cdot 10^{3} \cdot kg$	$mpMn = 38.09 \cdot kg$	$mpB = 30.47 \cdot kg$	$mpCr = 361.88 \cdot kg$	$mpNi = 257.12 \cdot kg$	$mpMo = 47.62 \cdot kg$
	$MG := VGUIDES \cdot \rho CS$	$mgFe := MG \cdot fFeCS$	$mgMn := MG \cdot fMnCS$				
GUIDES	$MG = 1.404 \cdot 10^{3} \cdot kg$	$mgFe = 1.38 \cdot 10^{3} \cdot kg$	$mgMn = 12.64 \cdot kg$				

TOTAL MASS Fe	$mtFe + mpFe + mgFe = 5.997 \cdot 10^{3} \cdot kg$
TOTAL MASS Mn	$mtMn + mpMn + mgMn = 82.357 \cdot kg$
TOTAL MASS B	$mpB = 30.474 \cdot kg$
TOTAL MASS Ni	$mpNi = 257.124 \cdot kg$
TOTAL MASS Cr	$mpCr = 361.879 \cdot kg$
TOTAL MASS Mo	$mpMo = 47.616 \cdot kg$

TOTAL MASS $MP + MT + MG = 6.823 \cdot 10^{3} \cdot kg$

TOTAL Fe EQUIVALENT MASS IN PLATES (Everything but B, S, P, Si, & C)

$$SSFeEQ := (1 - fBSS - fSSS - fPSS - fSiSS - fCSS) \cdot MP$$

$$SSFeEQ = 1.858 \cdot 10^{3} \cdot kg$$

Mass Conversions for Fe_2O_3 filled void space following total corrosion of SS plates and CS tubes

Mass of Fe for 30% of void space filled w/ oxide	$0.3\cdot VOIDNB\cdot \rho Fe2O3\cdot \frac{2\cdot AMFe}{2\cdot AMFe+3\cdot AMO}=6.283\cdot 10^{3}\cdot kg$
Mass of Fe for 25% of void space filled w/ oxide	$0.25\cdot VOIDNB\cdot \rho Fe2O3\cdot \frac{2\cdot AMFe}{2\cdot AMFe+3\cdot AMO}=5.235\cdot 10^{3}\cdot kg$
Mass of Fe for 20% of void space filled w/ oxide	$0.2\cdot VOIDNB\cdot \rho Fe2O3\cdot \frac{2\cdot AMFe}{2\cdot AMFe+3\cdot AMO}=4.188\cdot 10^{3}\cdot kg$
Mass of Fe for 10% of void space filled w/ oxide	$0.1\cdot VOIDNB\cdot \rho Fe2O3\cdot \frac{2\cdot AMFe}{2\cdot AMFe+3\cdot AMO}=2.094\cdot 10^{3}\cdot kg$

Constituent masses for various thicknesses of SS plates remaining

Mass of Fe in SS plate remaining at 50% original thickness	$SS50t := .5\cdot SSFeEQ$	$SS50t = 928.933\cdot kg$
Mass of Fe in SS plate remaining at 25% original thickness	$SS25t := .25\cdot SSFeEQ$	$SS25t = 464.467\cdot kg$
Mass of Fe in SS plate remaining at 10% original thickness	$SS10t := .1\cdot SSFeEQ$	$SS10t = 185.787\cdot kg$
Mass of B in SS plate remaining at 50% original thickness	$B50t := .5\cdot mpB$	$B50t = 15.237\cdot kg$
Mass of B in SS plate remaining at 25% original thickness	$B25t := .25\cdot mpB$	$B25t = 7.618\cdot kg$
Mass of B in SS plate remaining at 20% original thickness	$B20t := .2\cdot mpB$	$B20t = 6.095\cdot kg$
Mass of B in SS plate remaining at 15% original thickness	$B15t := .15\cdot mpB$	$B15t = 4.571\cdot kg$
Mass of B in SS plate remaining at 10% original thickness	$B10t := .1\cdot mpB$	$B10t = 3.047\cdot kg$
Mass of B in SS plate remaining at 5% original thickness	$B5t := .05\cdot mpB$	$B5t = 1.524\cdot kg$
Mass of B in SS plate remaining at 2% original thickness	$B2t := .02\cdot mpB$	$B2t = 0.609\cdot kg$

Mass Conversions for various thicknesses of SS plates remaining and parts of void space filled with Fe_2O_3

Mass of Fe in plates is same as indicated above.

Mass of Fe for 50% plates thickness and 10% of void space filled w/ oxide $0.1\cdot(\mathrm{VOIDNB} - .5\cdot\mathrm{VPLATES})\cdot\rho\mathrm{Fe2O3}\cdot\frac{2\cdot\mathrm{AMFe}}{2\cdot\mathrm{AMFe} + 3\cdot\mathrm{AMO}} + .5\cdot\mathrm{SSFeEQ} = 2.978\cdot10^{3}\cdot\mathrm{kg}$

Mass of Fe for 25% plates thickness and 20% of void space filled w/ oxide $0.2\cdot(\mathrm{VOIDNB} - .25\cdot\mathrm{VPLATES})\cdot\rho\mathrm{Fe2O3}\cdot\frac{2\cdot\mathrm{AMFe}}{2\cdot\mathrm{AMFe} + 3\cdot\mathrm{AMO}} + .25\cdot\mathrm{SSFeEQ} = 4.608\cdot10^{3}\cdot\mathrm{kg}$

Mass of Fe for 25% plates thickness and 15% of void space filled w/ oxide $0.15\cdot(\mathrm{VOIDNB} - .25\cdot\mathrm{VPLATES})\cdot\rho\mathrm{Fe2O3}\cdot\frac{2\cdot\mathrm{AMFe}}{2\cdot\mathrm{AMFe} + 3\cdot\mathrm{AMO}} + .25\cdot\mathrm{SSFeEQ} = 3.572\cdot10^{3}\cdot\mathrm{kg}$

Mass of Fe for 10% plates thickness and 25% of void space filled w/ oxide $0.25\cdot(\mathrm{VOIDNB} - .1\cdot\mathrm{VPLATES})\cdot\rho\mathrm{Fe2O3}\cdot\frac{2\cdot\mathrm{AMFe}}{2\cdot\mathrm{AMFe} + 3\cdot\mathrm{AMO}} + .1\cdot\mathrm{SSFeEQ} = 5.399\cdot10^{3}\cdot\mathrm{kg}$

Mass of Fe for 10% plates thickness and 20% of void space filled w/ oxide $0.2\cdot(\mathrm{VOIDNB} + .1\cdot\mathrm{VPLATES})\cdot\rho\mathrm{Fe2O3}\cdot\frac{2\cdot\mathrm{AMFe}}{2\cdot\mathrm{AMFe} + 3\cdot\mathrm{AMO}} + .1\cdot\mathrm{SSFeEQ} = 4.392\cdot10^{3}\cdot\mathrm{kg}$

Mass of Fe for 10% plates thickness and 10% of void space filled w/ oxide $0.1\cdot(\mathrm{VOIDNB} - .1\cdot\mathrm{VPLATES})\cdot\rho\mathrm{Fe2O3}\cdot\frac{2\cdot\mathrm{AMFe}}{2\cdot\mathrm{AMFe} + 3\cdot\mathrm{AMO}} + .1\cdot\mathrm{SSFeEQ} = 2.271\cdot10^{3}\cdot\mathrm{kg}$

ESTIMATED C-14 and Cl-36 PRODUCTION BY NEUTRON ACTIVATION DURING A WP CRITICALITY

REFERENCES (For Information Only)

5.4 "AUCF WP Criticality and SAS2H Evaluations," CRWMS M&O, IOC LV.WP.DAT.03/96.070, Dan Thomas, March 26, 1996.
5.6 "AUCF WP Design (21 PWR) Tube Design" Sketches, CRWMS M&O, BBAA00000-01717-2100-16000 thru 16022, REV00A.
5.7 "Characteristics of Potential Repository Wastes," U.S. Department of Energy, DOW/RW-0184-R1 Volume 1, July 1992.
5.14 M.J. Moran, H.N. Shapiro, "Fundamentals of Engineering Thermodynamics," John Wiley & Sons, 1988.
5.17 R.C. Weast, "CRC Handbook of Chemistry and Physics," 66th Edition, Boca Raton, FL, 1985 .
5.19 "Final Design Package, Babcock & Wilcox, BR-100 100 Ton Rail/Barge Spent Fuel Shipping Cask," FCF DI# 51-1203400-01, November 1991.
5.26 J.H. Perry, "Chemical Engineers Handbook," Third Edition, McGraw-Hill Publishing Company, New York, 1950.
5.33 "Nuclides and Isotopes," Fourteenth Edition, General Electric Company, 1989.
5.35 "Pitting, Galvanic, and Long-Term Corrosion Studies on Candidate Container Alloys for the Tuff Repository," U.S. Nuclear regulatory Commission, NUREG/CR-5709, January 1992.

MATHCAD UNITS DEFINITION

$\mathrm{kg} := 1\mathrm{M}$

$\mathrm{g} := 10^{-3}\cdot\mathrm{kg}$

$\mu\mathrm{g} := 10^{-6}\cdot\mathrm{g}$

$\mathrm{s} := 1\mathrm{T}$

$\mathrm{min} := 60\cdot\mathrm{s}$

$\mathrm{hr} := 60\cdot\mathrm{min}$

$\mathrm{day} := 24\cdot\mathrm{hr}$

$\mathrm{wk} := 7\cdot\mathrm{day}$

$\mathrm{yr} := 365\cdot\mathrm{day}$

$\mathrm{m} := 1\mathrm{L}$

$\mathrm{cm} := 10^{-2}\cdot\mathrm{m}$

$\mathrm{mm} := 10^{-3}\cdot\mathrm{m}$

$\mathrm{N} := \mathrm{kg}\cdot\frac{\mathrm{m}}{\mathrm{s}^2}$

$\mathrm{J} := \mathrm{N}\cdot\mathrm{m}$

$\mathrm{kJ} := 10^{3}\cdot\mathrm{J}$

$\mathrm{mL} := \mathrm{cm}^3$

$\mathrm{kmol} := \mathrm{mole}\cdot 10^{3}$

$\mathrm{barn} := 10^{-28}\cdot\mathrm{m}^2$

$\mathrm{Ci} := 3.7\cdot 10^{10}\cdot\mathrm{s}^{-1}$

$\mu\mathrm{Ci} := 10^{-6}\cdot\mathrm{Ci}$

$\mathrm{Pa} := \frac{\mathrm{N}}{\mathrm{m}^2}$

$\mathrm{MPa} := 10^{6}\cdot\mathrm{Pa}$

$\mathrm{bars} := 10^{5}\cdot\mathrm{Pa}$

INPUT PARAMETERS

WP Inner Diameter	$ID := 1.422 \cdot m$	Ref. 5.6
WP Inner Length	$IL := 4.665 \cdot m$	Ref. 5.6

Vol. of one PWR SNF Assembly $VSNF := 0.0807 \cdot m^3$ Ref. 5.19; B&W Mark B

Vol. of New 21 UCF WP Basket Assembly (tubes, SS-B plates, & structural members)

$VBAS := 8.731 \cdot 10^8 \cdot mm^3$ $VBAS = 0.873 \cdot m^3$ Ref 5.6. Determined using Pro-Engineer, which is the software used to create the sketches

Total volume occupied by all internal structures (basket & fuel)

$VINT := VBAS + 21 \cdot VSNF$ $VINT = 2.568 \cdot m^3$

Total WP interior void space

$VOID := \frac{\pi \cdot ID^2}{4} \cdot IL - VINT$ $VOID = 4.841 \cdot m^3$

Read in sat. liq. specific volume columns from temperature based steam table from Table A-2 of Ref. 5.14. Temperatures are in °C, Presures in bars, and Specific Volumes in cc/g

$SteamTable := READPRN(steamtab_{prn})$

Define vectors of second derivative coefficients using cubic spline function.

$SPVOL := cspline\left(SteamTable^{<0>}, SteamTable^{<2>}\right)$

Set up functions for interpolating pressure and specific volume as a function of the temperature

$\upsilon(T) := interp\left(SPVOL, SteamTable^{<0>}, SteamTable^{<2>}, T\right) \cdot \frac{cm^3}{g}$

Water Density as a function of Temperature $\rho(T) := \frac{1}{\upsilon(T)}$

MISC. INPUT DATA

Molecular Weight of Water	$M_1 := 18.02 \cdot \frac{kg}{kmol}$	Ref.5.14
Avagadro's Number	$Na := 6.022 \cdot 10^{23} \cdot mole^{-1}$	
Partial Pressure of N_2 in air at atm. pres.	$pN2 := 0.7808 \cdot atm$	Ref.5.17
Henry's law sol. of N_2 in 57.4°C water	$hN2 := 11.8 \cdot 10^4 \cdot \frac{atm}{mole}$	Ref.5.26 Ref. 5.26 by lin. interpolation
Abundance of N14	$aN14 := 0.9963$	Ref.5.33
N-14 n,p reaction thermal cross section	$N14\sigma np := 1.83 \cdot barn$	Ref.5.33
Critical WP total neutron flux	$\phi := 2.9 \cdot 10^8 \cdot \frac{1}{cm^2 \cdot s}$	Ref.5.34
Fraction of total flux in thermal part of spectrum	$f := 0.109$	Ref. 5.34
C-14 Half-Life	$C14half := 5730 \cdot yr$	Ref.5.33
Atomic Weight of Nitrogen	$M_2 := 14 \cdot \frac{kg}{kmol}$	Ref.5.33
Atomic Weight of Chlorine	$M_3 := 35.453 \cdot \frac{kg}{kmol}$	Ref.5.33
Atomic Weight of Oxygen	$M_4 := 15.9994 \cdot \frac{kg}{kmol}$	Ref.5.33
Concentration of Cl in J-13	$cCl := 7.5 \cdot \frac{\mu g}{mL}$	Ref.5.35
Concentration of Cl in J-13 after boiling for 1 yr.	$chCl := 161 \cdot \frac{\mu g}{mL}$	Ref.5.35
Abundance of Cl35	$aCl35 := 0.7577$	Ref.5.33
Cl35 n,γ reaction thermal cross section	$Cl35\sigma n\gamma := 43.6 \cdot barn$	Ref.5.33
Cl36 Half-Life	$Cl36half := 3.01 \cdot 10^5 \cdot yr$	Ref.5.33
Abundance of O-17	$aO17 := 0.0004$	Ref.5.33
O17 n,α reaction thermal cross section	$O17\sigma n\alpha \quad 0.24 \cdot barn$	Ref.5.33

PRODUCTION OF C14

C-14 is primarily generated by the N14 n,p reaction and the O17 n,α reaction.

The nitrogen concentration in water at equilibrium with air at atm. pressure is

$$Nsat := \frac{\rho(57.4)}{M_1}\cdot\frac{pN2}{hN2}\cdot 2\cdot M_2 \qquad Nsat = 1.012\cdot 10^{-2}\cdot kg\cdot m^{-3}$$

Number Density of Nitrogen in WP Water

$$Nn := \frac{Nsat}{M_2}\cdot Na \qquad Nn = 4.354\cdot 10^{17}\cdot cm^{-3}$$

Number Density of N14 in WP Water

$$Nn14 := Nn\cdot aN14 \qquad Nn14 = 4.337\cdot 10^{17}\cdot cm^{-3}$$

Production Rate of C14 during WP Criticality

$$C14 := (Nn14\cdot N14\sigma np + No17\cdot O17\sigma n\alpha)\cdot\phi\cdot f\cdot VOID$$

$$\lambda c14 := \frac{\ln(2)}{C14half} \qquad \lambda c14 = 3.836\cdot 10^{-12}\cdot sec^{-1}$$

$$\lambda c14\cdot C14 = 1.977\cdot\frac{\mu Ci}{yr}$$

Number Density of O17 in water

$$No17 := \frac{aO17\cdot\rho(57.4)}{M_1}\cdot Na \qquad No17 = 1.316\cdot 10^{19}\cdot cm^{-3}$$

Note that the small amount of dissolved oxygen is neglected. The production of O17 by neutron capture in the more abundant, but lower cross section O16 is also neglected.

PRODUCTION OF Cl36

Dominant means of Cl36 production is a Cl35 n,γ reaction

The Cl concentration in J-13 well water is 7.5 μg/ml, and was 161 μg/ml after 1 year of boiling with tuff & ss

$cCl = 0.007 \cdot kg \cdot m^{-3}$ (Nominal) $chCl = 0.161 \cdot kg \cdot m^{-3}$ (High)

Number Density of Chlorine in WP Water

$Ncl := \frac{cCl}{M_3} \cdot Na$ $Ncl = 1.274 \cdot 10^{17} \cdot cm^{-3}$ $Nhcl := \frac{chCl}{M_3} \cdot Na$ $Nhcl = 2.735 \cdot 10^{18} \cdot cm^{-3}$

Number Density of Cl35 in WP Water $Ncl35 := Ncl \cdot aCl35$ $Ncl35 = 9.653 \cdot 10^{16} \cdot cm^{-3}$ (High) $Nhcl35 := Nhcl \cdot aCl35$ $Nhcl35 = 2.072 \cdot 10^{18} \cdot cm^{-3}$

Production Rate of Cl36 during WP Criticality

$Cl36 := Ncl35 \cdot Cl35\sigma n\gamma \cdot \phi \cdot f \cdot VOID$ $Cl36 = 2.031 \cdot 10^{16} \cdot yr^{-1}$ $hCl36 := Nhcl35 \cdot Cl35\sigma n\gamma \cdot \phi \cdot f \cdot VOID$

$\lambda Cl36 := \frac{\ln(2)}{Cl36half}$ $\lambda Cl36 = 7.302 \cdot 10^{-14} \cdot sec^{-1}$ $hCl36 = 4.36 \cdot 10^{17} \cdot yr^{-1}$

$\lambda Cl36 \cdot Cl36 = 0.04 \cdot \frac{\mu Ci}{yr}$ (Nominal Concentration) $\lambda Cl36 \cdot hCl36 = 0.86 \cdot \frac{\mu Ci}{yr}$ (High Concentration)

NEITHER C14 OR Cl36 PRODUCTION RATES EXCEED THE NRC LIMITS FOR RELEASE OF .796 Ci/yr AND 7.13 mCi/yr, RESPECTIVELY.